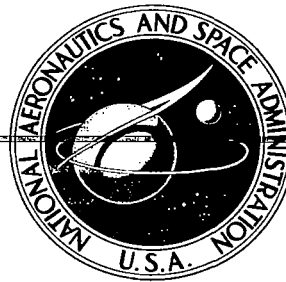


NASA CONTRACTOR REPORT



NASA CR-2708

0061452



TECH LIBRARY KAFB, NM

NASA CR-2708

LOAN COPY: RETURN TO
AFWL TECHNICAL LIBRARY
KIRTLAND AFB, N. M.

NOISE SUPPRESSION WITH HIGH MACH NUMBER INLETS

*Edward Lumsdaine, Jenn G. Cherng,
and Ismail Tag*

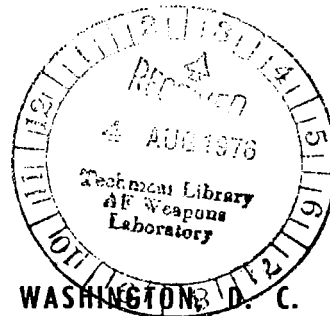
Prepared by

~~THE UNIVERSITY OF TENNESSEE~~ Univ.,

Knoxville, Tenn. 37916

for Langley Research Center

*Dept. of Mechanical
and Aerospace Engineering*



NATIONAL AERONAUTICS AND SPACE ADMINISTRATION • WASHINGTON, D. C. • JULY 1976



0061452

1. Report No. NASA CR-2708		2. Government Accession No.		3. Recipient's Catalog No.	
4. Title and Subtitle NOISE SUPPRESSION WITH HIGH MACH NUMBER INLETS				5. Report Date August 1976	
				6. Performing Organization Code	
7. Author(s) Edward Lumsdaine, Jenn G. Cherng, and Ismail Tag				8. Performing Organization Report No.	
9. Performing Organization Name and Address The University of Tennessee Department of Mechanical and Aerospace Engineering Knoxville, Tennessee 37916				10. Work Unit No.	
				11. Contract or Grant No.	
12. Sponsoring Agency Name and Address National Aeronautics and Space Administration Washington, D. C. 20546				13. Type of Report and Period Covered Contractor report	
				14. Sponsoring Agency Code	
15. Supplementary Notes The authors would like to acknowledge the assistance given to this program by Mr. Lorenzo R. Clark of the Acoustics Branch, Acoustics and Noise Reduction Division, Langley Research Center. Mr. Clark was responsible for coordinating the overall experimental effort. This included set-up of test hardware and instrumentation, operation of the Langley noise research compressor, and collection and reduction of data. These activities were essential to the completion of the research program and are greatly appreciated.					
16. Abstract Experimental results have been obtained for two types of high Mach number inlets, one with a translating centerbody and a fixed geometry inlet (collapsing cowl) with no centerbody. A study was made of the aerodynamic and acoustic performance of these inlets. The effects of area ratio, length/diameter ratio, and lip geometry were among several parameters investigated. The translating centerbody type inlet was found to be superior to the collapsing cowl both acoustically and aerodynamically, particularly for area ratios greater than 1.5. Comparison of length/diameter ratio and area ratio effects on performance near choked flow showed the latter to be more significant. Also, greater high frequency noise attenuation was achieved by increasing Mach number from low to high subsonic values.					
17. Key Words (Suggested by Author(s)) Acoustics, inlet, compressor, noise attenuation, aerodynamic performance, choked flow				18. Distribution Statement Unclassified - Unlimited Subject Category 71	
19. Security Classif. (of this report) Unclassified	20. Security Classif. (of this page) Unclassified	21. No. of Pages 106	22. Price* \$5.25		

CONTENTS

	<u>Page</u>
SUMMARY	iv
LIST OF ILLUSTRATIONS	v
1. INTRODUCTION	1
2. DESCRIPTION OF INLET CONFIGURATIONS	4
Table I	5
3. PROCEDURE FOR INLET DESIGN	6
4. TEST FACILITY, INSTRUMENTATION AND PROCEDURE	8
5. DISCUSSION OF RESULTS	11
6. COMPARISON OF RESULTS	14
7. EMPIRICAL EQUATIONS TO ESTIMATE NOISE ATTENUATION	17
8. CONCLUSION	20
9. REFERENCES	22
FIGURES	24
APPENDIX: REVIEW OF WORK ON SONIC AND NEAR-SONIC INLETS (TABLE A)	99

SUMMARY

A study was made of the parameters affecting the aerodynamic and acoustic performance of high Mach number inlets using the translating centerbody and fixed geometry configurations. The study included the effects of area ratio, length/diameter ratio, and lip geometry on the acoustic and aerodynamic performance when the rotor is at subsonic as well as supersonic tip speed.

The results support earlier findings by the authors that the translating centerbody type inlet is superior to the collapsing cowl, both acoustically and aerodynamically, especially at moderately high area ratios ($A_{\text{exit}}/A_{\text{throat}} > 1.5$). The length/diameter ratio does not seem to be as crucial to performance near choked flow as area ratio. Inlets operating at high Mach numbers are more effective in reducing high frequency noise. At choked flow, however, the low frequency noise is also effectively reduced.

This study also showed that the actual amount of noise reduction depends on the flow downstream of the throat (pressure recovery) in contradiction to inviscid theory. Choking does not guarantee a large amount of noise reduction if it is accompanied by high pressure loss. Thus, without boundary layer control, choked inlets are area ratio limited.

Using the present test results, an empirical formula was derived, relating the noise reduction to percent of maximum mass flow and pressure recovery. Results of previous studies, where noise attenuation was related to throat Mach number, are ambiguous and are difficult to assimilate for comparative purposes. The percent of maximum mass flow is a more satisfactory parameter, although accuracy in measurement is most vital.

Simulating forward speed by contouring the lips of the inlets was difficult, and the results were inconclusive. However, the lip design had a significant effect on the aerodynamic and acoustic performance of the inlets.

LIST OF ILLUSTRATIONS

<u>Figure</u>		<u>Page</u>
1	WALL AND CENTERLINE MACH NUMBERS FOR POTENTIAL FLOW IN TWO DIMENSIONS	24
2	INFLUENCE OF LENGTH/DIAMETER RATIO ON NOISE ATTENUATION (EJECTOR SOURCE)	25
3	SCHEMATIC AND AREA DISTRIBUTION OF TRANSLATING CENTER- BODY INLET CONFIGURATION 1	26
4	SCHEMATIC AND AREA DISTRIBUTION OF TRANSLATING CENTER- BODY INLET CONFIGURATION 2	27
5	SCHEMATIC AND AREA DISTRIBUTION OF TRANSLATING CENTER- BODY INLET CONFIGURATION 3	28
6	SCHEMATIC AND AREA DISTRIBUTION OF TRANSLATING CENTER- BODY INLET CONFIGURATION 4	29
7	SCHEMATIC AND AREA DISTRIBUTION OF FIXED GEOMETRY (COLLAPSING COWL) INLET CONFIGURATION 5	30
8	SCHEMATIC AND AREA DISTRIBUTION OF FIXED GEOMETRY (COLLAPSING COWL) INLET CONFIGURATION 6	31
9	SCHEMATIC AND AREA DISTRIBUTION OF FIXED GEOMETRY INLET CONFIGURATIONS 7,8,9	32
10	AERODYNAMIC AND ACOUSTIC PERFORMANCE OF INLET WITH DIFFERENT LENGTH/DIAMETER RATIOS	33
11	OPTIMUM L/D FOR A GIVEN AREA RATIO AT DIFFERENT THROAT MACH NUMBERS FOR CIRCULAR AND SQUARE DIFFUSERS	34
12	OPTIMUM L/D FOR A GIVEN AREA RATIO AT DIFFERENT THROAT MACH NUMBERS FOR ANNULAR DIFFUSERS	35
13	THEORETICAL POTENTIAL FLOW AND EXPERIMENTAL RESULTS FOR CONFIGURATION 1 WITH CENTERBODY AT 0 CM DISPLACEMENT	36
14	THEORETICAL POTENTIAL FLOW AND EXPERIMENTAL RESULTS FOR CONFIGURATION 1 WITH CENTERBODY AT 5.1 CM DISPLACEMENT	37

<u>Figure</u>		<u>Page</u>
15	THEORETICAL POTENTIAL FLOW AND EXPERIMENTAL RESULTS FOR CONFIGURATION 1 WITH CENTERBODY AT 12.7 CM DISPLACEMENT	38
16	THEORETICAL POTENTIAL FLOW AND EXPERIMENTAL RESULTS FOR CONFIGURATION 1 WITH CENTERBODY AT 17.8 CM DISPLACEMENT	39
17	THEORETICAL POTENTIAL FLOW AND EXPERIMENTAL RESULTS FOR CONFIGURATION 1 WITH CENTERBODY AT 20.3 CM DISPLACEMENT	40
18	NASA-LANGLEY RESEARCH CENTER ANECHOIC-CHAMBER TRANSONIC COMPRESSOR FACILITY	41
19	INSTRUMENTATION ROOM, ANECHOIC-CHAMBER TRANSONIC COMPRESSOR FACILITY, NASA-LANGLEY RESEARCH CENTER	42
20	SCHEMATIC OF INLET CONFIGURATIONS 2, 3 AND 4 WITH AERODYNAMIC INSTRUMENTATION	43
21	SCHEMATIC OF INLET CONFIGURATION 5 WITH AERODYNAMIC INSTRUMENTATION	44
22	ILLUSTRATION OF INLET AND COMPRESSOR OPERATING CONDITIONS FOR DATA ACQUISITION	45
23	NOISE ATTENUATION FOR INLET CONFIGURATION 1	46
24	MASS FLOW FOR INLET CONFIGURATION 1	47
25	AVERAGE MAXIMUM MACH NUMBER OF INLET CONFIGURATION 1	48
26	PRESSURE RECOVERY FOR INLET CONFIGURATION 1	49
27	PRESSURE DISTORTION FOR INLET CONFIGURATION 1	50
28	NOISE ATTENUATION FOR INLET CONFIGURATION 2	51
29	MASS FLOW FOR INLET CONFIGURATION 2	52
30	AVERAGE MAXIMUM MACH NUMBER OF INLET CONFIGURATION 2	53
31	PRESSURE RECOVERY FOR INLET CONFIGURATION 2	54
32	PRESSURE DISTORTION FOR INLET CONFIGURATION 2	55
33	NOISE ATTENUATION FOR INLET CONFIGURATION 3	56
34	MASS FLOW FOR INLET CONFIGURATION 3	57

<u>Figure</u>		<u>Page</u>
35	AVERAGE MAXIMUM MACH NUMBER FOR INLET CONFIGURATION 3	58
36	PRESSURE RECOVERY FOR INLET CONFIGURATION 3	59
37	PRESSURE DISTORTION FOR INLET CONFIGURATION 3	60
38	NOISE ATTENUATION FOR INLET CONFIGURATION 4	61
39	MASS FLOW FOR INLET CONFIGURATION 4	62
40	AVERAGE MAXIMUM MACH NUMBER FOR INLET CONFIGURATION 4	63
41	PRESSURE RECOVERY FOR INLET CONFIGURATION 4	64
42	PRESSURE DISTORTION FOR INLET CONFIGURATION 4	65
43	EFFECT OF PERCENTAGE OF MAXIMUM MASS FLOW ON NOISE ATTENUATION FOR INLET CONFIGURATION 2	66
44	EFFECT OF PERCENTAGE OF MAXIMUM MASS FLOW ON NOISE ATTENUATION FOR INLET CONFIGURATION 3	67
45	EFFECT OF PERCENTAGE OF MAXIMUM MASS FLOW ON NOISE ATTENUATION FOR INLET CONFIGURATION 4	68
46	NOISE ATTENUATION FOR INLET CONFIGURATIONS 5 AND 6	69
47	MASS FLOW FOR INLET CONFIGURATIONS 5 AND 6	70
48	PEAK WALL MACH NUMBER OF INLET CONFIGURATIONS 5 AND 6	71
49	PRESSURE RECOVERY FOR INLET CONFIGURATIONS 5 AND 6	72
50	PRESSURE DISTORTION FOR INLET CONFIGURATIONS 5 AND 6	73
51	EFFECT OF PERCENTAGE OF MAXIMUM MASS FLOW ON NOISE ATTENUATION FOR INLET CONFIGURATIONS 5 AND 6	74
52	MASS FLOW FOR INLET CONFIGURATIONS 7, 8 AND 9	75
53	PEAK WALL MACH NUMBER OF INLET CONFIGURATIONS 7, 8 AND 9	76
54	PRESSURE RECOVERY FOR INLET CONFIGURATIONS 7, 8 AND 9	77
55	PRESSURE DISTORTION FOR CONFIGURATIONS 7,8,9	78
56	COMPARISON OF OVERALL NOISE ATTENUATION CHARACTERISTICS OF INLETS OPERATING AT SUBSONIC MACH NUMBERS	79
57	COMPARISON OF BLADE PASSAGE FREQUENCY ATTENUATION CHARACTERISTICS OF INLETS OPERATING AT SUBSONIC MACH NUMBERS	80

<u>Figure</u>		<u>Page</u>
58	FREQUENCY SPECTRA FOR CONFIGURATION 2 AT 17,500 RPM	81
59	FREQUENCY SPECTRA FOR CONFIGURATION 2 AT 20,000 RPM	82
60	INFLUENCE OF LIP GEOMETRY ON NOISE ATTENUATION	83
61	INFLUENCE OF LIP GEOMETRY ON NOISE ATTENUATION AND PRESSURE RECOVERY	84
62	INFLUENCE OF LIP GEOMETRY ON NOISE ATTENUATION AND PRESSURE RECOVERY	85
63	INFLUENCE OF LIP GEOMETRY ON NOISE ATTENUATION AND PRESSURE RECOVERY	86
64	INFLUENCE OF LIP GEOMETRY ON NOISE ATTENUATION AND PRESSURE RECOVERY	87
65	INFLUENCE OF CENTERBODY ON NOISE LEVEL	88
66	POLAR GRAPHS SHOWING THE INFLUENCE OF LIP GEOMETRY OF INLETS OPERATING AT SUBSONIC MACH NUMBER	89
67	INFLUENCE OF COMPRESSOR PRESSURE RATIO ON NOISE	90
68	COMPARISON OF NOISE ATTENUATION CHARACTERISTICS OF INLETS OPERATING AT HIGH SUBSONIC MACH NUMBER WITH COMPRESSOR OPERATING AT SUPERSONIC ROTOR TIP SPEED	91
69	EFFECT OF AREA RATIO ON NOISE ATTENUATION AND PRESSURE RECOVERY	92
70	INFLUENCE OF PRESSURE RECOVERY ON THE EXPONENTIAL PARAMETER α	93
71	COMPARISON BETWEEN EMPIRICAL EQUATIONS AND EJECTOR TEST DATA	94
72	COMPARISON BETWEEN EMPIRICAL EQUATIONS AND COMPRESSOR TEST DATA	95
73	PRESSURE RECOVERY FOR DIFFUSERS WITH DIFFERENT AREA RATIOS	96
74	COMPARISON OF EMPIRICAL EQUATIONS WITH EXPERIMENTAL RESULTS	97

1. INTRODUCTION

Feasibility demonstrations of sonic and near-sonic inlets are numerous. Table A in the Appendix gives a brief summary of tests that have been conducted during the past few years. A large number of these were conducted by aircraft and engine manufacturers with applications directed toward specific engines. Despite this continual effort, and although most demonstration-of-concept studies yield impressive amounts of noise attenuation, this method of noise reduction has not achieved the status of acceptability as other methods of noise reduction (i.e. acoustic liners).

Presently, results from laboratory or full scale (static) demonstrations have not yet been transferred to practical applications on aircraft. A detailed understanding of the interaction of the acoustic and aerodynamic fields is hampered by the fact that the flow is near-sonic at the throat, making both analytical description and careful experimental measurements difficult due to the dominance of non-linear effects. However, from a compilation of the available data, some general trends can be discerned which can be used to indicate certain design limits or show if some form of boundary layer control is required.

The purpose of this research project was to develop some fundamental aerodynamic and acoustic information on the sonic and near-sonic inlets. Specifically, this research program attempts to provide aerodynamic and acoustic data of a sufficiently general nature in order to keep open the options of various configurations in choked inlet design. The experimental research results reported here are complemented by a continuing theoretical study. The emphasis in the experimental study was on the translating center-body type inlet, although comparisons are made with fixed geometry

(collapsing cowl) inlets. With the exception of one test on a Viper-8 jet engine in 1966 (Cawthorn et al., see Appendix A), there have been no other tests on translating centerbody type inlets outside those conducted by one of the authors (Lumsdaine, see Appendix A). Besides type comparison, the study involved an investigation of such parameters as area ratio, length/diameter ratio, and lip effects to determine their influence on the acoustic and aerodynamic performance.

For purpose of definition, sonic inlets are those where the flow is accelerated until a sonic surface exists near the throat of the inlet and the inlet is aerodynamically choked (or nearly so) with a corresponding large noise reduction. These inlets are known to be very effective acoustically since the only noise that can propagate upstream in this case is the noise escaping through the boundary layer. The problems associated with the sonic inlet are primarily aerodynamic, that is, how to achieve a sonic surface with the shortest inlet, with low distortion, negligible instability, and minimum pressure loss.

In the near-sonic (or accelerating) inlet the flow near the throat is at a velocity which results in noise reduction but has not yet reached the aerodynamic choking point. For one-dimensional flow, such a differentiation would not be necessary since the two types of inlets need only be divided by an arbitrary throat Mach number (say 0.8). This oversimplification, however, can cause problems when data from different tests are compared, because for inlets of practical length and for near-sonic velocities, the flow deviates greatly from the one-dimensional potential flow approximation. As can be seen in Figure 1* (from Reference 1), the centerline throat Mach number is a very inadequate parameter, since it remains nearly constant for the three very different flow conditions (a,b,c) with differing amounts of mass flow. This can also lead to the mistaken notion that near sonic inlets are effective, when the throat centerline Mach number indicates subsonic flow even though supersonic conditions exist downstream of the throat.

*The figures are given at the end of each chapter.

Another point concerns the noise attenuation characteristics. In Reference 2, tests were conducted using an ejector with inlets of different length/diameter ratio but with the same area ratio and noise source. The attenuations obtained have different values for the same maximum average axial Mach number. (In this report, the average throat Mach number refers to the Mach number at the geometric throat. The maximum average axial Mach number refers to the maximum average Mach number inside the channel taken normal to the flow direction.) It was noted in these tests (see Figure 2) that the shorter diffusers tend to be more effective in terms of noise reduction at subsonic speeds, whereas the longer diffusers produce little or no noise reduction until the flow is close to being aerodynamically choked. The reason for this can be attributed either to a supersonic pocket near the throat for the shorter diffusers (due to the smaller radius of curvature at the throat) which is effective in reducing some of the noise propagated, or to the larger axial pressure gradient for the same overall pressure difference. In any case, Figure 2 points out the inadequacy of plotting noise reduction versus a single parameter (in this case the maximum axial Mach number) since extrapolation or comparison of data will not be reliable because conditions downstream of the throat have an influence on the noise attenuation. The percentage of maximum mass flow is a better parameter for plotting noise reduction. However, it is very sensitive near choke flow; a change of about 4 percent in mass flow changes the Mach number from 0.8 to 1.0.

2. DESCRIPTION OF INLET CONFIGURATIONS

Table I gives a summary of the inlets tested. Figures 3 to 9 show the schematic of these inlets including the area distributions at the centerbody positions tested. Besides the two basic configurations (fixed and variable geometry) the inlets can be classified in the following way for test identification: 1. Sonic inlet for subsonic and supersonic rotor tip speed, 2. Accelerating (near-sonic) inlet for subsonic tip speed, and 3. Accelerating inlet for supersonic tip speed. The rotor achieved supersonic tip speeds at approximately 22,000 rpm. However, far field data did not show the propagation of multiple pure tones until fan speed was in excess of 23,500 rpm.

In order to obtain the flexibility required to determine the different effects desired in this study, the translating centerbody type inlet was used. This type of inlet was also found to be more satisfactory in earlier concept evaluation studies (as compared to the collapsing cowl, for example). The present tests also confirm the translating centerbody type to be more superior in regard to pressure loss, noise attenuation and flow stability.

Configuration 1 was used to determine the effect of sonic and near sonic flow on noise for both subsonic and supersonic tip speeds. Configurations 2 to 4 were first used to determine area ratio effects on performance for sonic inlets with subsonic tip speeds and later to determine lip effects for supersonic tip speeds. Configurations 5 and 6 were fixed geometry type inlets mainly used for comparison purposes (aerodynamic and acoustic). The fixed positions which were tested simulate the collapsing cowl type inlet. Configurations 7 to 9 were low area ratio inlets for the primary purpose of testing the influence of high subsonic Mach number on supersonic tip speed rotor noise. The three basic types of lips tested were the short bellmouth, the simulated landing (equal to 0.2 Mach number forward speed) and the takeoff lip. The diffuser sections for Configurations 2 to 4 and 7 to 9 were nearly identical.

TABLE I - LIST OF INLET CONFIGURATIONS TESTED

CONF. NO.	INLET TYPE	TYPE OF LIP	MAX. TIP SPEED (MAX. RPM)	LENGTH/ DIAMETER	C.B. POS. (CM)	AREA RATIO	REMARKS	DESIGNED MAX.MASS FLOW (KG/SEC)
1	translating centerbody	flight lip	supersonic (25,000)	1.90	0.0	-	sonic (and near-sonic) inlet	19.0
					5.1	-		-
					12.7	2.35		12.0
					17.8	2.90		9.75
					20.3	3.20		8.6
					25.4	3.50		7.9
2	translating centerbody	short bellmouth	subsonic (21,000)	1.68	0.0	1.40	sonic (and near-sonic) inlet	10.0
					3.8	1.80		8.6
					7.6	2.20		7.5
					11.4	2.60		6.35
3	translating centerbody	simulated landing	subsonic (21,000)	1.68	0.0	1.40	sonic (and near-sonic) inlet	10.0
					3.8	1.80		8.6
					7.6	2.20		7.5
					11.4	2.60		6.35
4	translating centerbody	flight lip	subsonic (21,000)	1.68	0.0	1.40	sonic (and near-sonic) inlet	10.0
					3.8	1.80		8.6
					7.6	2.20		7.5
					11.4	2.60		6.35
5	fixed geometry	simulated landing	subsonic (20,000)	1.54	-	2.60	sonic (and near-sonic) inlet	6.35
6	fixed geometry	simulated landing	subsonic (20,000)	1.54	-	2.30	sonic (and near-sonic) inlet	7.5
7	fixed geometry	short bellmouth	supersonic (25,000)	1.68	-	1.20	near sonic inlet	15.2
8	fixed geometry	simulated landing	supersonic (25,000)	1.68	-	1.20	near sonic inlet	15.2
9	fixed geometry	flight lip	supersonic (25,000)	1.68	-	1.20	near sonic inlet	15.2

3. PROCEDURE FOR INLET DESIGN

Two types of inlets were designed for these tests: 1) with a translating centerbody and 2) without centerbody. The translating centerbody type inlets were designed to produce a high pressure gradient near the throat; the inlets without centerbody were designed with a more gradual pressure gradient for the same overall area ratio. The sharp pressure gradient was placed near the throat (where for transonic flow the streamlines are very stiff) because earlier tests conducted under this program showed that for a given overall pressure ratio, sound attenuation at near sonic conditions was more effective when the pressure gradient was high. This is also evident from Figure 2. Recent tests by General Electric³ confirmed this effect. Because a high constant Mach number section (constant area) is also effective in reducing the noise, particularly for supersonic tip speeds, a rapid diffusion near the throat was followed by a constant area section in the design.

The length/diameter ratio for the area ratios of the preliminary design was selected based on some earlier work which found that an optimum length/diameter ratio existed for a given area ratio. Figure 10 shows the results of some earlier tests conducted under this program using six annular-type inlets of different diffuser lengths but with the same area ratio of 3.2. Although parameters such as throat blockage due to boundary layer development and increasing Mach number have a considerable effect on decreasing the pressure recovery, this does not seem to have a significant influence on the optimum point. Also, a literature search uncovered a large number of tests with circular and square diffusers; some of the important results are compiled in Figure 11 which shows the approximate relationship between area ratio and optimum length/diameter ratio. For the case of annular diffusers the number of tests that could be used for such a graph were not as numerous;

they are brought together in Figure 12. The term "flow diameter" for an annular diffuser indicates the inner diameter minus the centerbody diameter at the exit. From these graphs it can be seen that the centerbody type inlet requires a shorter length for the same area ratio than an inlet without centerbody.

From an initial estimate of the length/diameter ratio for a given area ratio requirement, the inlet was designed based on a smooth area progression for both the choked and unchoked positions. After the contour was laid out, a transonic potential flow program⁴ was used to calculate the flow field. The results were then substituted into a boundary layer program to determine corrections for the contour. In almost all these calculations, some flow separation was predicted by the boundary layer analysis because of the wide range of operating conditions occurring in the inlet and in order to keep the inlet within reasonable length for a given area ratio. Figures 13 to 17 give the streamlines and Mach number distribution along the wall and centerbody for Configuration 1 (takeoff configuration or flight lip) for five of the centerbody positions tested. These results were used in the boundary layer program to determine boundary layer growth. Because of the high adverse pressure gradient when the centerbody is translated to 12.7 cm and beyond, some flow separation had been predicted from boundary layer calculations. However, for this particular configuration, the actual separation was more severe as indicated by the experimental surface pressure distribution and the total pressure probes at the exit. The experimental surface Mach numbers are also indicated on these figures.

Three types of lips were designed: the flight lip, the contoured lip simulating the streamline at 0.2 freestream Mach number, and a short bellmouth. Furthermore, the fixed geometry inlets were designed with a straight wall since contouring the wall does not have a significant influence on the aerodynamic performance. These inlets were designed with a slightly shorter length than the optimum (if Figure 11 is followed) for the purpose of maintaining the same area ratio and approximately the same length/diameter ratio as the translating centerbody type inlets (see Table I) in order to compare the effectiveness of the two types of inlets.

4. TEST FACILITY, INSTRUMENTATION AND PROCEDURE

The inlets were tested in the anechoic-chamber transonic compressor facility of the NASA-Langley Research Center. The test vehicle was a 30.5 cm-tip diameter single-stage transonic compressor with 19 rotor blades. Figure 18 shows the anechoic chamber facility with one of the choked inlets in place. The far field noise measurements were made with a movable boom microphone (foreground) at 4.57 m from the inlet.

Figure 19 shows the instrumentation room where the speed of the compressor, the position of the translating centerbody, and the boom microphone position were controlled. In addition, aerodynamic output was recorded on punch cards from the scanivalves, and acoustic output was recorded on magnetic tape. On-line far field noise data were taken with a 1/3-octave real-time analyzer at two locations by an independent system for comparison and quick-look monitoring. The following aerodynamic instrumentation was used:

1. Four static pressure taps were located circumferentially upstream of the cowl highlight.
2. Sixty static pressure taps located axially in two circumferential stations (12 on one and 48 on the other) were used for Configuration 1; 45 were used for each of the other configurations. In addition, there were 12 static pressure taps on each centerbody.
3. One kiel head total pressure traverse probe and two 20-element total pressure rakes were located at the exit plane of the inlet.
4. One fixed kiel head probe read pressure and temperature at the exit plane.
5. Centerbody translation was controlled by a hydraulic cylinder. The centerbody position was indicated by a voltmeter at the control panel.

A schematic of some of the aerodynamic instrumentation and their approximate location is shown on Figure 20 for a translating centerbody type inlet and on Figure 21 for a fixed geometry type inlet.

The acoustic instrumentation consisted of

1. A traveling boom 0.635-cm condenser microphone located 4.57 m from the inlet plane and reading at 15-degree increments,
2. 0.635-cm condenser microphones also located at 4.57 m for on-line data acquisition,
3. an acoustic traversing probe placed at the exit plane of the inlet, and
4. four flush-mounted 0.635 cm microphones (or six depending on the inlet) located on the cowl as shown on Figures 3 to 9.

All microphones were calibrated before and after each test. The boom microphone measured the far field noise at 15-degree intervals from 0-degrees to 90 degrees. Two far field microphones at 0-degrees and 15-degrees recorded the far field data continuously and were monitored on a 1/3-octave real-time analyzer. This analyzer was also used to monitor choking speed and to regulate the operating points for the compressor. Acoustic traverses were made only near the choke point and traverse data were recorded for a minimum of 10 seconds (for stabilization) at each point. Steady acoustic data (on walls, far field, etc.) were recorded for a minimum of one minute at each data point. Only one traverse probe was operated at a given time. The acoustic traverse was immersed at five radial positions for data acquisition.

Aerodynamic inlet performance data were recorded on punch cards, with each parameter sampled several times per data point. The total pressure kiel probe data was recorded on an X-Y plotter. Data were recorded at fixed immersion points and continuously during the traverse; each fixed immersion was sampled for 10 seconds.

Typically, the test operation for a translating centerbody inlet followed this sequence: With the centerbody completely retracted, the compressor rotor

was gradually accelerated to some prescribed maximum rpm and stabilized; acoustic and aerodynamic data were recorded at prescribed intervals during this acceleration, and the centerbody was then translated to the next test position.

The on-line 1/3-octave real-time analyzer monitored the sound levels until the choking (acoustic) rpm point was reached. Data were recorded for several rpm and centerbody positions. The back pressure ratio was adjusted to near maximum (blade stall) and also to minimum (valve wide open) with one intermediate point to give different blade loading for the same rpm. A typical set of data points for a given centerbody position is shown in Figure 22 for inlet Configuration 1. Other inlets were run with the back pressure valve wide open only.

5. DISCUSSION OF RESULTS

Noise attenuation for inlets under near-sonic conditions seems to depend on the source (tip speed, peak frequency) as well as on the flow conditions (axial velocity gradient, radial gradient, peak Mach number); thus the choice of parameters to represent the acoustic and aerodynamic conditions should be made very carefully. Figures 23 to 27 give the five parameters which largely define the performance of inlet Configuration 1: a) noise attenuation, b) mass flow, c) average maximum Mach number (cowl and centerbody), d) pressure recovery, and e) pressure distortion. The detailed Mach number distributions along the cowl and centerbody for each one of these data points are given in a separate volume (presently being compiled). The constant noise attenuation lines on the mass flow versus rpm graphs (i.e. Figure 24) are interpolations.

For this inlet only, the noise attenuation values were taken with respect to the fully retracted position. For all other configurations, the values were taken with respect to a baseline, normally without the centerbody. It is typical of high area ratio short inlets that the noise attenuation is very gradual, that is, the noise does not drop rapidly as the choke point is approached. This was also evident in past tests using an ejector. In Figure 2 (for the same area ratio but different lengths), the noise reduction as a function of rpm is gradual for the shorter inlet but increases sharply for the long inlet. The distortion level for this high area ratio short inlet is very low, due to a long constant area section downstream of the throat.

Figures 28 to 42 are performance results for inlet Configurations 2 to 4. These configurations differ only in the shape of the lip; the centerbody and the diffusers are the same. For these inlets with relatively low area ratios, noise attenuation is quite sudden and occurs within 5 to 10 percent of maximum mass flow as can be seen from Figures 43 to 45 where the far

field noise is plotted as a function of mass flow. The noise reduction occurs for all three configurations in the interval of 90 to 100 percent of mass flow. It should be noted that the major noise drop is within a narrow (5 percent) range of mass flow. On a one-dimensional basis, this means a move from very little noise reduction to almost full choke for a 5 percent change in area. Near Mach one, a 5 percent change in area causes the average Mach number to change from 0.75 to 1.0. Also, when the centerbody was translated, there was an increase in the noise level from the compressor. This can be readily seen in Figures 28, 33, and 38.

As a result of mechanical problems in the design, a slightly higher pressure loss than expected was encountered with the translating type inlet because there was a discontinuity between the cylinder and centerbody (which slid over the cylinder). Also, there was a groove which was exposed when the centerbody was translated forward. This groove was necessary in order to keep the centerbody from rotating, but when a configuration was tested with the centerbody, the presence of the groove may have contributed to the increased far field noise. The noise level rose as the centerbody was translated further, exposing a larger segment of the groove (i.e. see Figure 45). Also, with the centerbody translated, the higher pressure gradient caused some flow separation which contributed to the increased noise level.

Figures 46 to 50 show the performance results for two fixed-geometry type inlets (simulating a collapsing cowl type inlet) without centerbody. Although the area ratios are not very high (see Table I), both inlets performed very poorly. The flow was so unstable and the monitor for the far field noise showed such large variations that the average noise reduction shown on Figure 46 is very approximate. It appeared that even under choke conditions the amount of noise reduction was very small. The test was discontinued at around 17,000 rpm because of severe pressure and acoustic fluctuations for inlet Configuration 5, and at 19,000 rpm for Configuration 6. The high distortion can be seen on Figure 50. Note that the Mach number plot (Figure 48) is represented by the wall Mach number and not the average Mach number as in the previous graphs. The average values would be

lower than the peak wall Mach number. Figure 51 is a graph of noise reduction as a function of mass flow for Configurations 5 and 6. These poor results were quite unexpected, since the same guidelines were followed in the design of Configurations 5 and 6 as for the other inlets.

Configurations 7 to 9 were run to obtain baseline data for Configurations 2 to 4 as well as data for noise reduction at high throat Mach numbers when the fan is at supersonic tip speeds. They were also used to determine the lip effect. Figures 52 to 55 show the basic flow characteristics of Configurations 7 to 9. Note that here, too, the Mach number plot is represented by the wall Mach number and not the average Mach number. Figure 56 shows the far field acoustic characteristics for these three inlets (with Configuration 1 at 0 cm centerbody displacement given for comparison). For lower rpm (lower Mach number) the inlet with the centerbody appears to give a few decibels more attenuation than the same inlet without centerbody. This is only true when comparisons are made with the centerbody retracted. Although Configuration 9 (flight lip) has a consistently higher noise level at lower rpm this is decreasing more rapidly at higher rpm. This is more evident from the results of blade passage frequency shown in Figure 57. Thus the high velocity around the lip seems to influence the attenuation.

Figure 58 shows the frequency spectrum for inlet Configuration 2 at approximately 17,500 rpm (an exact rpm is difficult to maintain) and different centerbody positions. It can be seen that the amount of noise reduction at the blade passage frequency is much higher than the overall noise reduction and that the higher frequencies are attenuated much more than the lower frequencies for high Mach numbers. At fully choked conditions, however, the amount of noise reduction of the different frequencies is more uniform, as seen in Figure 59.

6. COMPARISON OF RESULTS

Configuration 1 was used to test choking at very high area ratios (maximum of 3.5) while maintaining a reasonable length/diameter ratio of 1.9. The remaining configurations were shorter with lower area ratios. These configurations showed some flow separation when the centerbody was near maximum translation. The computer program required the introduction of a forward speed (free stream Mach number = 0.1) which is acceptable during flight but does not represent the static test conditions accurately. The acceleration around the lip in Configuration 1 during static tests caused some separation and is partially responsible for the low pressure recovery.

In comparing Configurations 2 to 4 to determine the influence of the lip, Figure 60 shows the difference in noise reduction for the three lips with the centerbody retracted. It is seen that at lower rpm there is some noise reduction for the flight lip but not for the contoured lips. The acceleration around the lip causes a high-velocity pocket around the lip which improves the acoustic performance, but decreases pressure recovery.

Figures 61 to 64 show the influence of the lip on noise attenuation and pressure recovery at different positions of the centerbody. The short bell-mouth appears to have better noise reduction characteristics than the flight lip. Contouring the lip slightly (to simulate approach streamline patterns) does not seem to improve the noise reduction characteristics. In fact, at some higher mass flow rates, the flight lip appears to have a higher noise reduction for the same pressure loss compared to the simulated landing lip. For small area ratios, the pressure recovery is high enough so that changes in the lip do not have a large effect on the pressure recovery. The difference in pressure recovery seems to increase for increasing area ratios until a fairly large area ratio is reached. With forward speed, the flow will more

closely approximate the short bellmouth, and thus the noise reduction and pressure recovery should improve over static conditions. Tests in Reference 5 showed that during choke and with 100 feet/sec upstream blowing the pressure recovery increased only slightly. However, the area ratio for these inlets was large; thus it appears for high area ratio, forward speed may not increase the pressure recovery and noise attenuation but should do so for low area ratio. This is also consistent with the results of Figures 61 to 64. When Figures 61, 62 and 63 are compared with Figure 64 (large area ratio), it is seen that there is very little difference between the simulated landing lip and the short bellmouth.

Figure 65 compares the lip effect with and without centerbody for two configurations (short bellmouth and flight lip). Considering the case without centerbody, it is quite clear that noise reduction is more gradual for the case of the flight lip (Configuration 4) than for the short bellmouth. The noise reduction for the short bellmouth occurs quite suddenly and over a very small span of increasing rpm. This also points out the difficulty of simulating forward speed using static tests. Figure 66 is a polar plot of the far field noise at 15-degree intervals for the fixed geometry inlets (Configurations 7, 8 and 9). The difference in the lip shape causes a slight dip at an angle of 15 degrees for the case of the contoured lip; for the flight lip, the distribution is quite uniform.

Figure 67 shows the influence of a change in compressor pressure ratio on noise. Variation in the back pressure of the compressor does not seem to change the noise in the far field, except when the back pressure is high enough to cause the inlet to go from choke point to unchoke; however, the mass flow also drops. As seen from this figure, there is very little change in the far field noise as a result of changing the compressor back pressure for the same mass flow. The data points were slightly scattered; thus the straight lines are only approximate. The influence of compressor blade loading on far field noise with the inlet at high Mach numbers is an important problem, and further tests are necessary to gain more precise and useful information in this area.

Figure 68 is a comparison of the results of the present tests with data published in Reference 3 using the same compressor running at supersonic relative Mach numbers at the tip. It was found that the amount of noise reduction was much less than that predicted by the methods of either Fisher⁶ or Matthews⁷.

The crucial aerodynamic parameters for any inlet to be used on an aircraft engine are pressure recovery and distortion, and low pressure recovery is usually coupled with high distortion. The controlling geometric parameters are length/diameter ratio and area ratio. The area ratio required is dictated by a given application, and the optimum length/diameter ratio is selected from which the best design contour is made. It appears that large area ratio choked inlets would be difficult to design with realistic lengths. For example, without modification to the JT3D engine, if it were necessary to design the inlet to choke (or nearly choke) during approach for a Boeing 707 with normal load and full flaps, an area ratio of higher than three would be required. But for a STOL aircraft with blown flaps, the required area ratio would be less than two. The influence of area ratio on aerodynamic and acoustic performance thus was one of the parameters studied, and Figure 69 gives a comparison of inlets with different area ratios and length/diameter ratios. It appears here that the length/diameter ratio is not as crucial as the area ratio. For large area ratios, the choked inlet seems to produce high losses and distortion even with a centerbody-type inlet. For the centerbody-type inlet with low area ratios ($A_{\text{exit}}/A_{\text{throat}}$ less than 2), the choked inlet operates with acceptable pressure recovery and distortion and from all indications appears to provide stable flow.

7. EMPIRICAL EQUATIONS TO ESTIMATE NOISE ATTENUATION

Assuming the forward and rearward noise distribution from the fan to be equal and assuming that the mean flow velocity is one-dimensional and constant, the sound propagation from a cylindrical element dA is, in the forward direction,

$$dW_f = (1 - M) \frac{dW}{2} = (1 - M) \frac{I}{2} r d\theta dr \quad (1)$$

and rearward

$$dW_r = (1 + M) \frac{dW}{2} = (1 + M) \frac{I}{2} r d\theta dr \quad (2)$$

where I is the sound intensity, M the Mach number, r the radial position, W_f, W_r the total forward and rearward propagating sound power, and θ the angular position.

When Equations (1) and (2) are integrated over a circular plane, the following correction factors are obtained:

$$C_f = \frac{1}{1 - M}, \quad C_r = \frac{1}{1 + M}$$

Thus the noise reduction in the forward direction due to the opposing flow is

$$\Delta dB = -10 \log C_f = -10 \log \left[\frac{1}{1 - M} \right] \quad (3)$$

This empirical formula has been used to estimate noise reduction in high speed flow^{8,9,10}. A modification of this formula (again using the mean throat Mach number as the variable) was suggested in Reference 8. The

problem with using these formulas is the lack of a proper definition for the Mach number of an actual inlet and is quite evident from Figure 1.

It is more realistic to describe noise reduction with an empirical formula based on percent of maximum mass flow. One such formula was recently given in Reference 11: for one-dimensional isentropic flow of air, the relationship between Mach number and percent mass flow is

$$\dot{m}/\dot{m}_{\max} = 1.73M(1+0.2M^2)^{-3} \quad (4)$$

Equation (3) can be rewritten in the form

$$\Delta \text{dB} = -10 \log \left[\frac{1}{1 - f(\dot{m}/\dot{m}_{\max})} \right] \quad (5)$$

To determine $f(\dot{m}/\dot{m}_{\max})$ from experimental data, it was found that a function such as $(\dot{m}/\dot{m}_{\max})^{1/\alpha}$, where $0 < \alpha \leq 1$, appears to best fit the experimental data. The constant α appears to depend on the pressure recovery near choke point. Figure 70 shows the value of α as a function of pressure recovery. The probable cause of the relationship between α and pressure recovery is that for inlets with relatively low pressure recovery, there exists a rather thick boundary layer where the noise can escape. This is the reason why there exists a large variation in the reported results of the effectiveness of choked inlets (from a few decibels as given by Cawthorn et al to over 40 dB in some references such as 5,8,14). Inlets with high losses will not produce large noise reductions even though the flow is choked. However, high loss inlets normally produce larger noise reduction than inlets with low loss at subsonic Mach numbers, possibly because of the large gradients existing in these inlets. This phenomenon is now the subject of further investigation.

Figures 71 and 72 are comparisons of Equation (5) with experimental data reported in References 14 and 15. Reference 14 used the ejector as a source, and Reference 16 used a 12-inch compressor. Also plotted for comparison is

Equation (3). It is not necessary to compare Equation (5) with the present results since the curve for α versus pressure recovery was derived by using the present experimental data; obviously the empirical formula agrees very well with the experimental results.

However, in order to gain some confidence in the method, the pressure recovery for two types of diffusers was calculated for different area ratios and at two mass flow ratios of interest. The results are shown on Figure 73. The lower curves are for large area ratio diffusers, and the upper curves are for straight wall diffusers with near-optimum length/diameter ratios. In each case, the initial boundary layer thickness was considered small. These curves, together with Equation (5), can be used effectively to estimate the amount of noise reduction for a given inlet. Consider the case of three inlets with an area ratio of 2.2. Using the upper set of curves, several pressure recoveries can be determined for mass flow ratios between 94 percent and 100 percent. Each point then determines a value of α and consequently the noise reduction. The approximate curve is shown on Figure 74; it appears to estimate the noise reduction quite well when compared with experimental results.

For the case of blade passage frequency tones, Equation (5) should be modified to

$$\Delta dB = -10 \beta \log \left[\frac{1}{1 - (\dot{m}/\dot{m}_{\max})^{1/\alpha}} \right] \quad (6)$$

Present tests and those reported in Reference 8 indicate that β increases with increasing frequency. Further work is presently being planned to determine the influence of high speed flow on the attenuation of various frequencies.

8. CONCLUSION

Some general qualitative remarks concerning high Mach number inlets appear appropriate following the detailed examination of data from these tests as well as from other sources (listed in Table A of the Appendix). Whether a choked inlet can actually be used depends to a large extent on the maximum area ratio required for a particular application. As shown in Figure 10, increasing the length of the inlet for a given area ratio does not necessarily increase the pressure recovery near transonic flow, or assuming that a very long inlet is practical for a given application requiring a large area ratio for choked flow does not assure a high pressure recovery. Thus without boundary layer control, choked inlets are area-ratio limited. It appears that for low area ratios, high Mach number inlets can be used to reduce noise with sufficiently high pressure recovery and acceptable distortion if the favorable effects of forward speed are added which tend to reduce the distortion and increase the pressure recovery¹.

Boundary layer control can always be used to increase recovery and reduce distortion. For inlets with high area ratios this may be necessary. Vortex generators are only nominally effective when properly placed and when the degree of separation is small. Injection can be effective and is easily added because of the high pressure source available on the aircraft¹². Suction is an alternative since the high pressure source can be used to drive an ejector.

For low area ratios (less than 1.5) fixed geometry inlets without centerbody appear feasible. This type of inlet, however, will require a change in the engine operating cycle to maintain high mass flow during landing. This can possibly be done by using a variable geometry exit nozzle which can also be used to maintain choked flow during landing.

¹ Private communication from B. Miller, Lewis Research Center.

For higher area ratios, the centerbody type inlet appears superior when compared to the collapsing cowl type for the same area ratio and length/diameter ratio. The inlets without centerbodies have performed poorly both acoustically and aerodynamically when compared to the centerbody type. The translating centerbody can also be modulated to maintain choked flow during landing¹³. For hybrid inlets the centerbody type inlet provides an additional advantage because of the curvature. For these high Mach number inlets with liners, the centerbody type provides a reduced channel height and additional surface for treatment; both of these are favorable factors in noise control, improving the effectiveness of acoustic liners.

At high Mach numbers, noise reduction appears to be frequency-dependent. The relationship between the amount of attenuation, frequency, and flow conditions is being further investigated. The present trend suggests that high Mach numbers are more effective in reducing high-frequency noise. Most of the noise reduction from high Mach number inlets takes place at a value of \dot{m}/\dot{m}_{\max} between 90 and 100 percent. On a one-dimensional basis, this means a throat Mach number variation of 0.68 to 1.0. Despite the problem of accuracy, the measured percent mass flow plotted against attenuation is a better parameter for comparison between inlets than the throat Mach number. Thus the equation relating noise reduction to Mach number

$$\Delta dB = -10 \log(1 / 1-M)$$

should be rewritten in the form

$$\Delta dB = -10 \log \left[\frac{1}{1 - (\dot{m}/\dot{m}_{\max})^{1/\alpha}} \right]$$

where $0 < \alpha \leq 1$ and α depends on the pressure recovery.

The amount of noise reduction depends on the flow downstream of the throat. Thus inlets with high losses will not produce large noise attenuation even when aerodynamically choked.

9. REFERENCES

- 1 H.W. Emmons, "The Theoretical Flow of a Frictionless, Adiabatic, Perfect Gas Inside a Two-Dimensional Hyperbolic Nozzle," NACA TN 1003, 1944.
- 2 E. Lumsdaine and L.R. Clark, "Noise Suppression with Sonic and Near-Sonic Inlets," Proceedings of the Second Interagency Symposium on University Research on Transportation Noise, North Carolina State University, June 5-7, 1974, pp. 432-447.
- 3 J.M. Wilson and C.T. Savell, "Inlet Flowpath Design to Attenuate Supersonic Rotor Noise," General Electric Report No. R73-AEG-412.
- 4 Transonic Computer Program - NASA Langley, Hampton, Virginia (used with permission of E.M. Boxer).
- 5 E. Lumsdaine, "Results of the Development of a Choked Inlet," Inter-Noise Proceedings, 1972, pp. 501-506.
- 6 C.L. Morfey and M.J. Fisher, "Shock-Wave Radiation from a Supersonic Duct Rotor," Journal of the Royal Aeronautical Society, Vol. 74, July 1970, p. 579.
- 7 D.C. Matthews and R.T. Nagel, "Inlet Geometry and Axial Mach Number Effects on Fan Noise Propagation," AIAA Paper No. 73-1022, AIAA Aero-Acoustics Conference, Seattle, Washington, October 1973.
- 8 Y. Tuan, "A Survey of Sonic Inlet Concepts for Inlet Noise Reduction," Boeing Document D6-40573, May 1972.

- 9 Anon., Project Status Report PE-8217-R6, Airesearch Manufacturing Company of Arizona, Garrett Corporation, November 1971.
- 10 M.J.T. Smith and M.E. House, "Internally Generated Noise from Gas Turbine Engines - Measurements and Predictions," ASME Paper No. 66-GT/N-43, March 1966.
- 11 E. Lumsdaine, "Fan Noise Reduction at Subsonic and Supersonic Tip Speeds with High Mach Number Inlets," Inter-Noise Proceedings, Sendai, Japan, 1975.
- 12 E. Lumsdaine and A. Fathy, "Theoretical Study of Boundary Layer Control by Blowing for Axisymmetric Flow and Its Application to the Sonic Inlet," Engineering Experiment Station Bulletin 16, South Dakota State University, October 1970.
- 13 J. Jibben and E. Lumsdaine, "An Automatic Control System for Sonic Inlets," to be presented at the ASME Automatic Controls Conference, Houston, Texas, December 1975.
- 14 David Chestnutt and Lorenzo R. Clark, "Noise Reduction by Means of Variable-Geometry Inlet Guide Vanes in a Cascade Apparatus," NASA TM X-2392, October 1971.
- 15 F. Klujber, K.C. Bosch, R.W. Demetrick, W.R. Robb, "Investigation of Noise Suppression by Sonic Inlets for Turbofan Engines - Final Report, Volumes I and II," Boeing Document D6-40855, NASA CR-121126, CR-121127, July 1973.

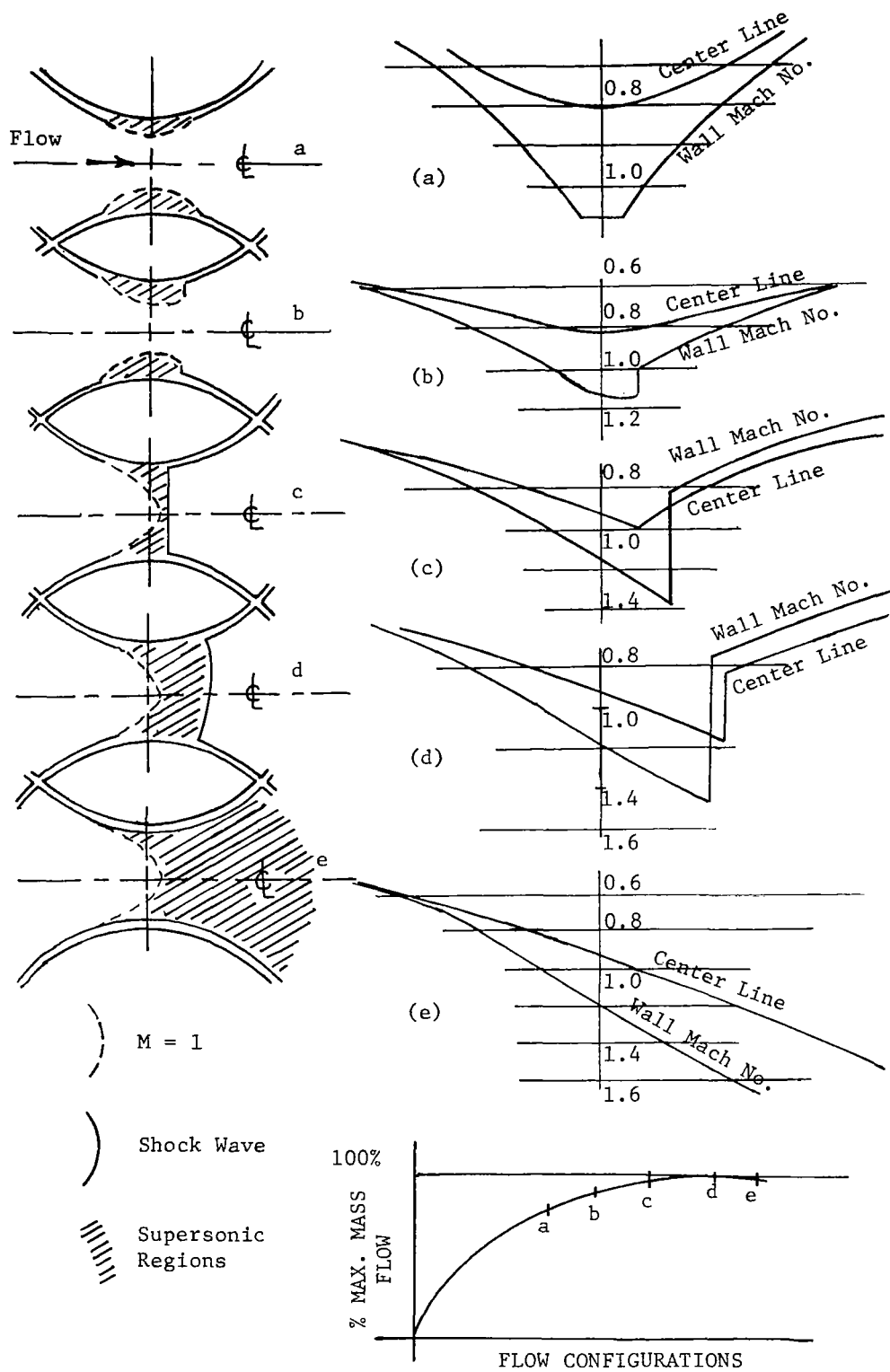


FIG. 1 WALL AND CENTERLINE MACH NUMBERS FOR POTENTIAL FLOW IN TWO DIMENSIONS

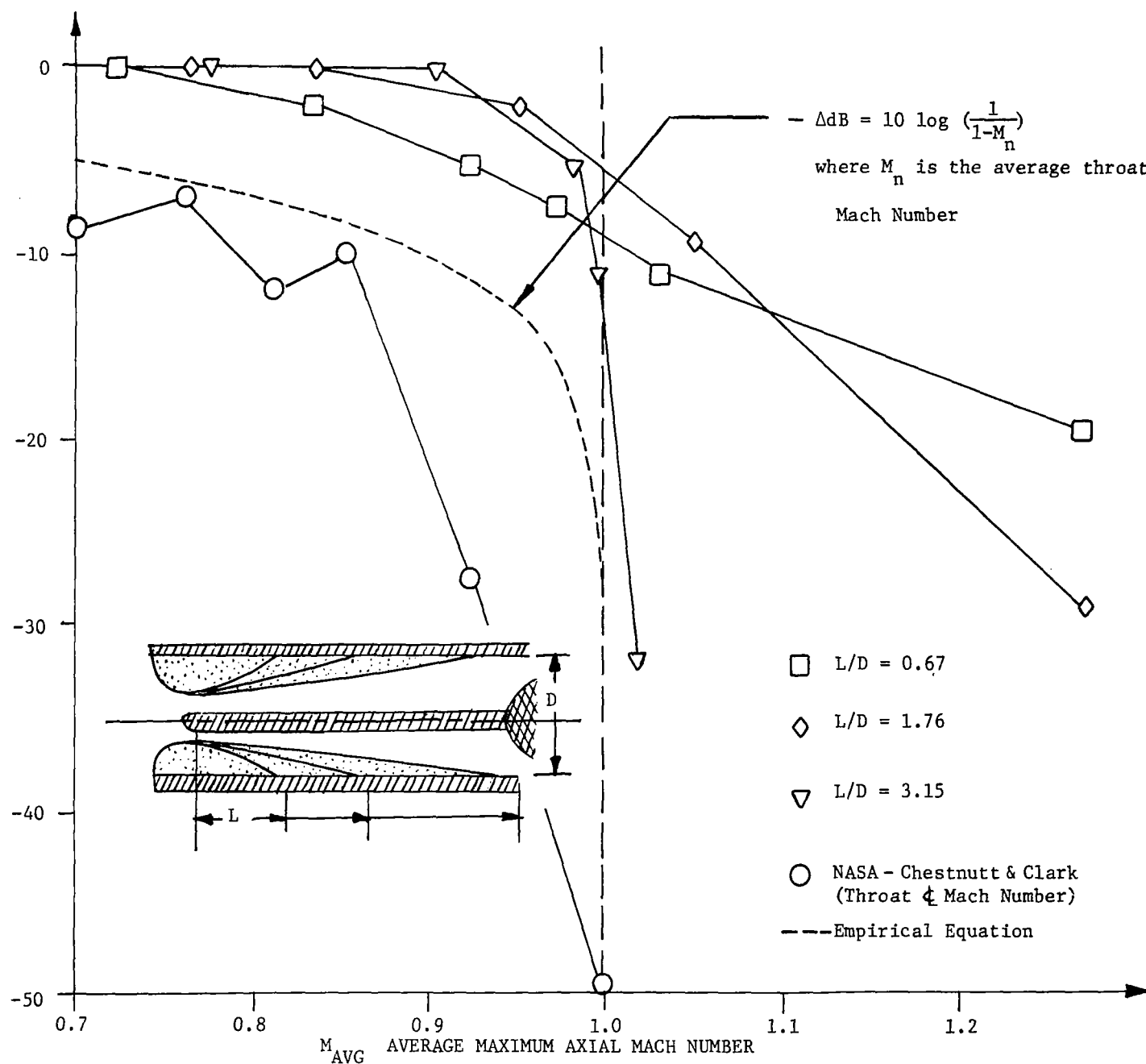
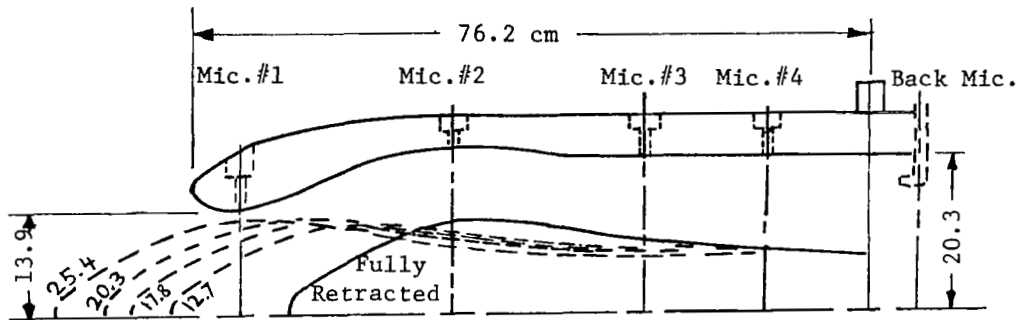
CHANGE IN OVERALL SOUND PRESSURE LEVEL, ΔdB 

FIG.2 INFLUENCE OF LENGTH/DIAMETER RATIO ON NOISE ATTENUATION (EJECTOR SOURCE)



CONFIGURATION NO. 1

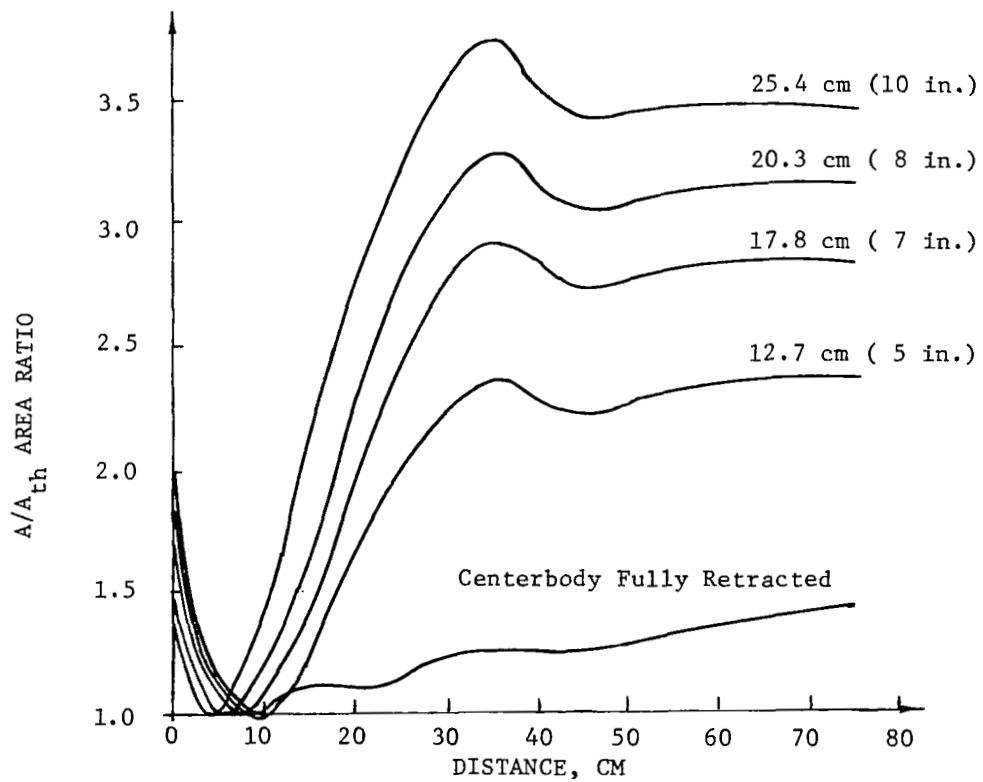
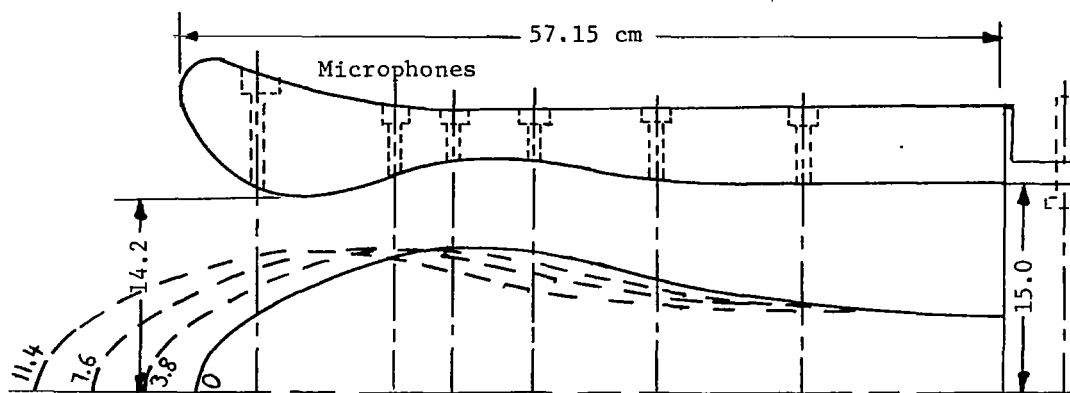


FIG. 3 SCHEMATIC AND AREA DISTRIBUTION OF TRANSLATING CENTERBODY INLET CONFIGURATION 1



CONFIGURATION NO. 2

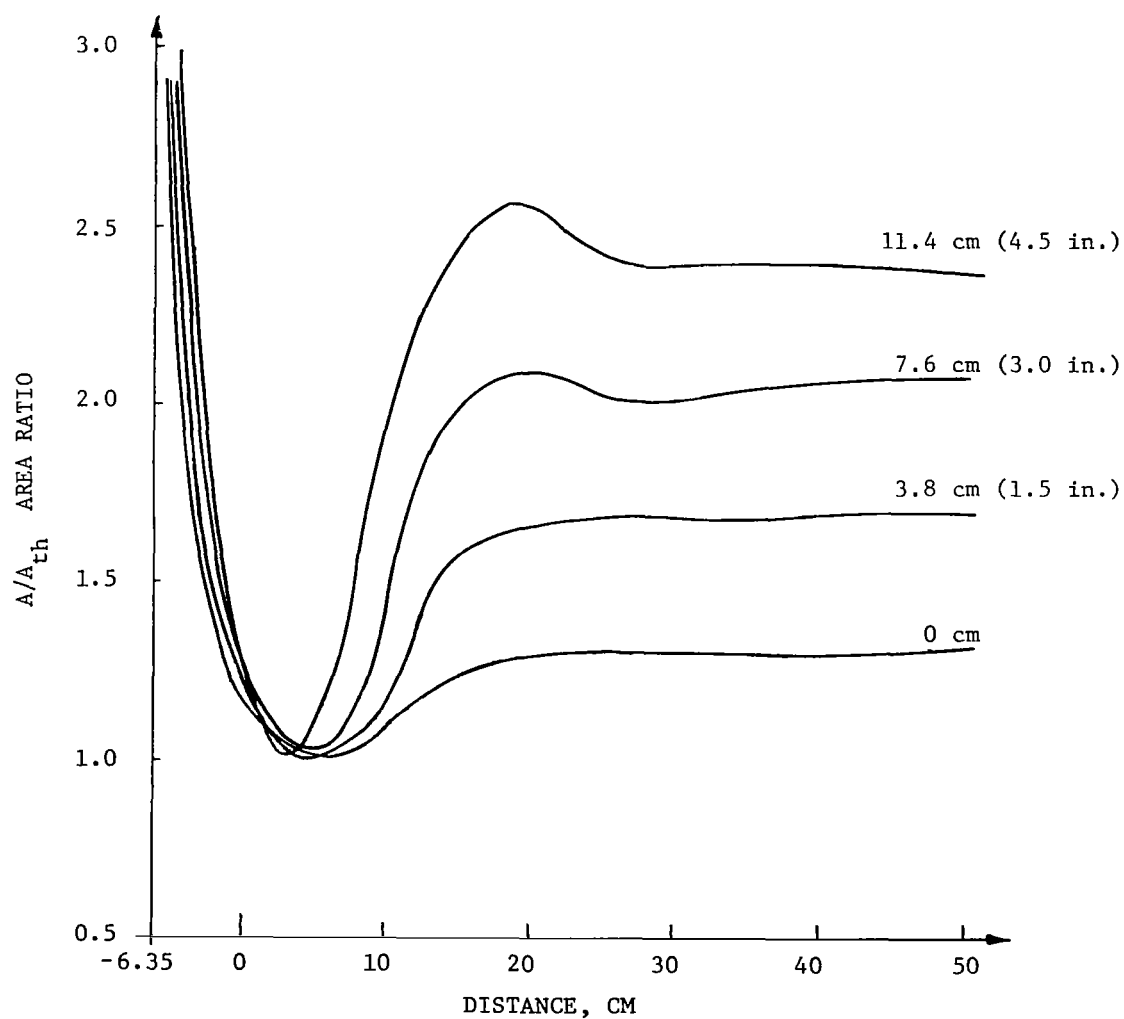
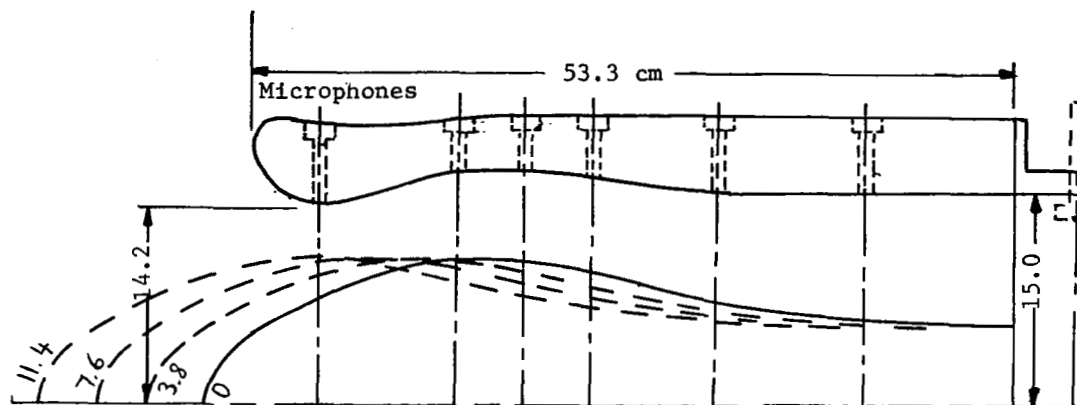


FIG.4 SCHEMATIC AND AREA DISTRIBUTION OF TRANSLATING CENTERBODY INLET
CONFIGURATION 2



CONFIGURATION NO. 3

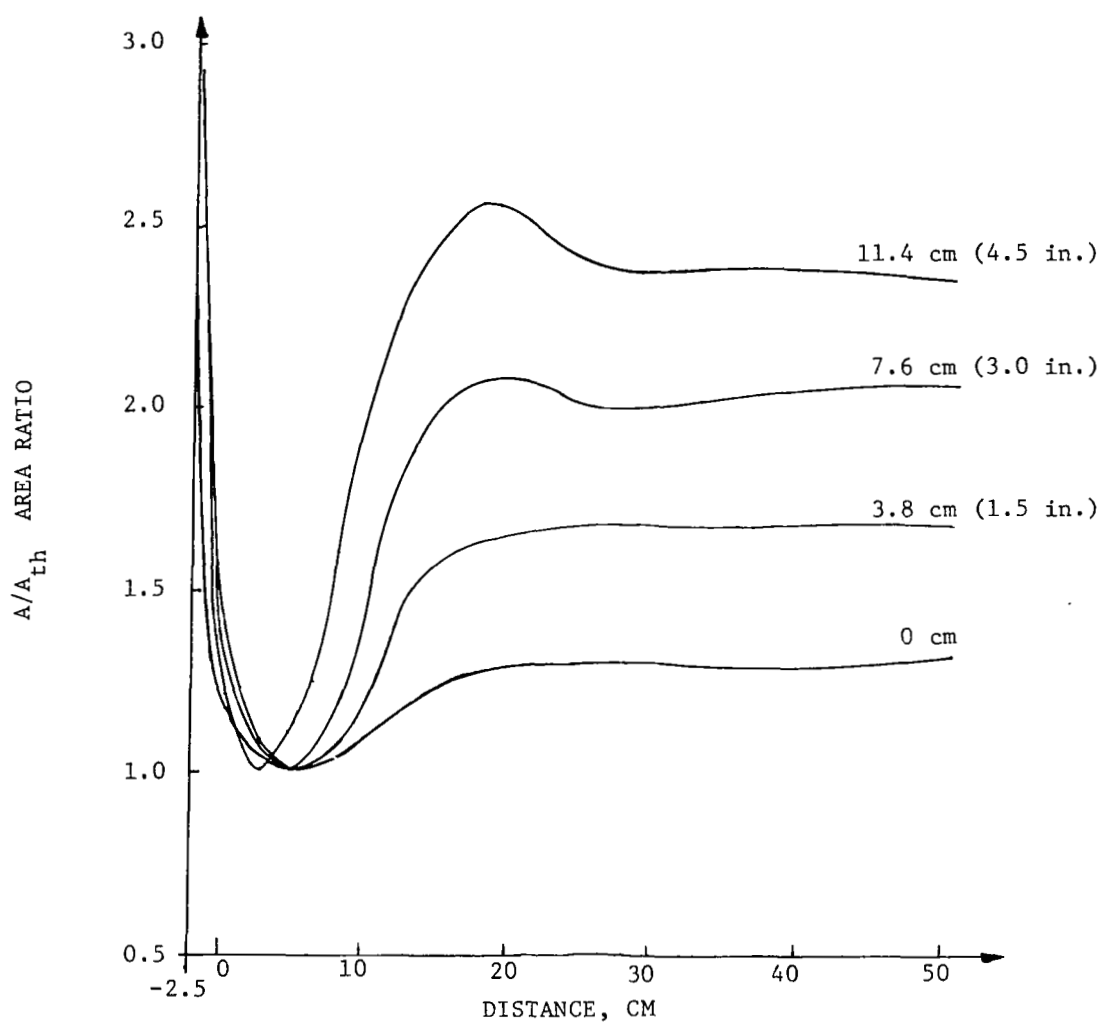
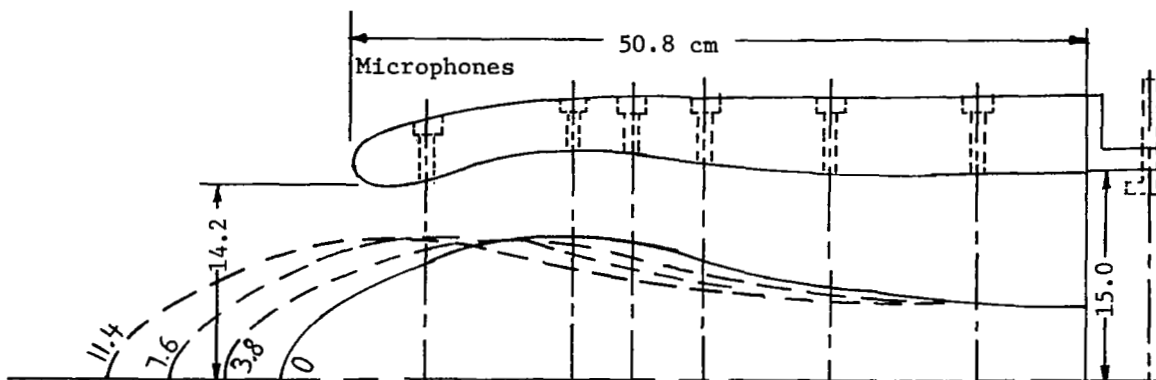


FIG.5 SCHEMATIC AND AREA DISTRIBUTION OF TRANSLATING CENTERBODY INLET CONFIGURATION 3



CONFIGURATION NO. 4

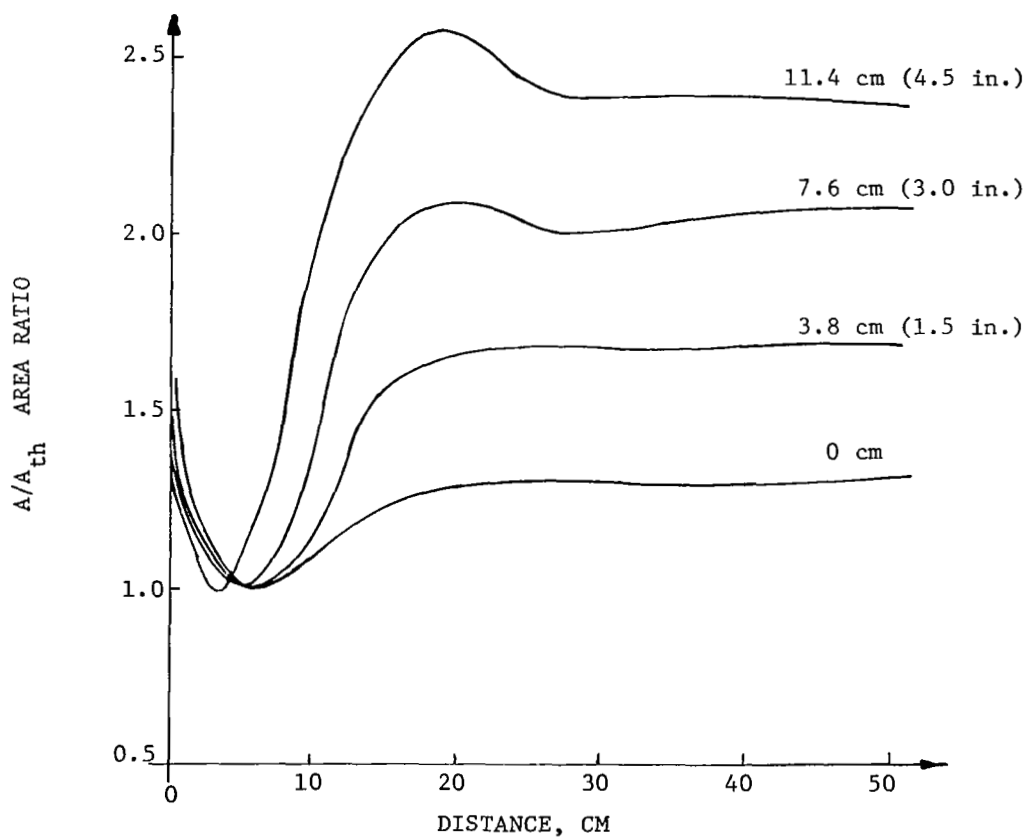
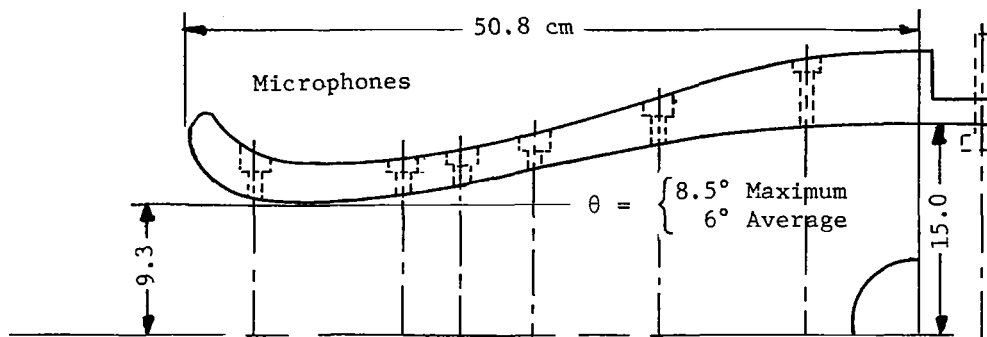


FIG.6 SCHEMATIC AND AREA DISTRIBUTION OF TRANSLATING CENTERBODY INLET CONFIGURATION 4



CONFIGURATION NO. 5

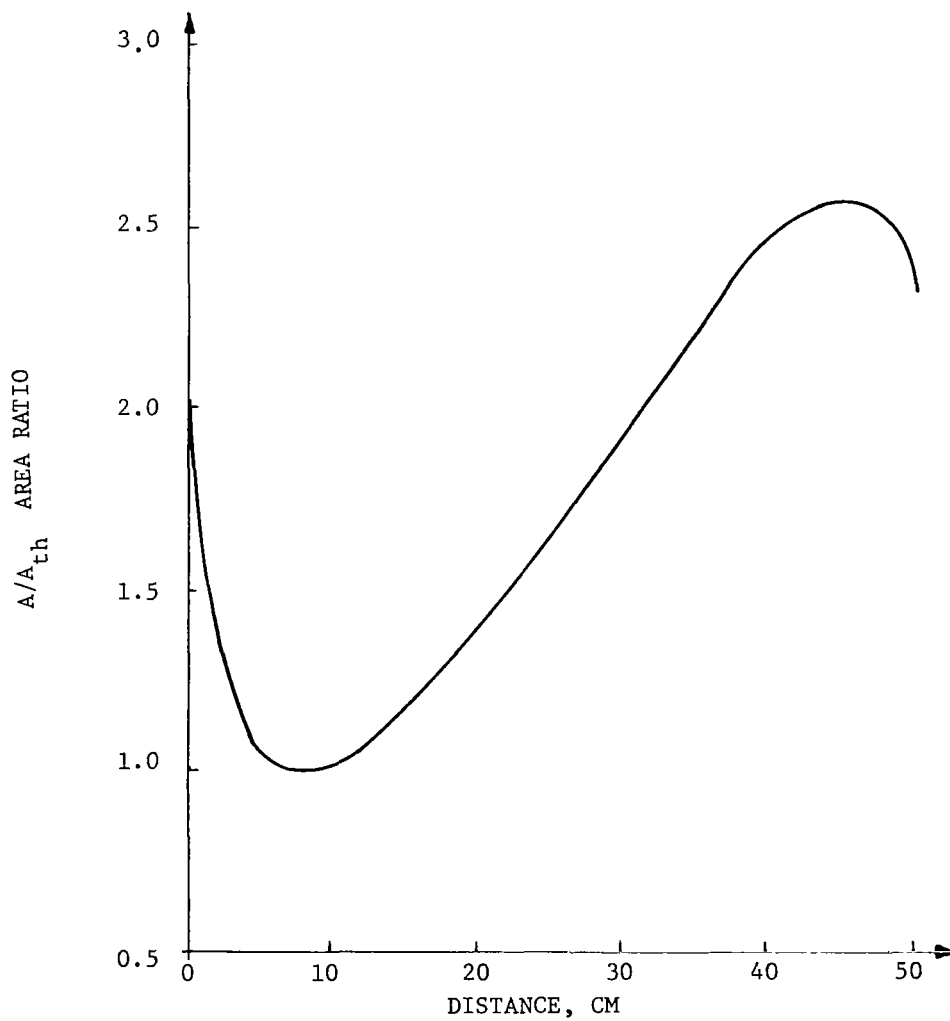
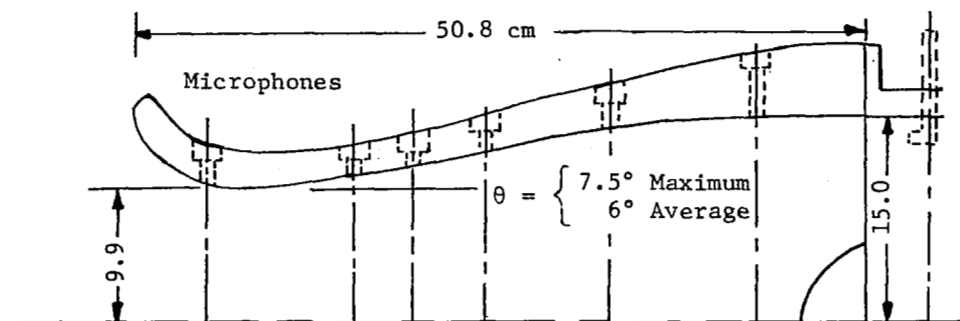


FIG.7 SCHEMATIC AND AREA DISTRIBUTION OF FIXED GEOMETRY (COLLAPSING COWL) INLET CONFIGURATION 5



CONFIGURATION NO. 6

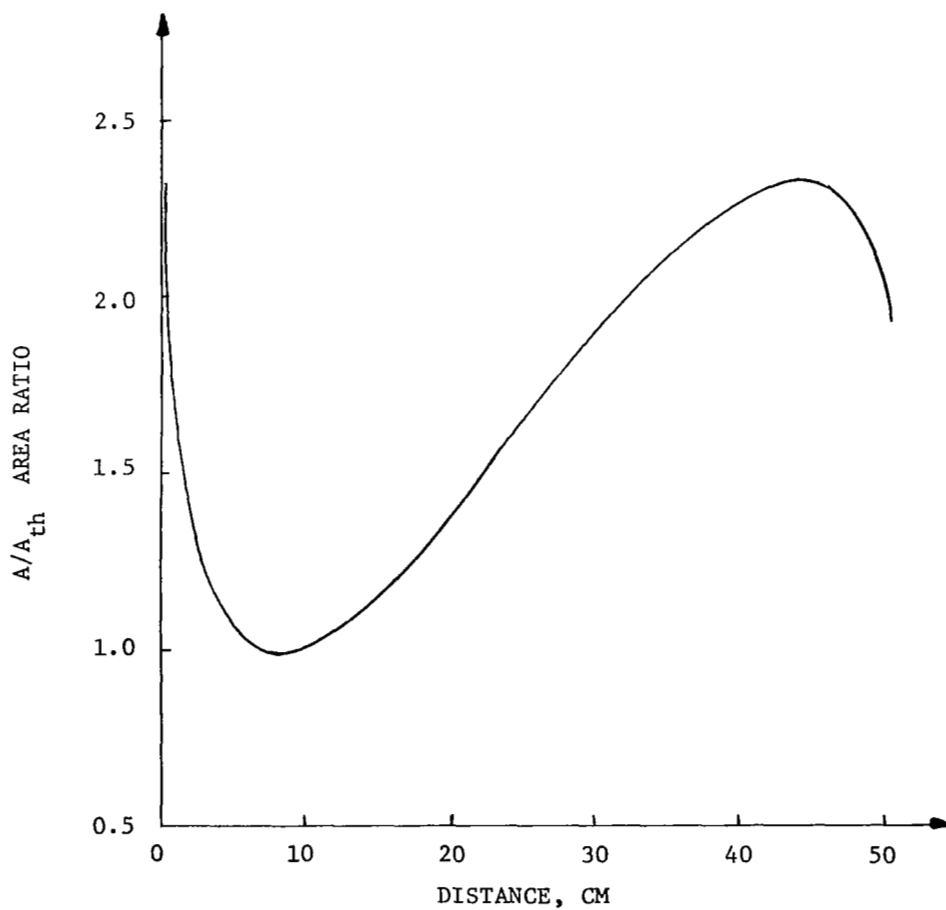
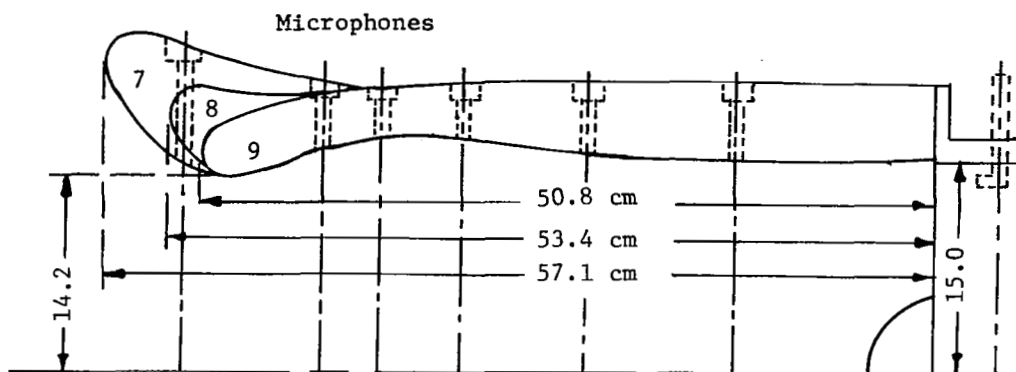


FIG.8 SCHEMATIC AND AREA DISTRIBUTION OF FIXED GEOMETRY (COLLAPSING COWL)
INLET CONFIGURATION 6



CONFIGURATIONS NO. 7,8,9

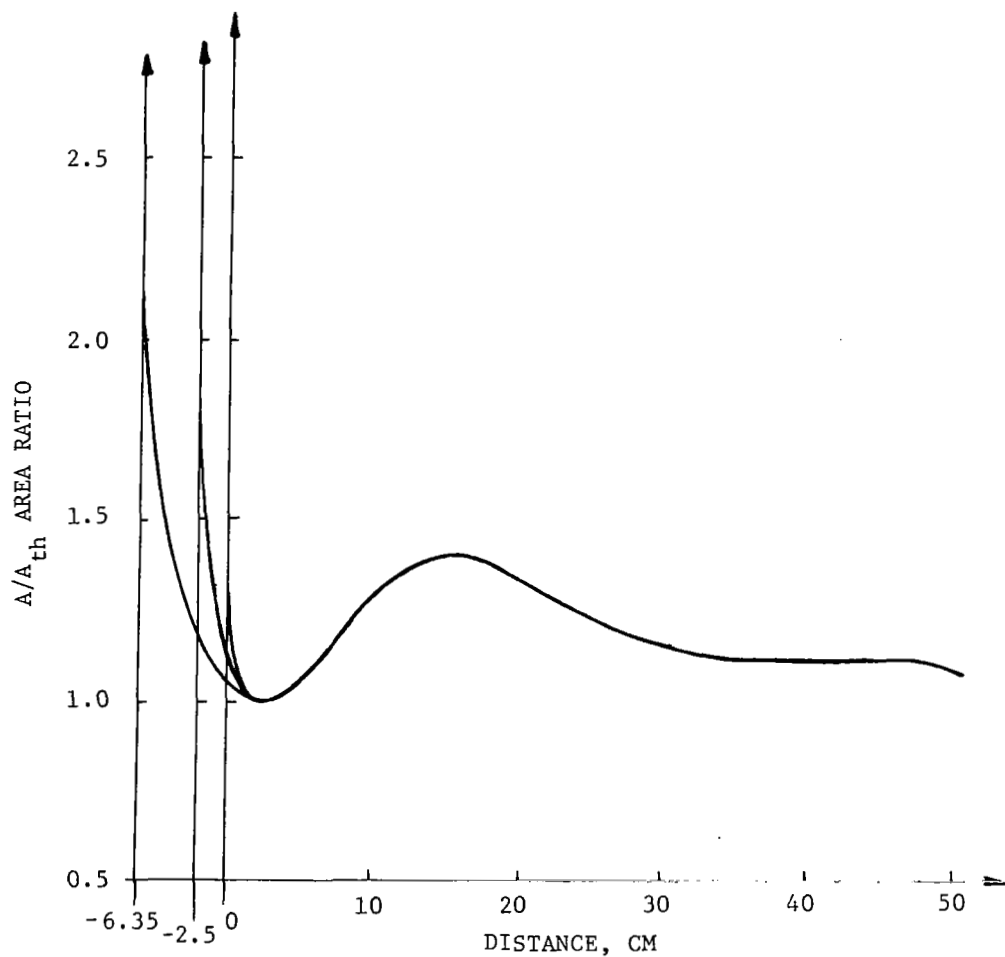


FIG.9 SCHEMATIC AND AREA DISTRIBUTION OF FIXED GEOMETRY INLET CONFIGURATIONS 7,8,9

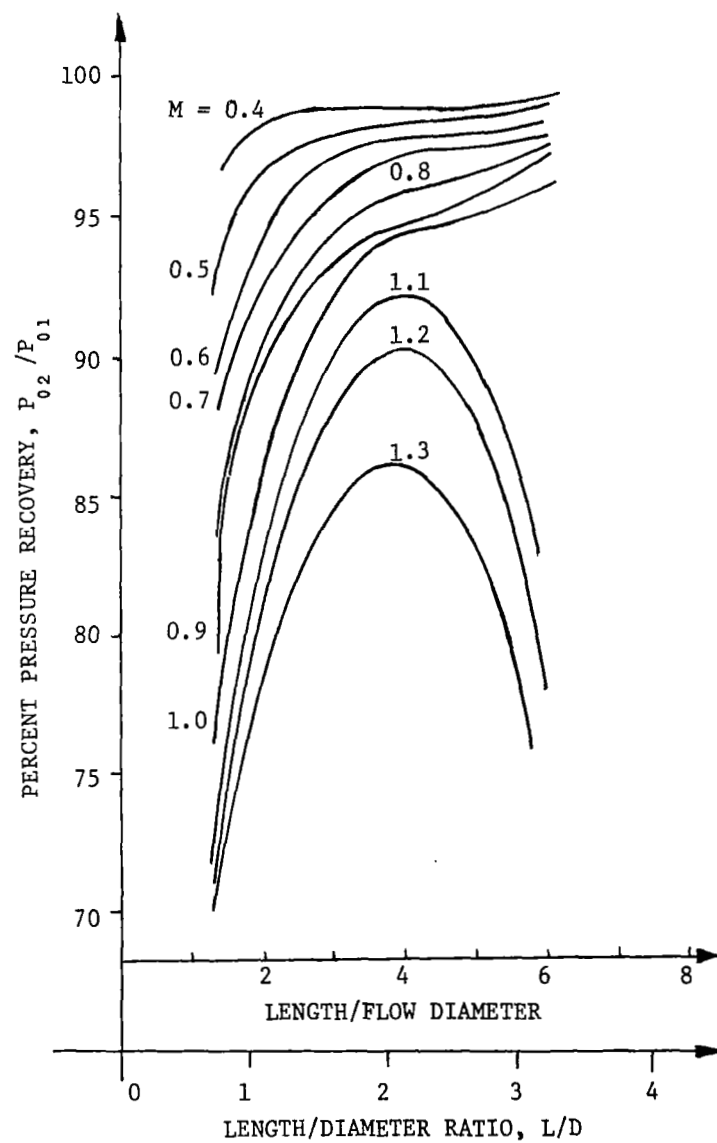
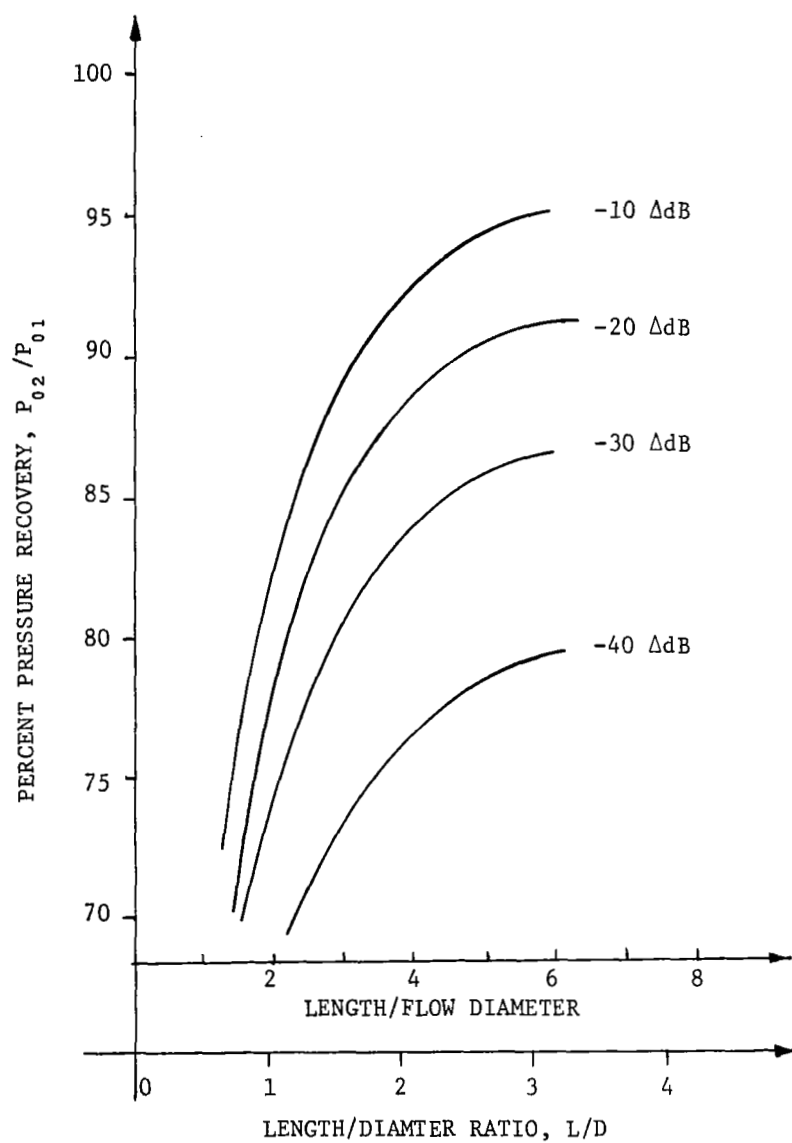


FIG.10 AERODYNAMIC AND ACOUSTIC PERFORMANCE OF INLETS WITH DIFFERENT LENGTH/DIAMETER RATIOS

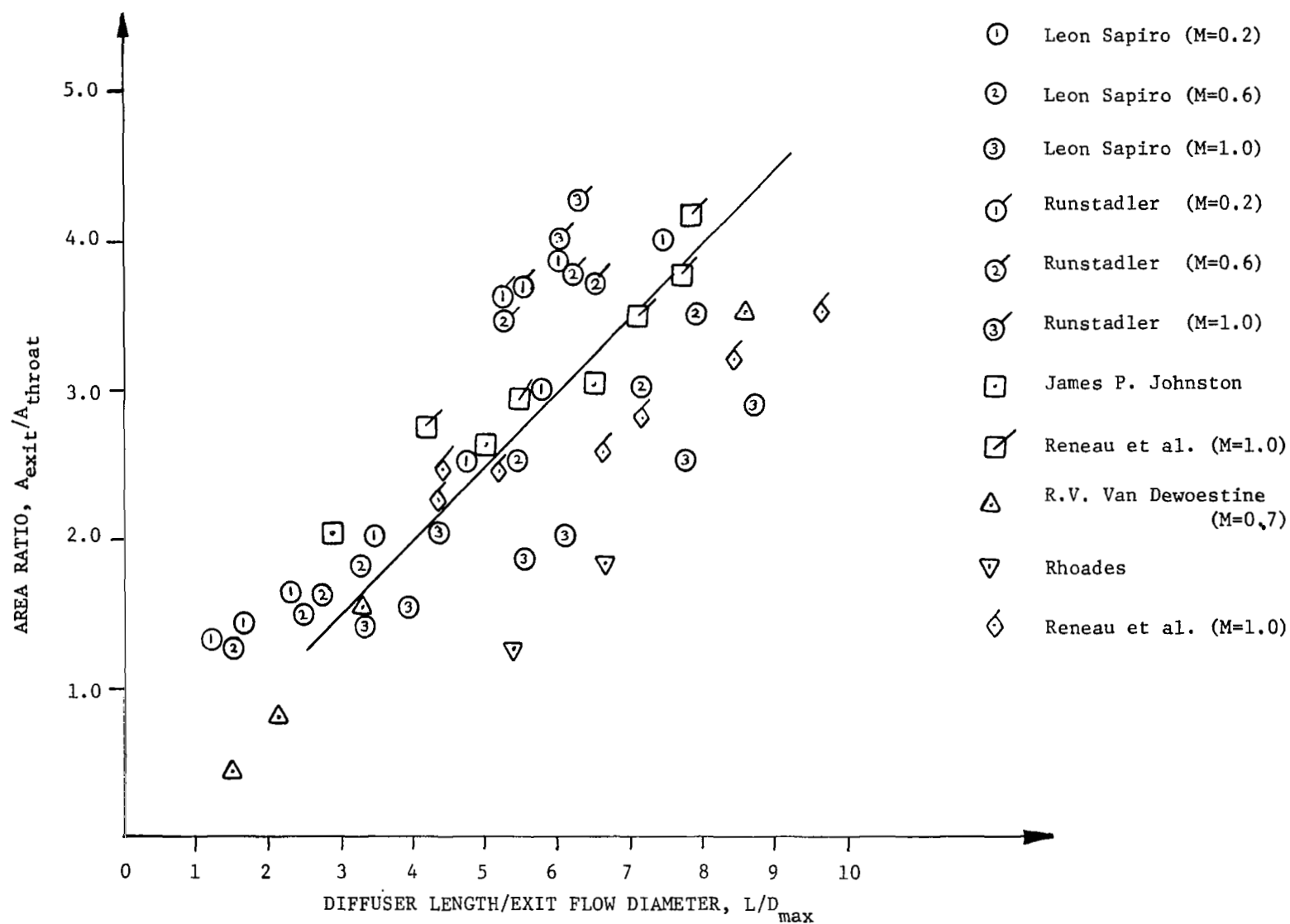


FIG.11 OPTIMUM L/D FOR A GIVEN AREA RATIO AT DIFFERENT THROAT MACH NUMBERS FOR CIRCULAR AND SQUARE DIFFUSERS

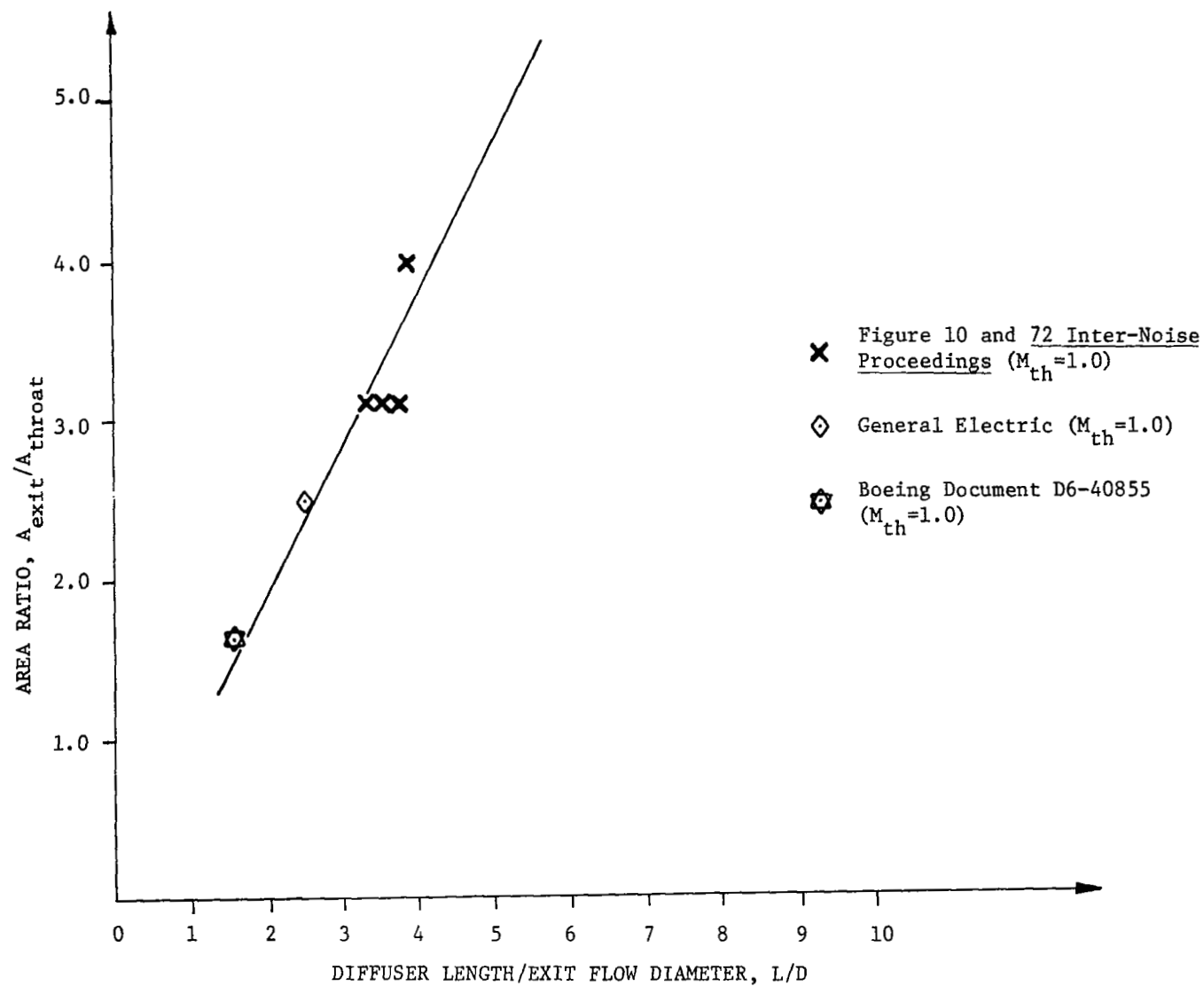


FIG.12 OPTIMUM L/D FOR A GIVEN AREA RATIO AT DIFFERENT THROAT MACH NUMBERS FOR ANNULAR DIFFUSERS

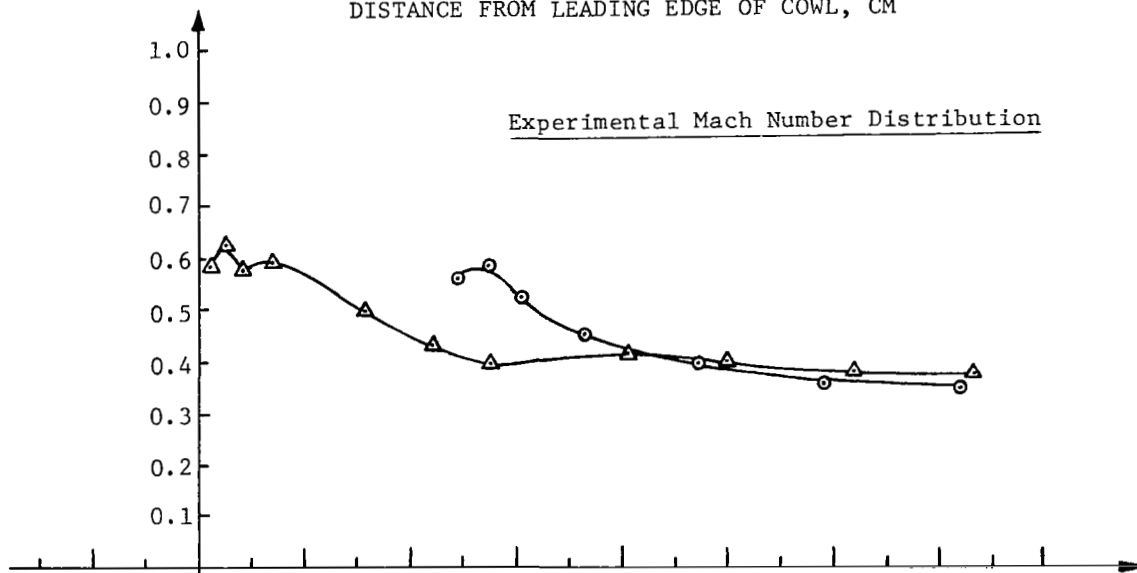
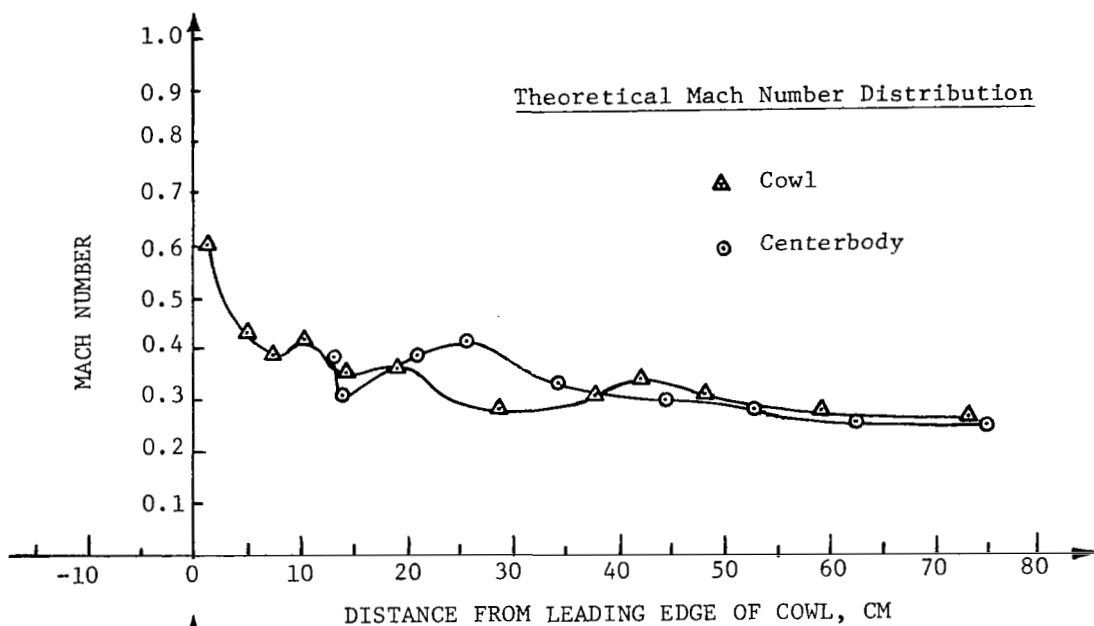
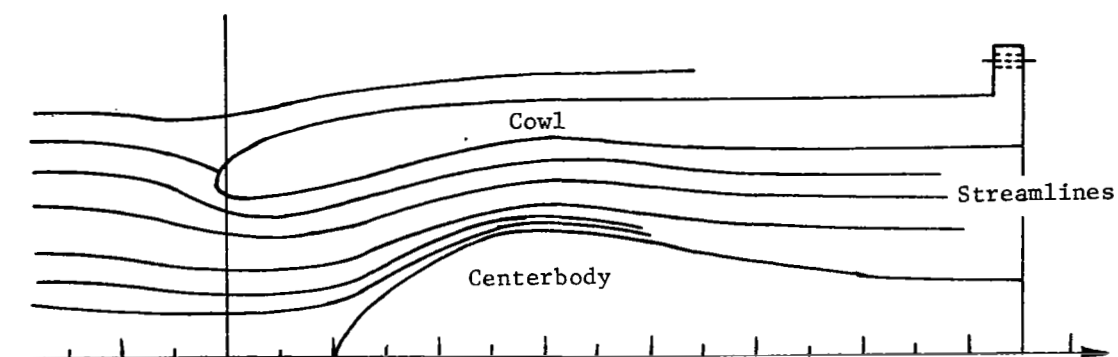


FIG.13 THEORETICAL POTENTIAL FLOW AND EXPERIMENTAL RESULTS FOR CONFIGURATION 1 WITH CENTERBODY AT 0 CM DISPLACEMENT

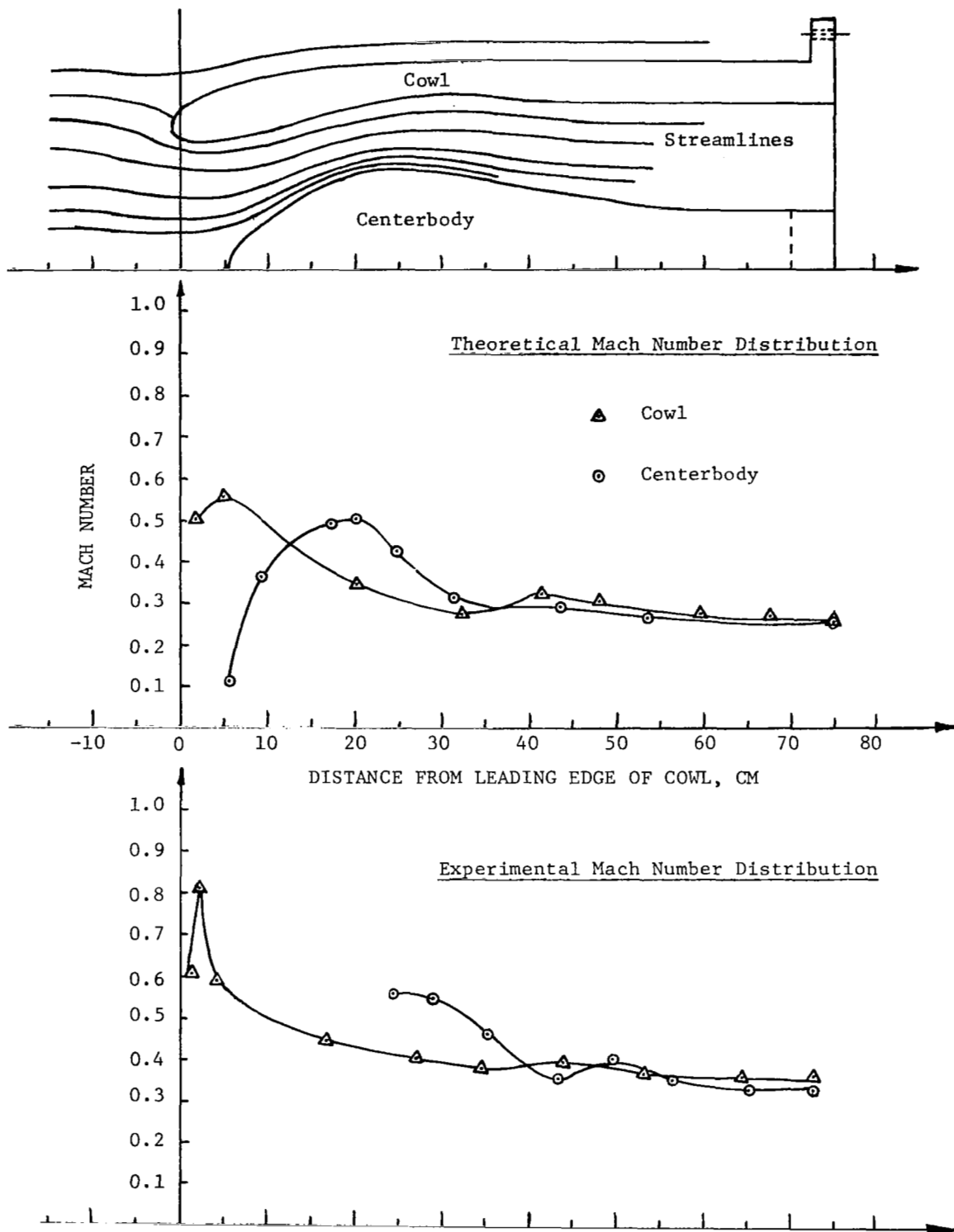


FIG.14 THEORETICAL POTENTIAL FLOW AND EXPERIMENTAL RESULTS FOR CONFIGURATION 1 WITH CENTERBODY AT 5.1 CM DISPLACEMENT

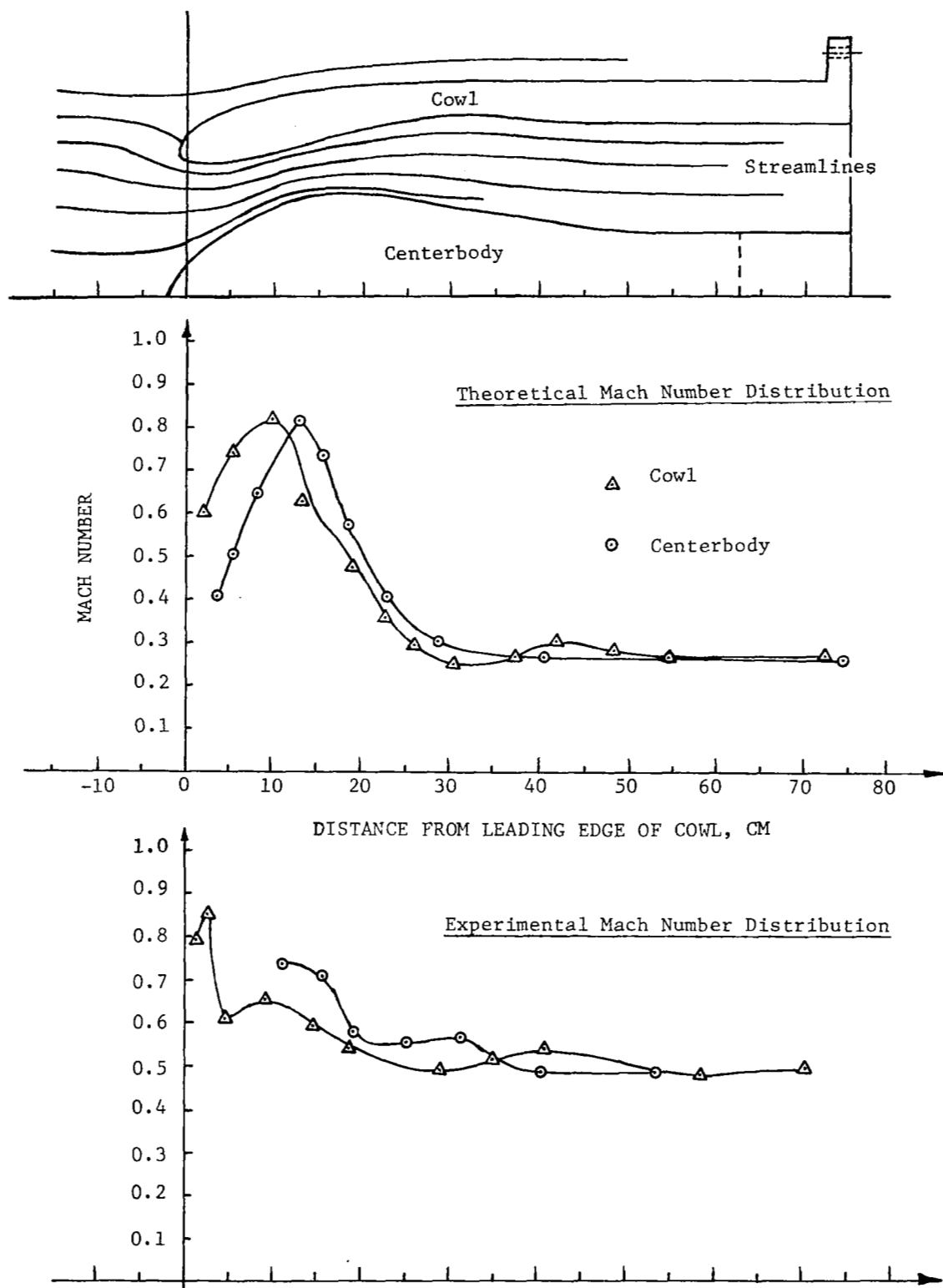


FIG.15 THEORETICAL POTENTIAL FLOW AND EXPERIMENTAL RESULTS FOR CONFIGURATION 1 WITH CENTERBODY AT 12.7 CM DISPLACEMENT

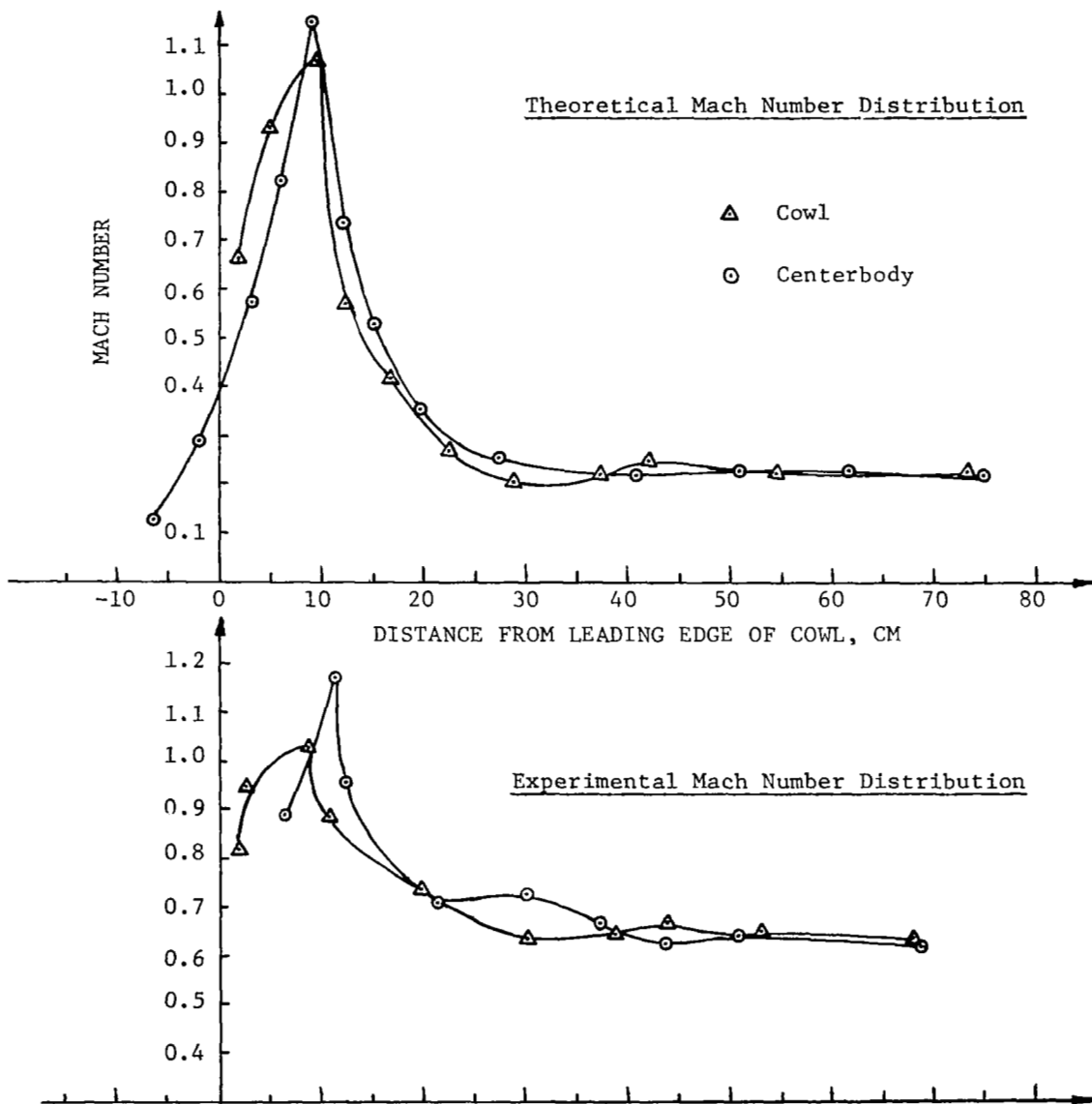
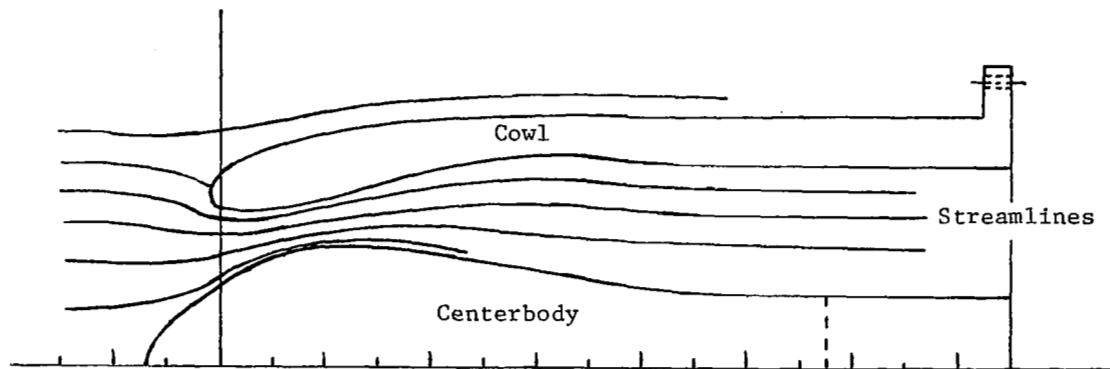


FIG.16 THEORETICAL POTENTIAL FLOW AND EXPERIMENTAL RESULTS FOR CONFIGURATION 1 WITH CENTERBODY AT 17.8 CM DISPLACEMENT

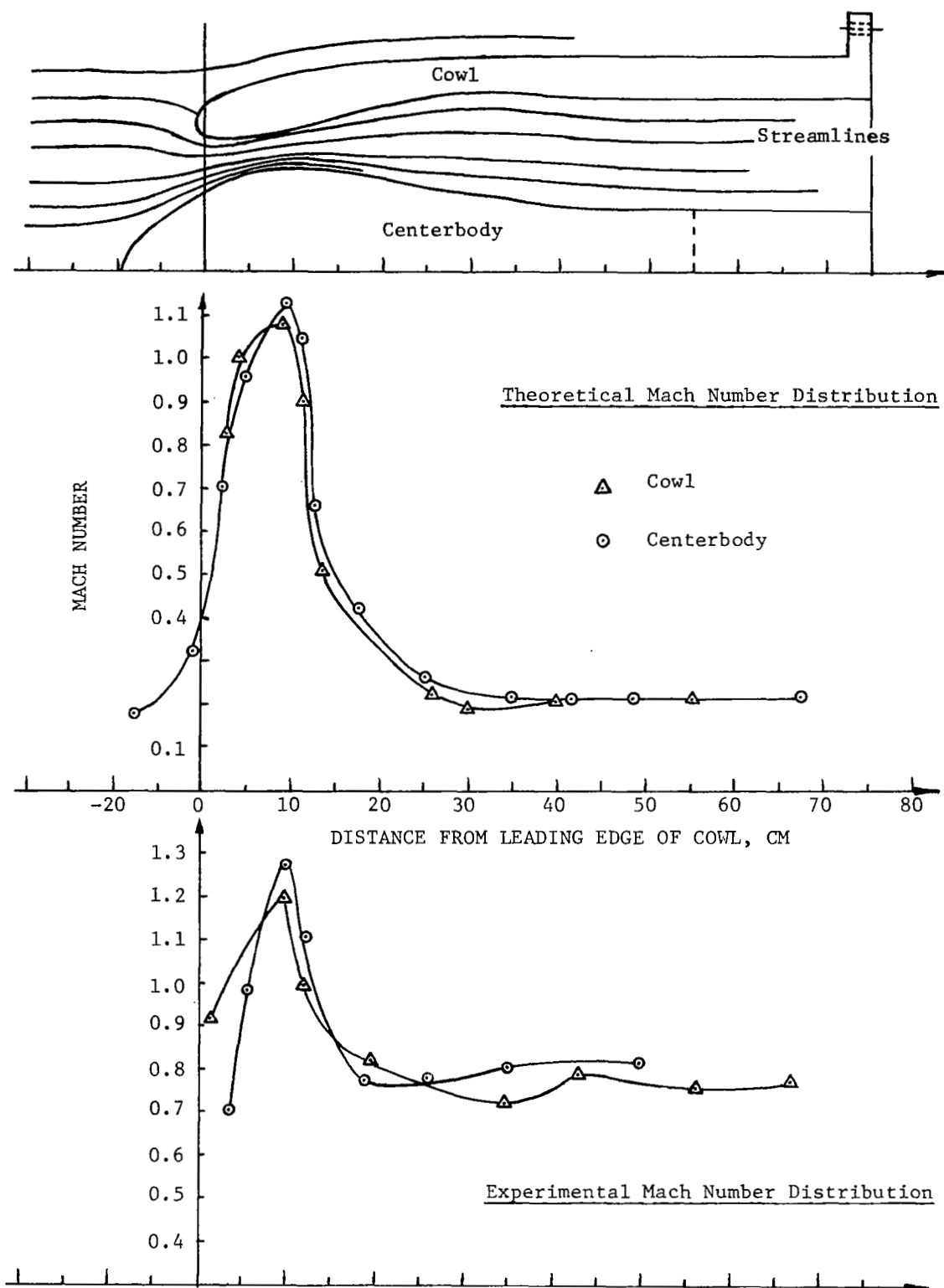


FIG.17 THEORETICAL POTENTIAL FLOW AND EXPERIMENTAL RESULTS FOR CONFIGURATION 1 WITH CENTERBODY AT 20.3 CM DISPLACEMENT

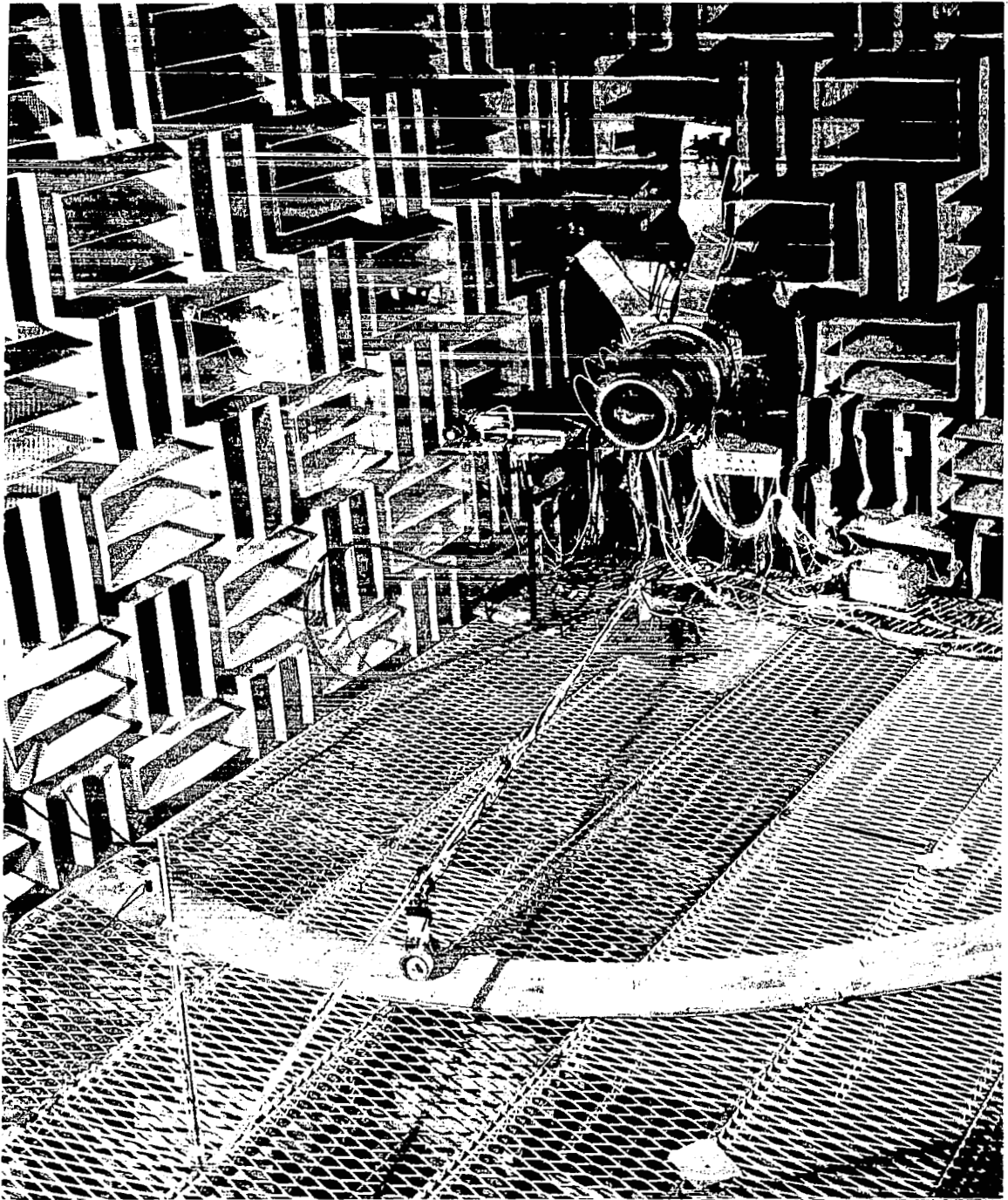


FIG.18 NASA-LANGLEY RESEARCH CENTER ANECHOIC-CHAMBER TRANSONIC COMPRESSOR FACILITY



FIG.19 INSTRUMENTATION ROOM, ANECHOIC-CHAMBER TRANSONIC COMPRESSOR FACILITY, NASA-LANGLEY RESEARCH CENTER

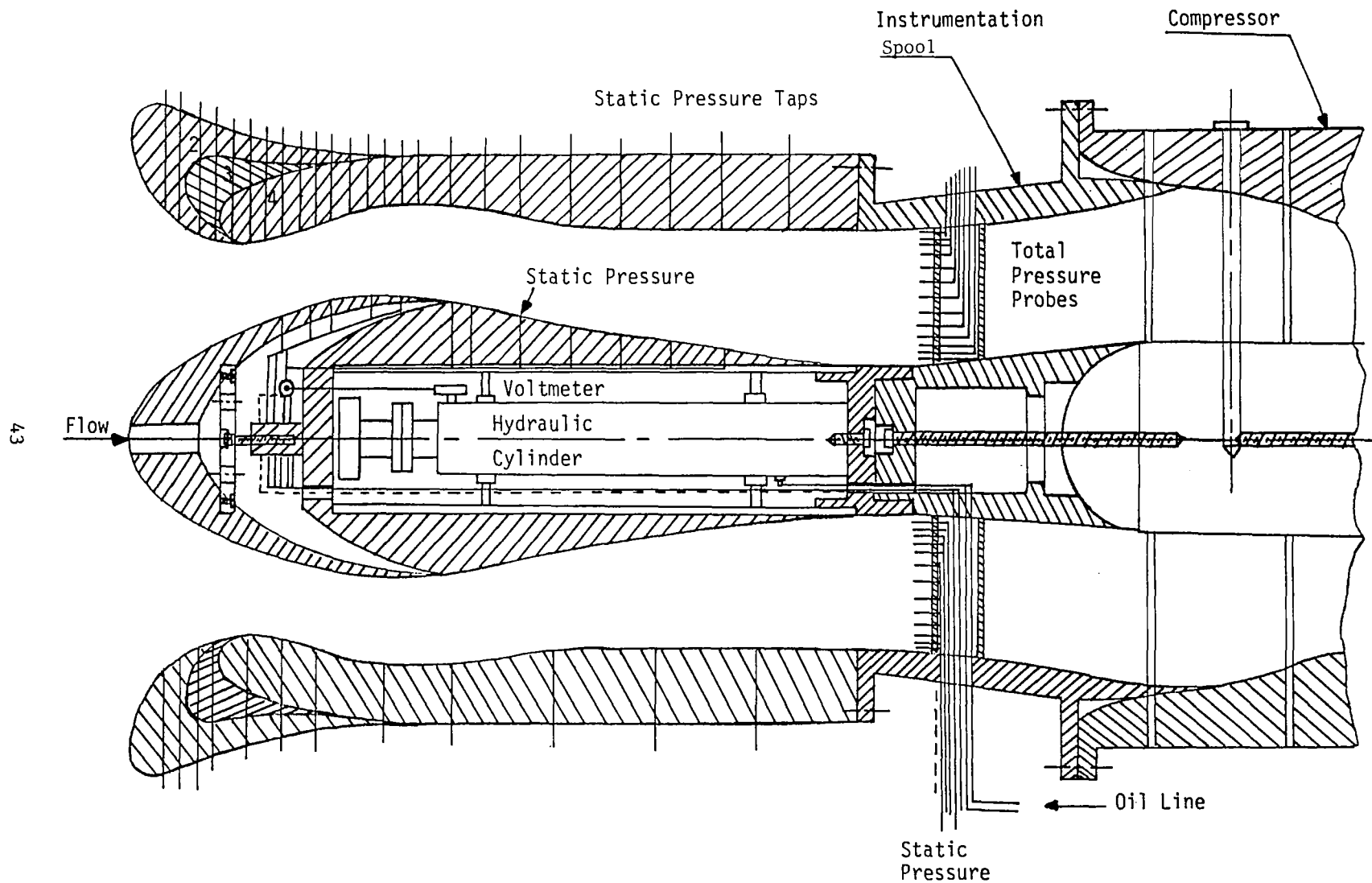


FIG.20 SCHEMATIC OF INLET CONFIGURATIONS 2, 3 AND 4 WITH AERODYNAMIC INSTRUMENTATION

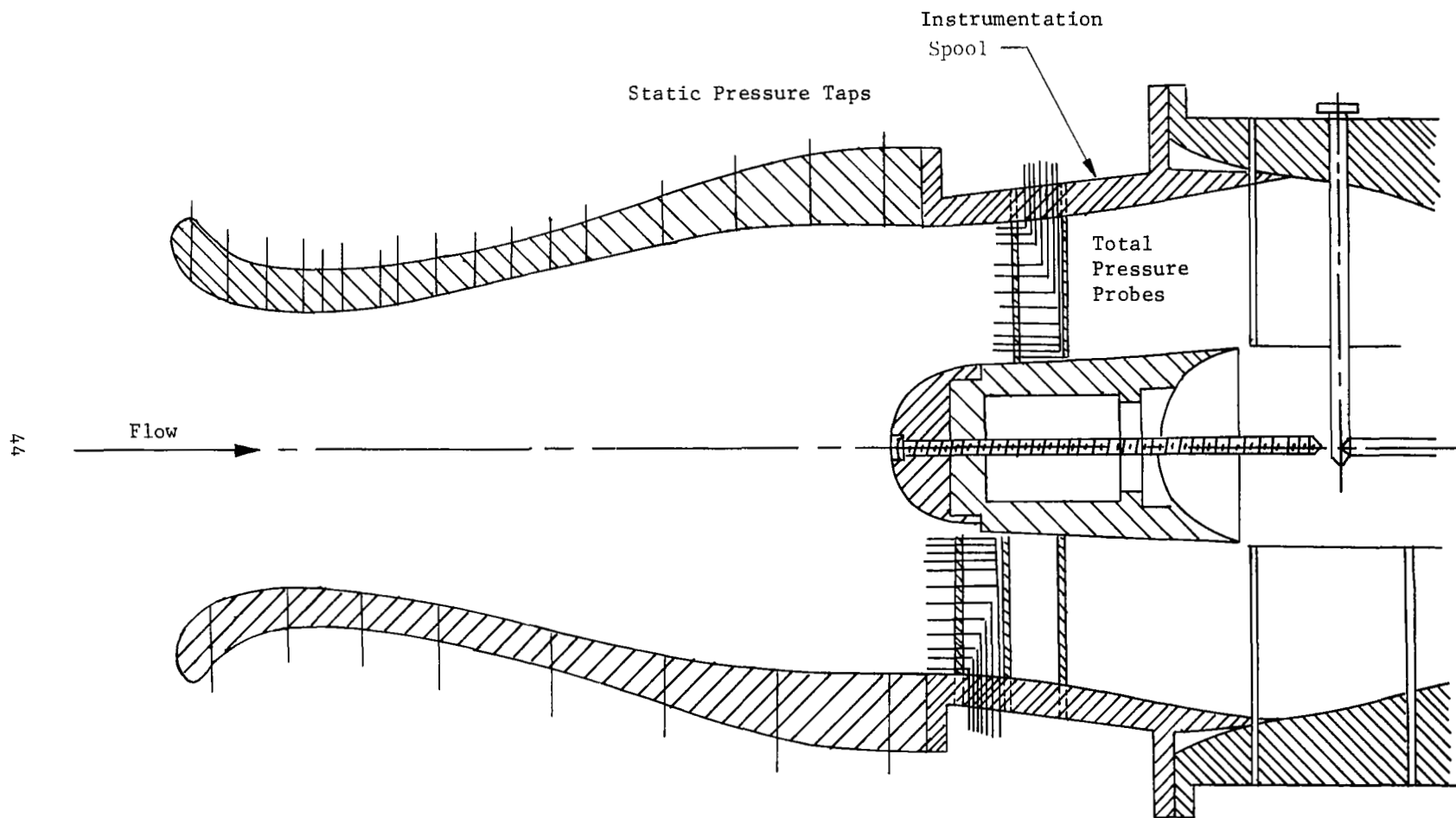


FIG.21 SCHEMATIC OF INLET CONFIGURATION 5 WITH AERODYNAMIC INSTRUMENTATION

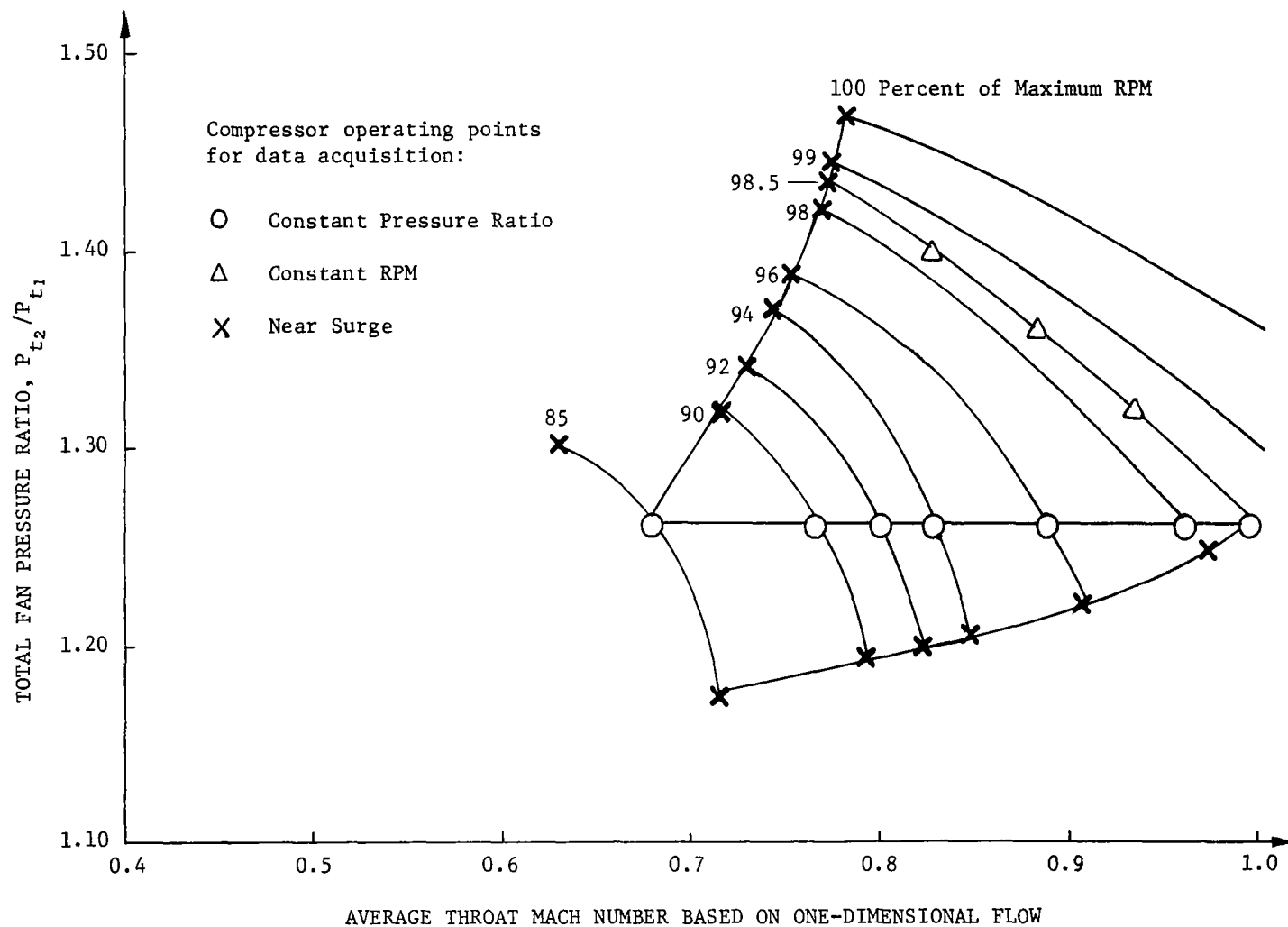


FIG.22 ILLUSTRATION OF INLET AND COMPRESSOR OPERATING CONDITIONS FOR DATA ACQUISITION

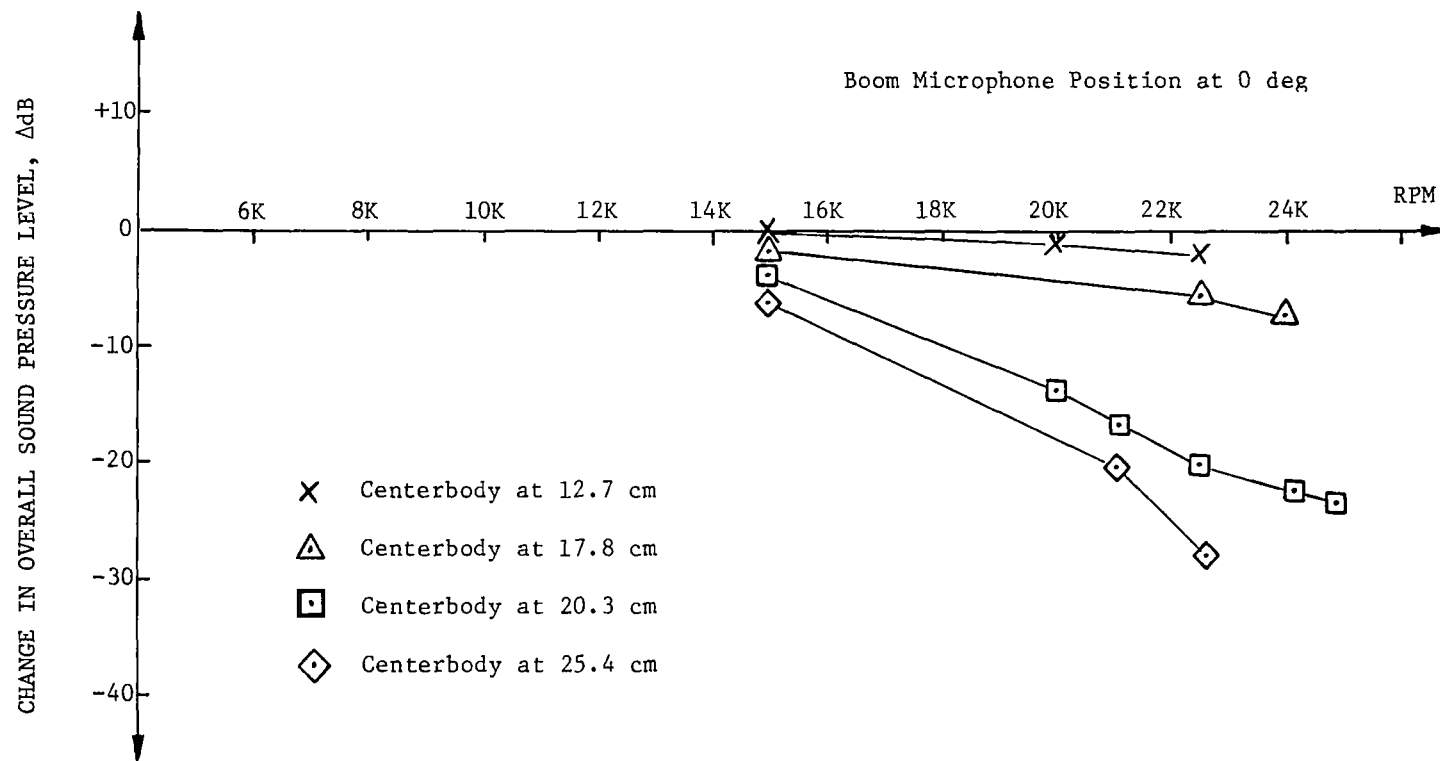


FIG.23 NOISE ATTENUATION FOR INLET CONFIGURATION 1

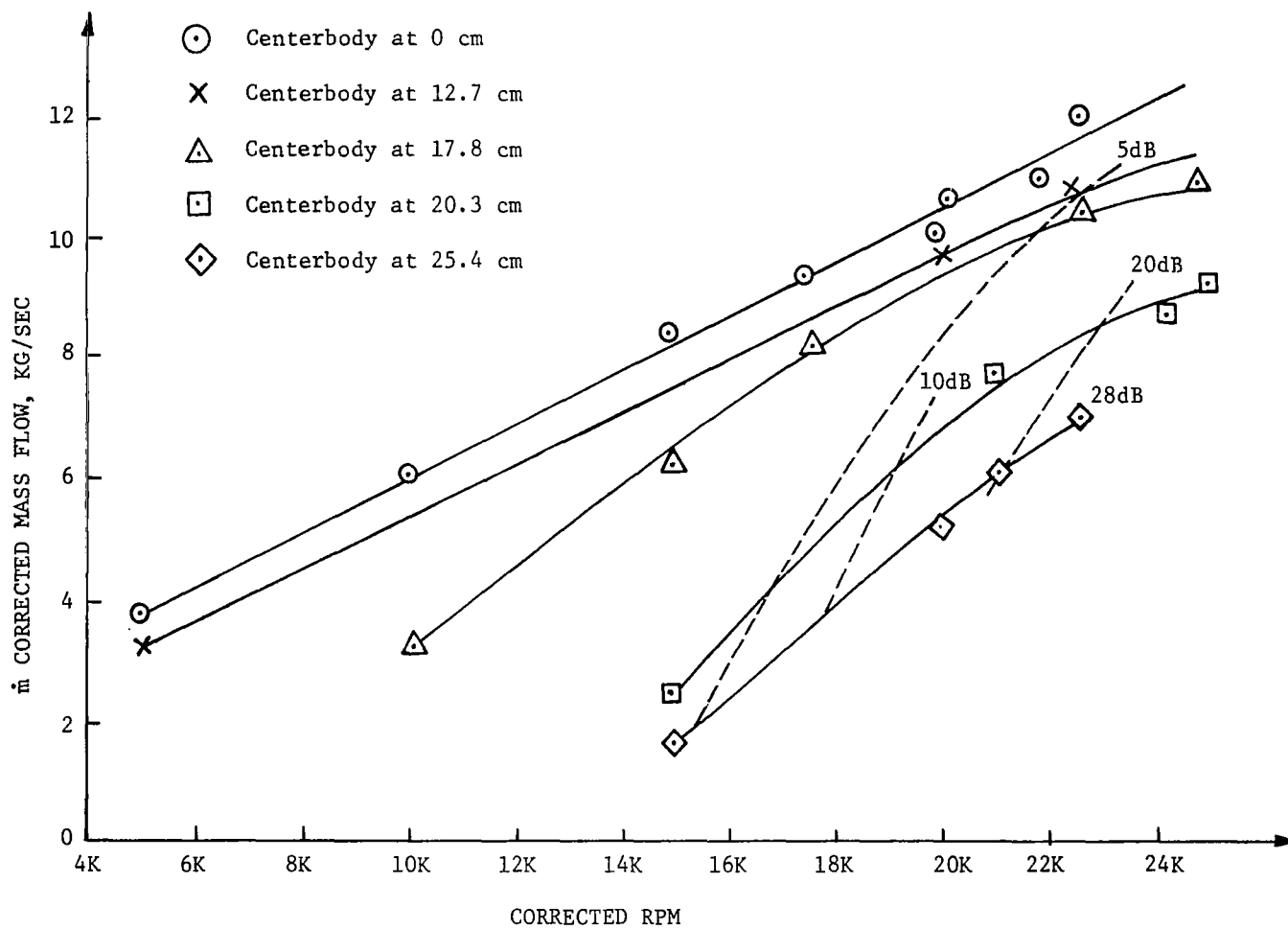


FIG.24 MASS FLOW FOR INLET CONFIGURATION 1

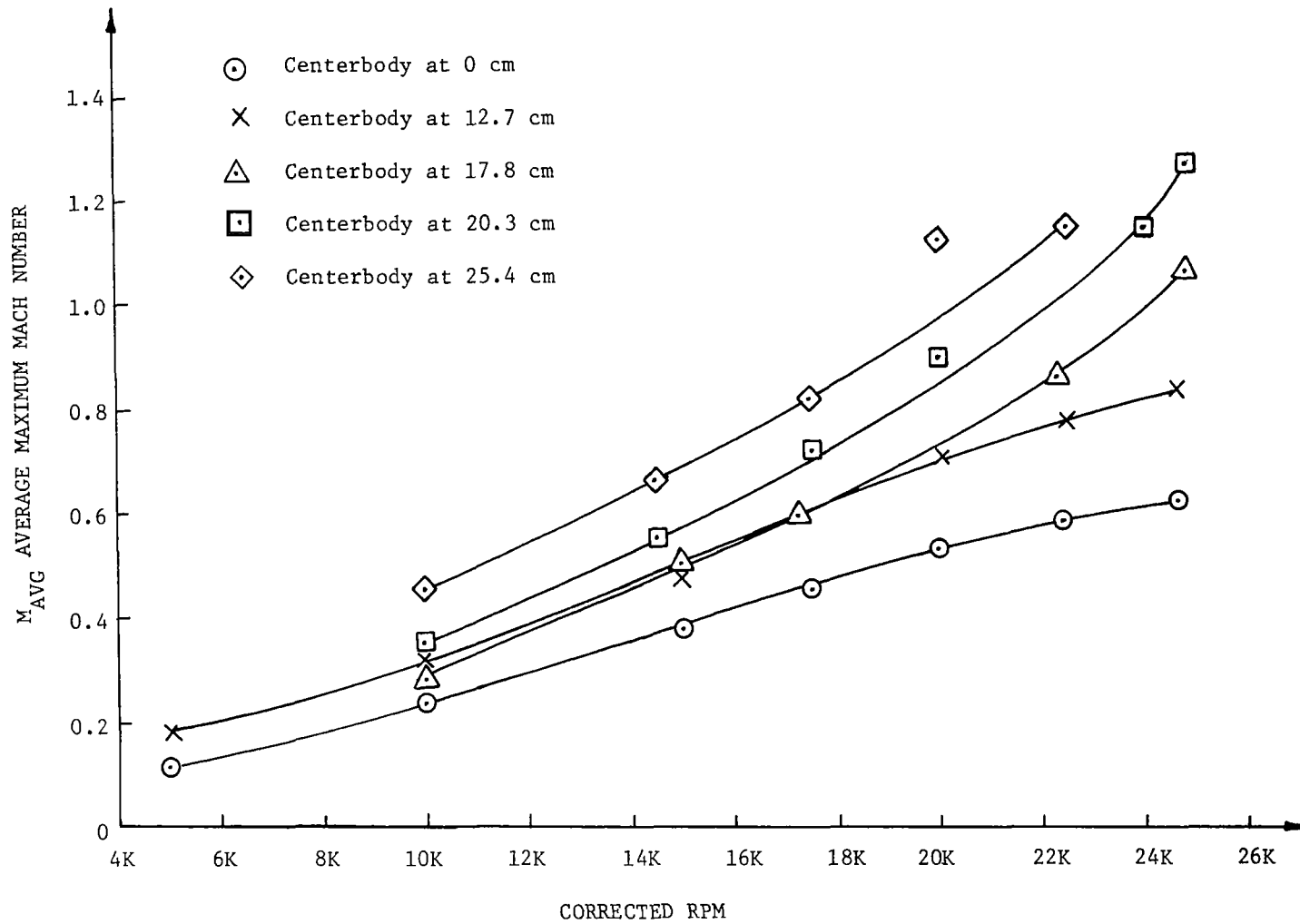


FIG.25 AVERAGE MAXIMUM MACH NUMBER OF INLET CONFIGURATION 1

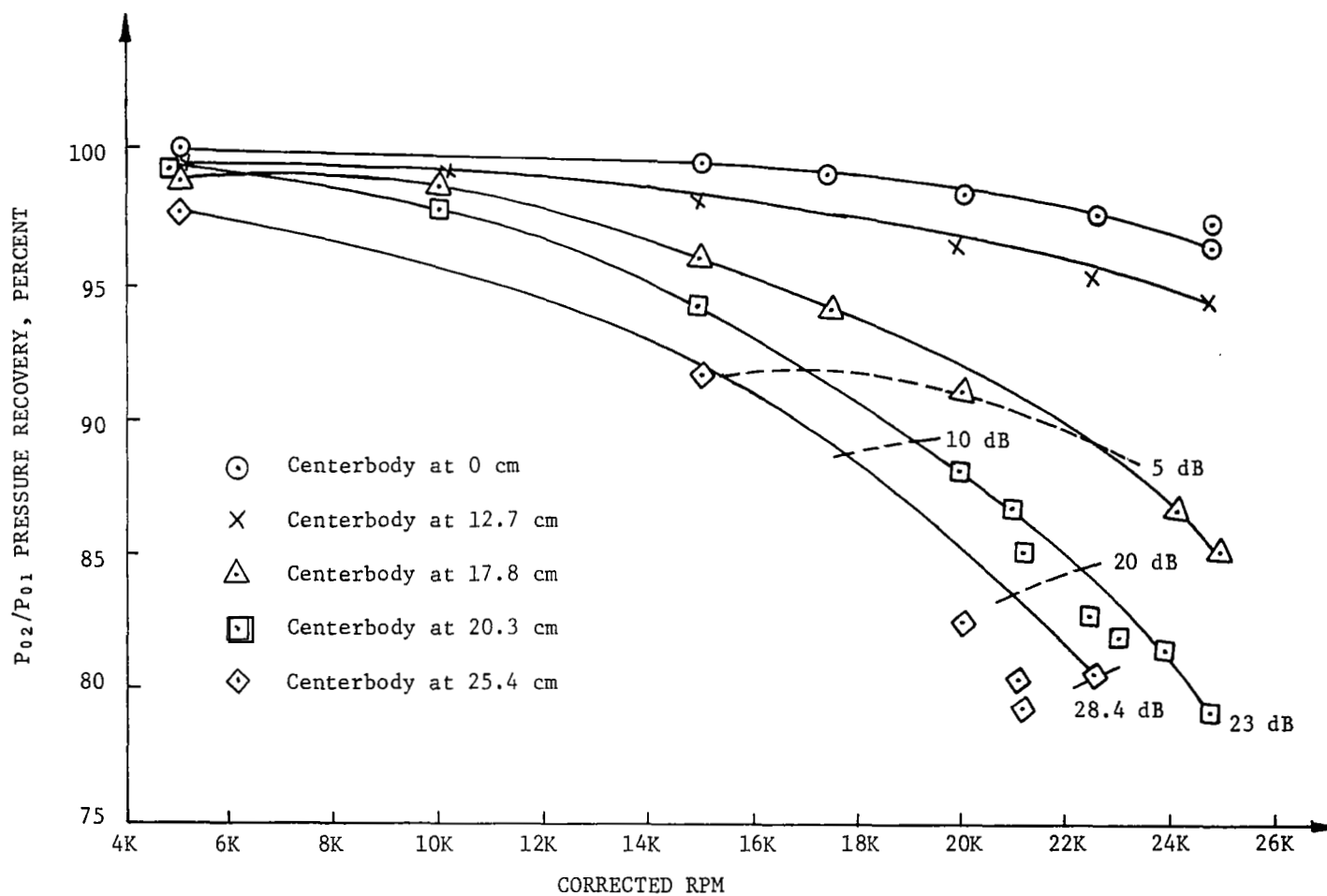


FIG.26 PRESSURE RECOVERY FOR INLET CONFIGURATION 1

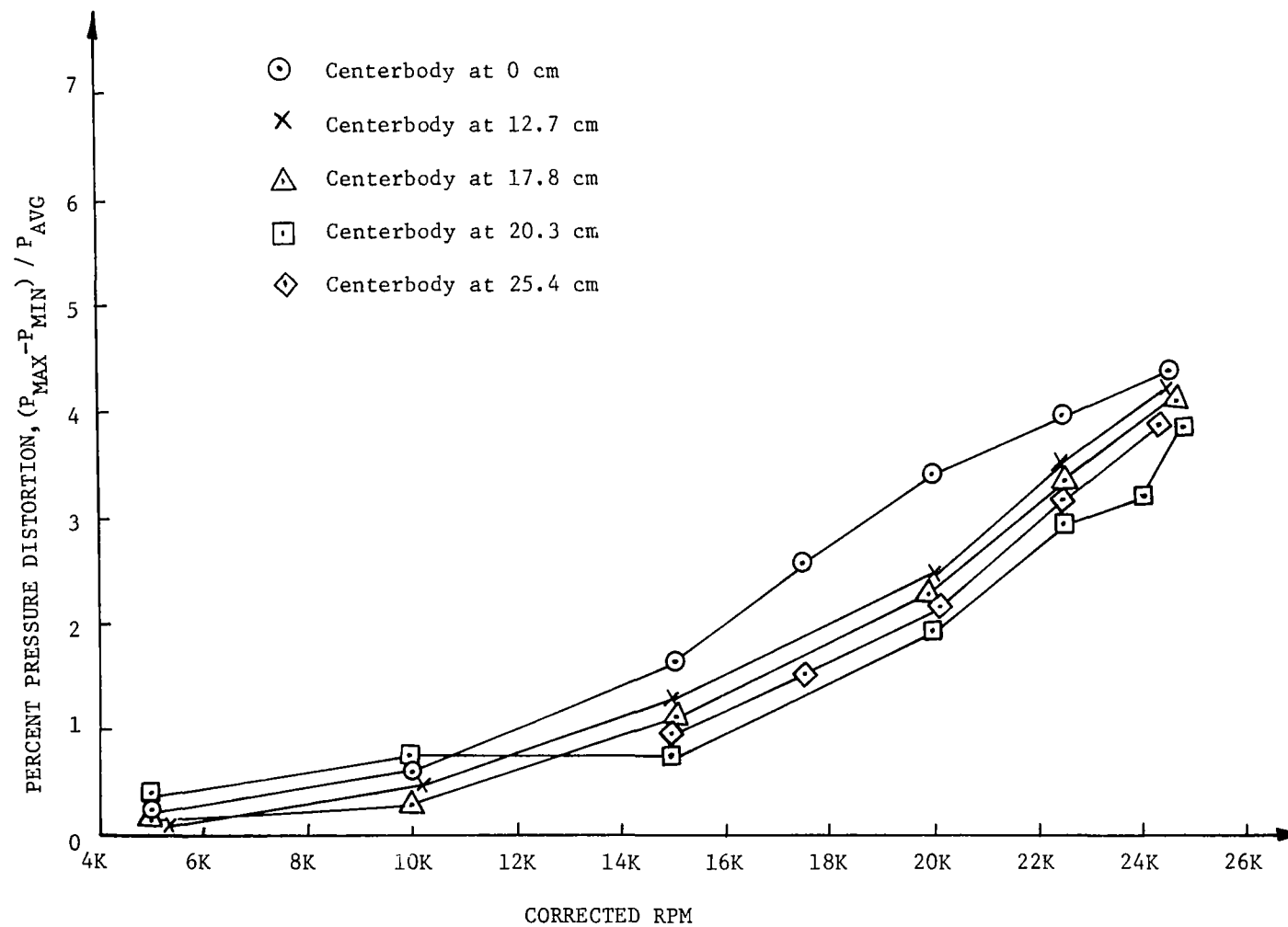


FIG.27 PRESSURE DISTORTION FOR INLET CONFIGURATION 1

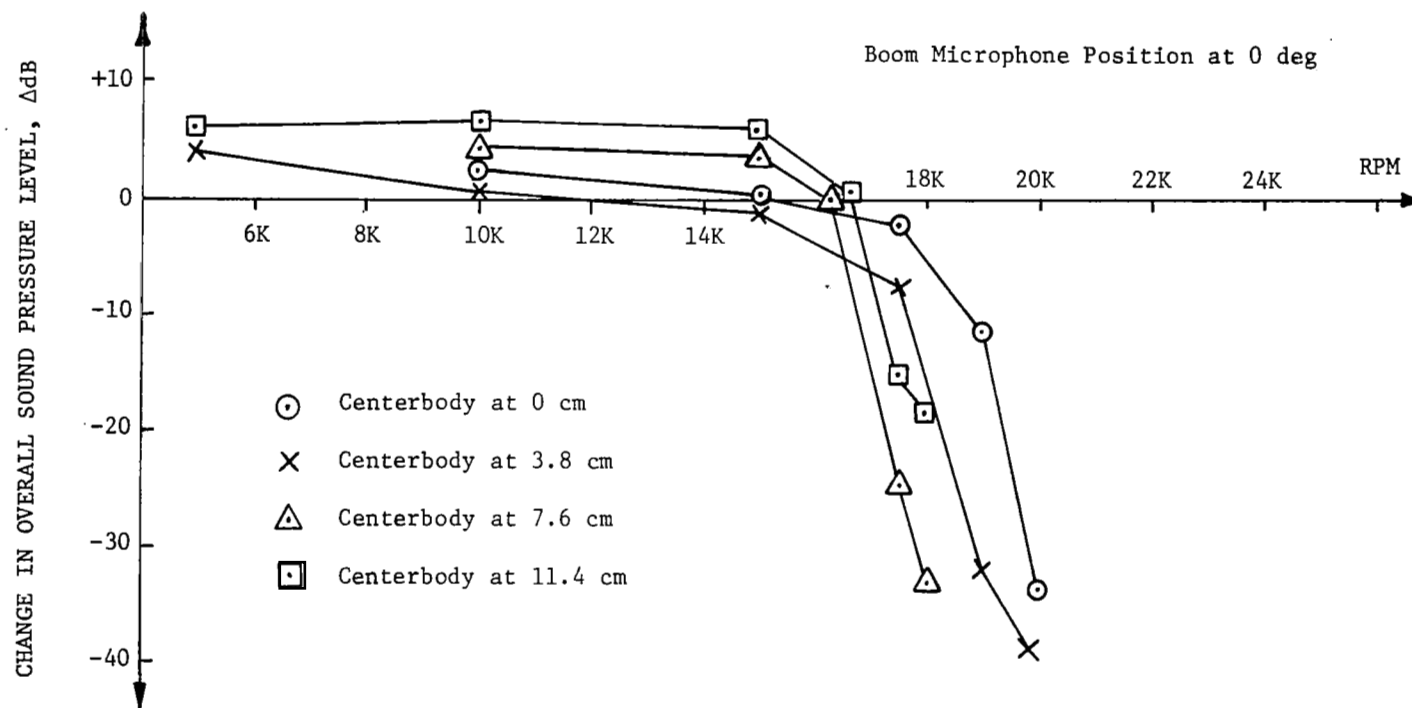


FIG.28 NOISE ATTENUATION FOR INLET CONFIGURATION 2

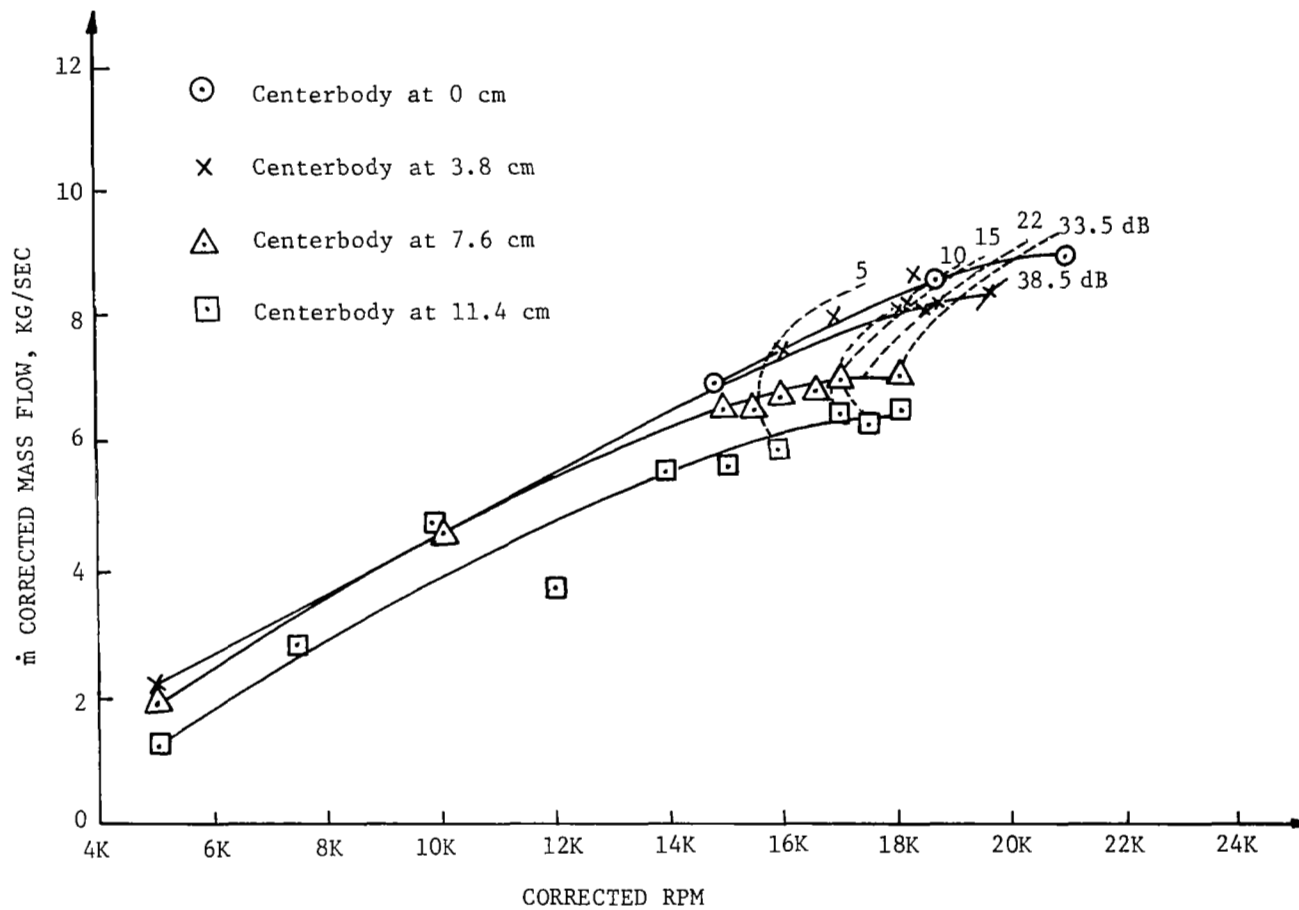


FIG.29 MASS FLOW FOR INLET CONFIGURATION 2

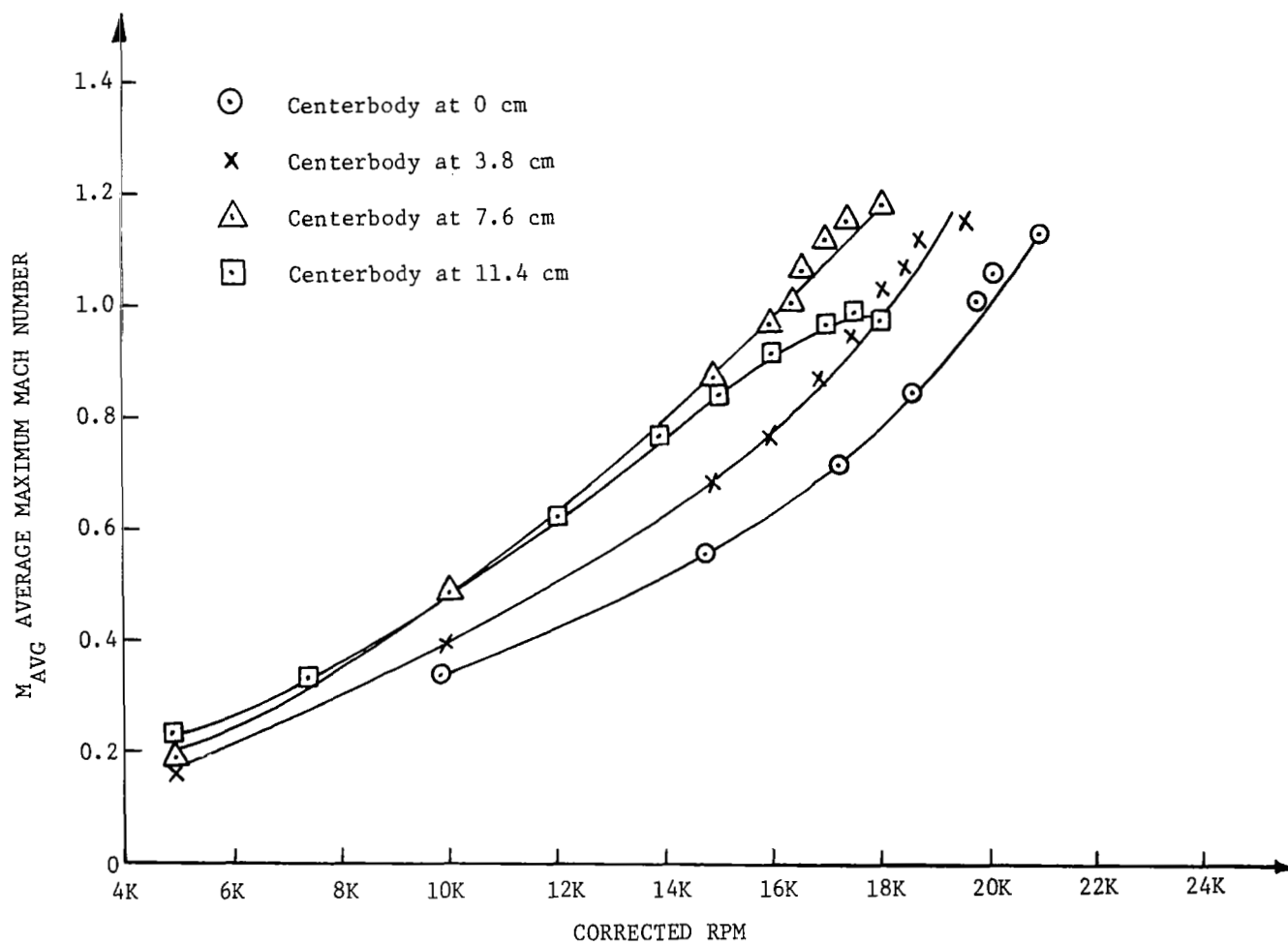


FIG.30 AVERAGE MAXIMUM MACH NUMBER OF INLET CONFIGURATION 2

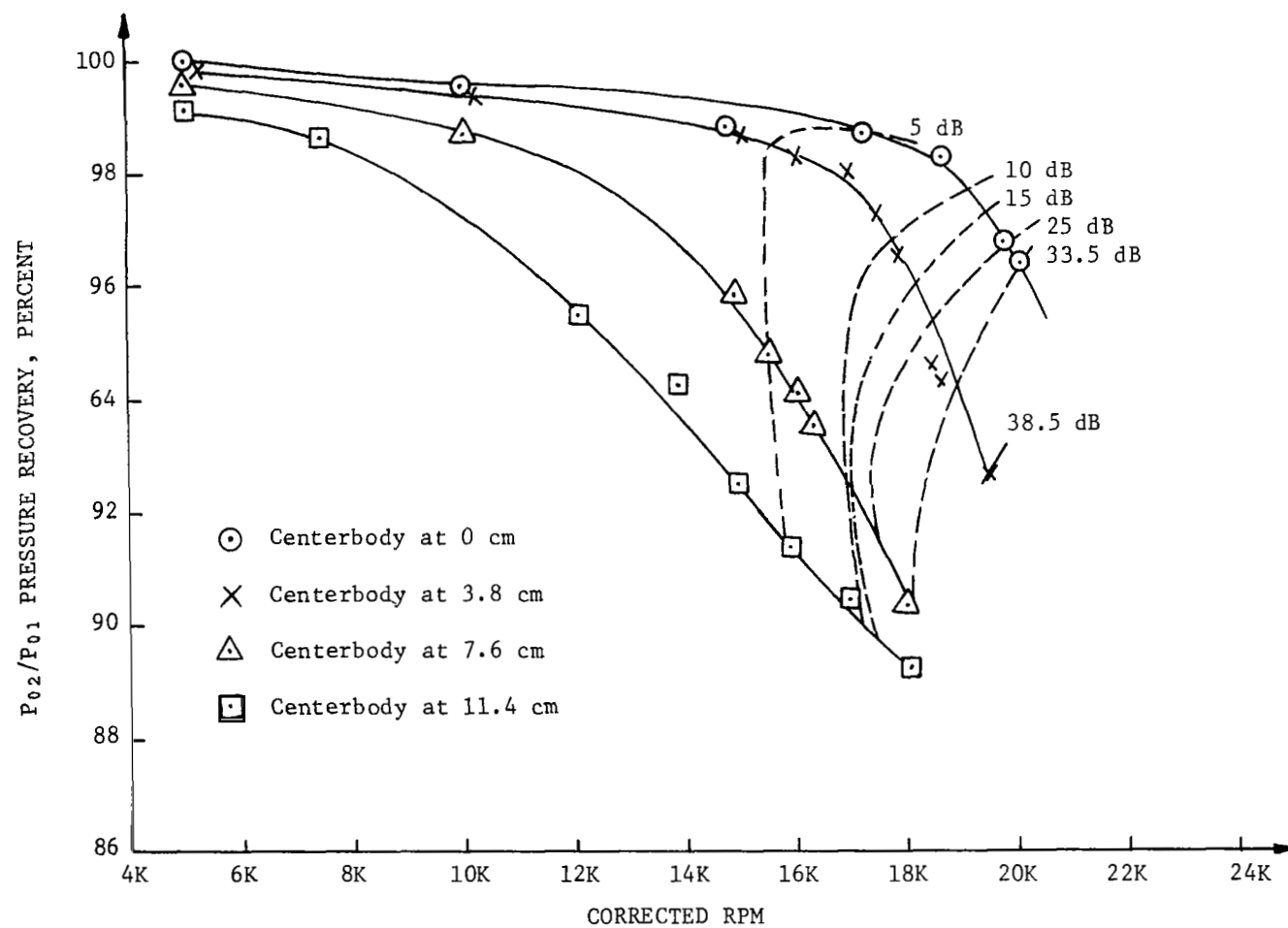


FIG.31 PRESSURE RECOVERY FOR INLET CONFIGURATION 2

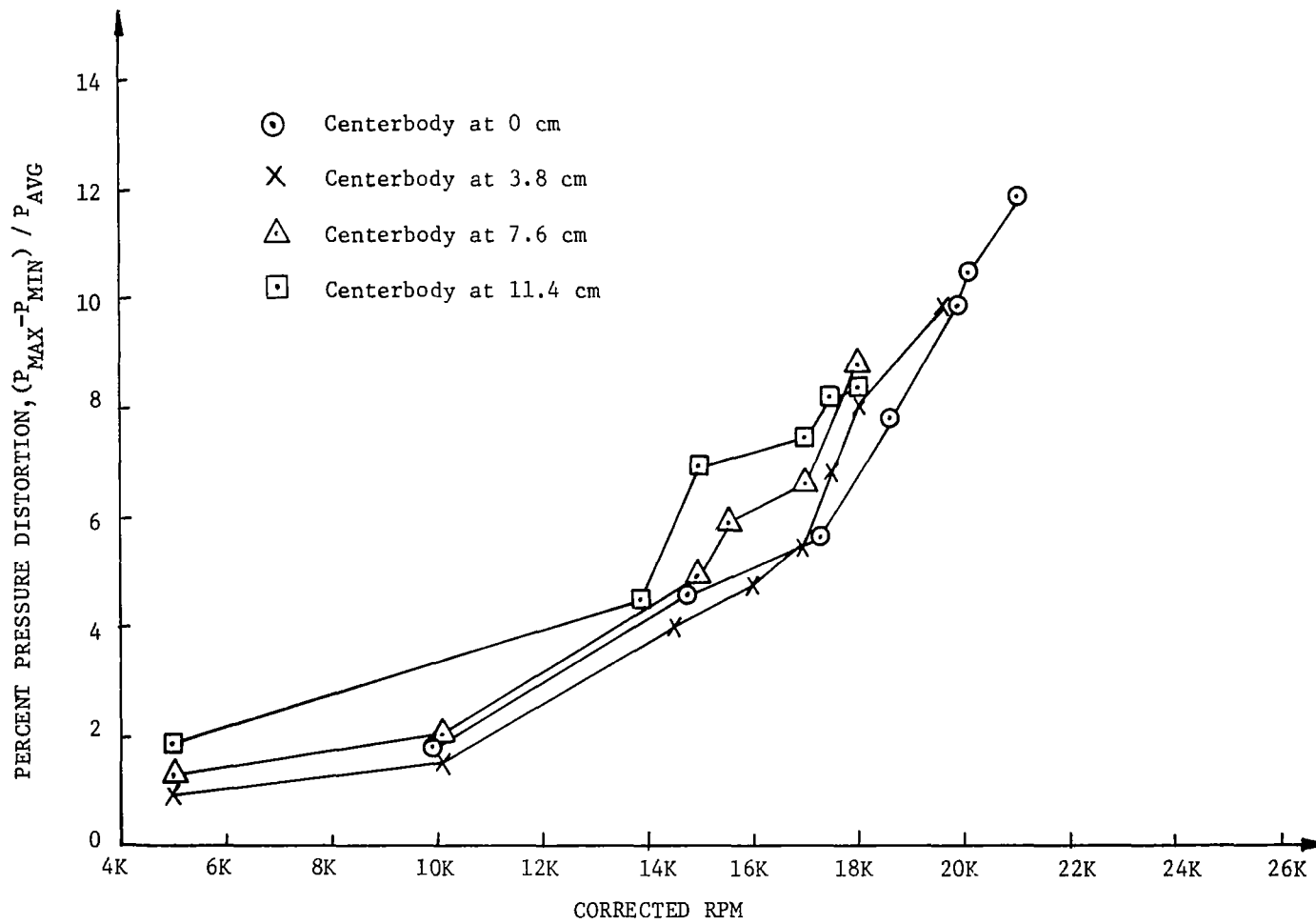


FIG.32 PRESSURE DISTORTION FOR INLET CONFIGURATION 2

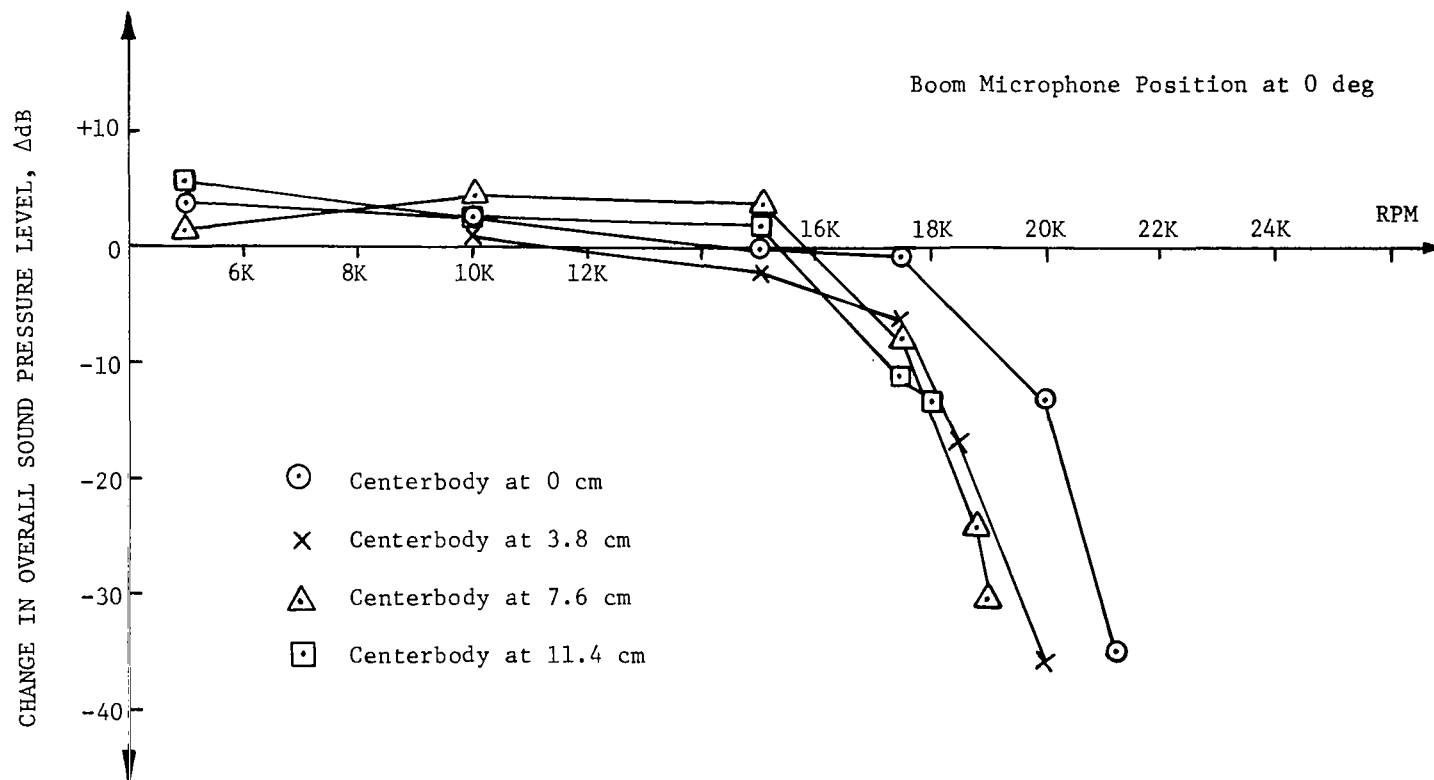


FIG.33 NOISE ATTENUATION FOR INLET CONFIGURATION 3

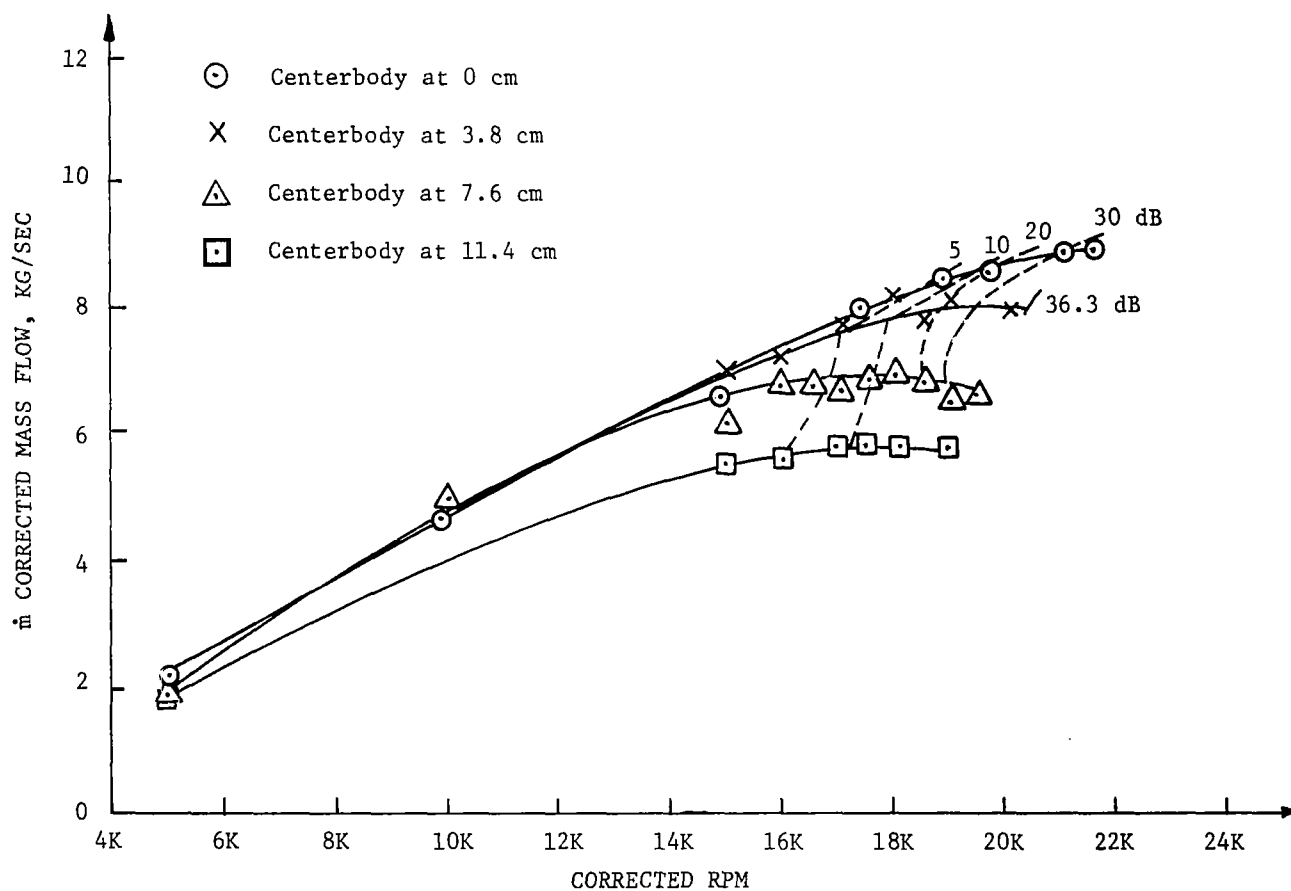


FIG.34 MASS FLOW FOR INLET CONFIGURATION 3

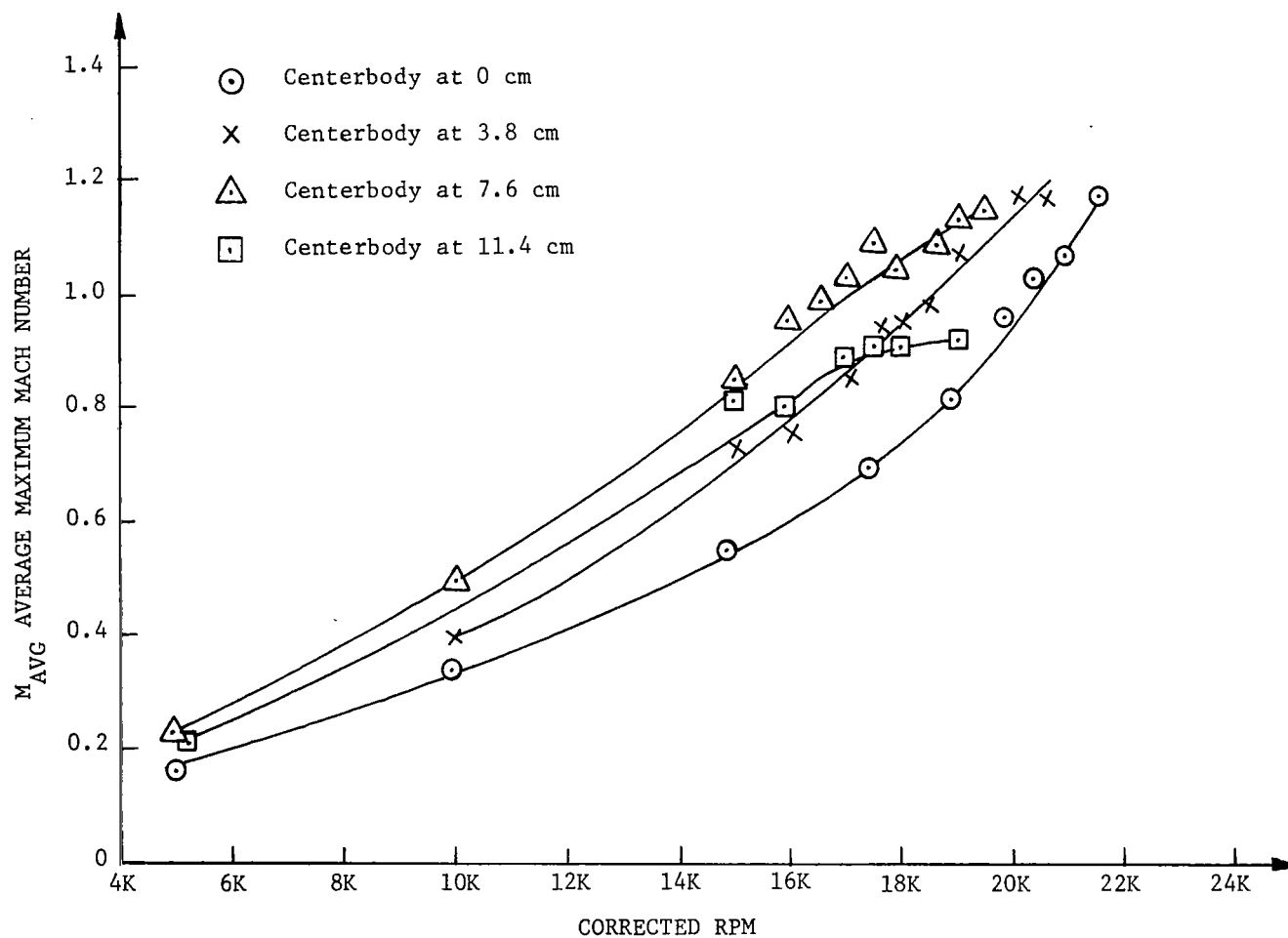


FIG.35 AVERAGE MAXIMUM MACH NUMBER FOR INLET CONFIGURATION 3

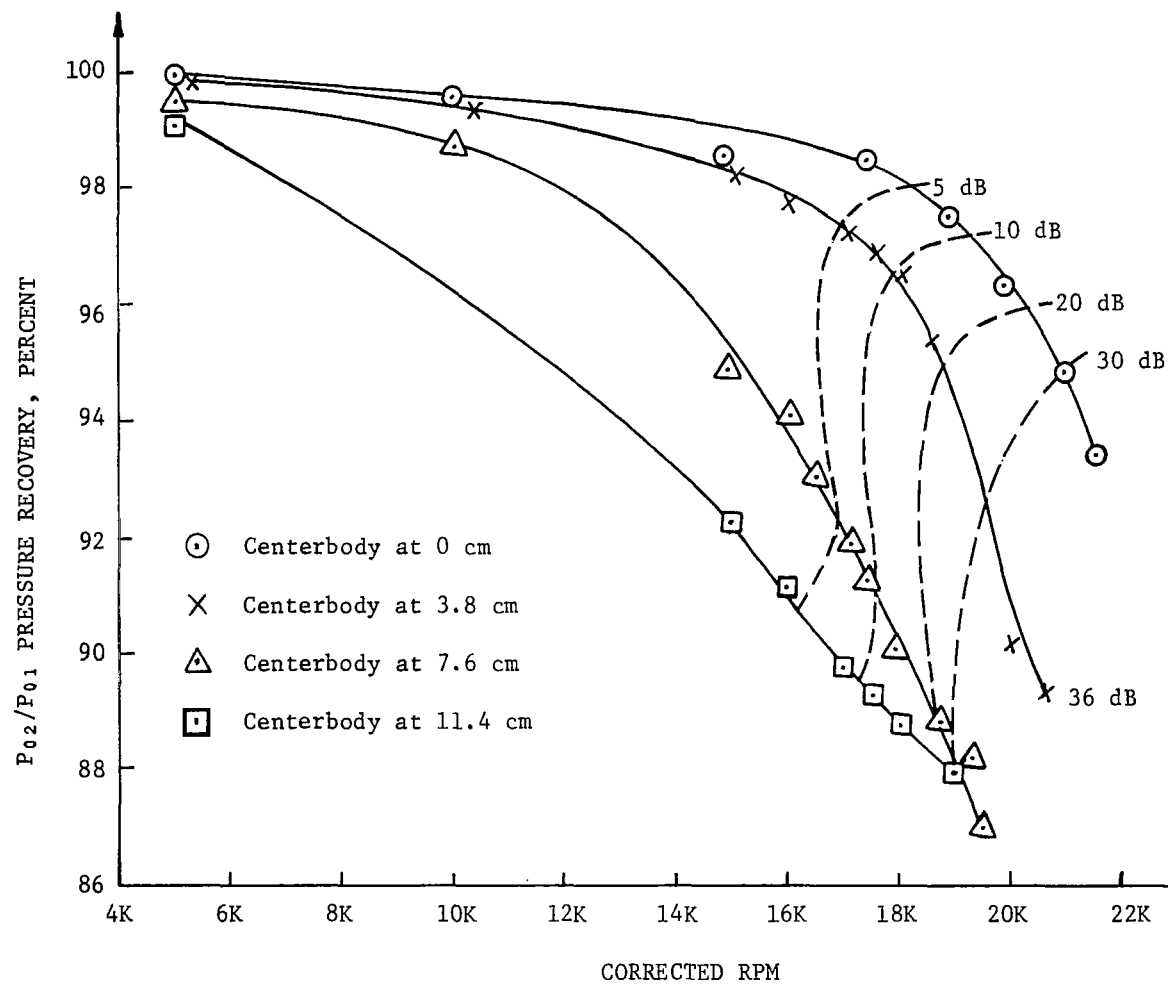


FIG.36 PRESSURE RECOVERY FOR INLET CONFIGURATION 3

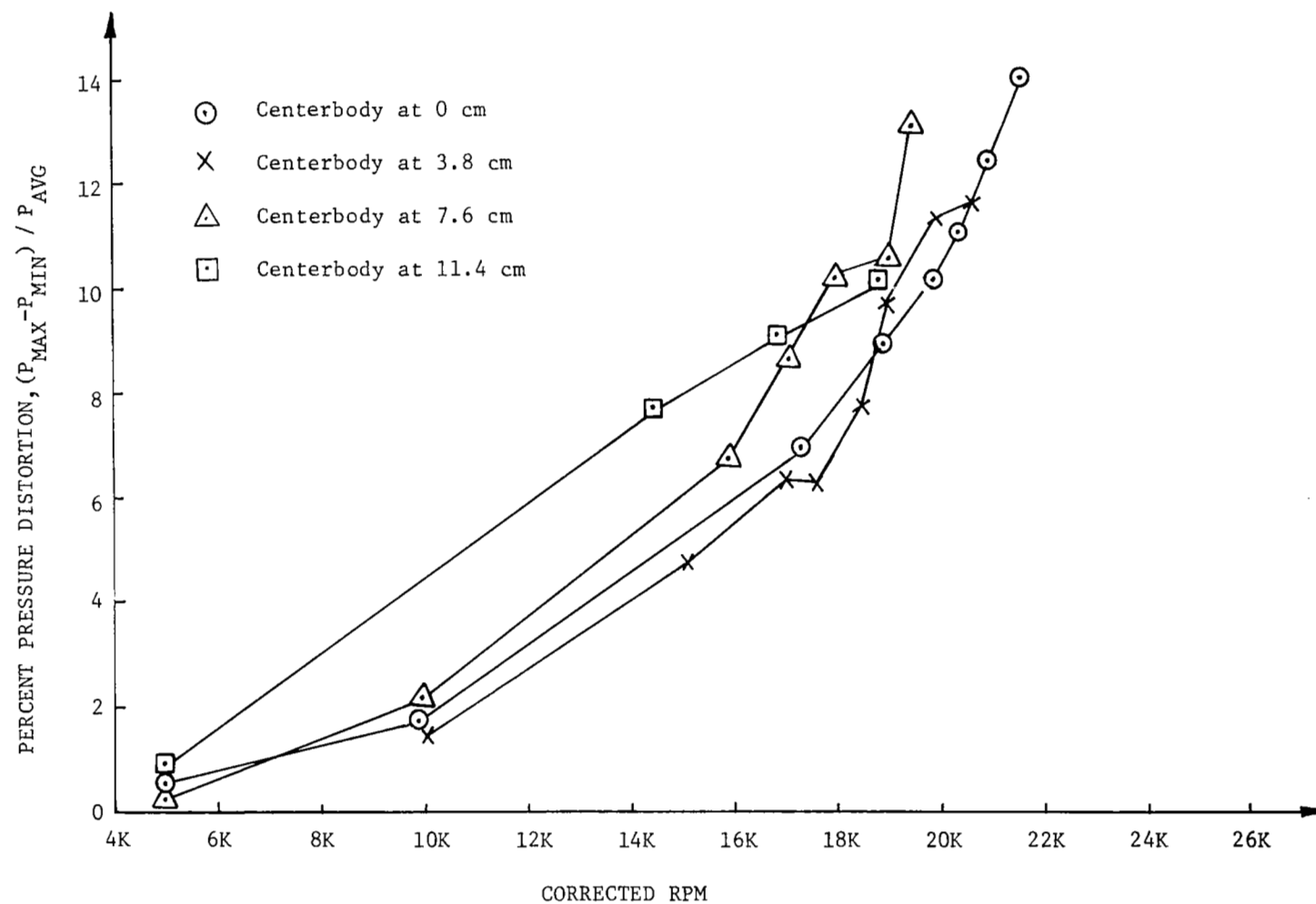


FIG.37 PRESSURE DISTORTION FOR INLET CONFIGURATION 3

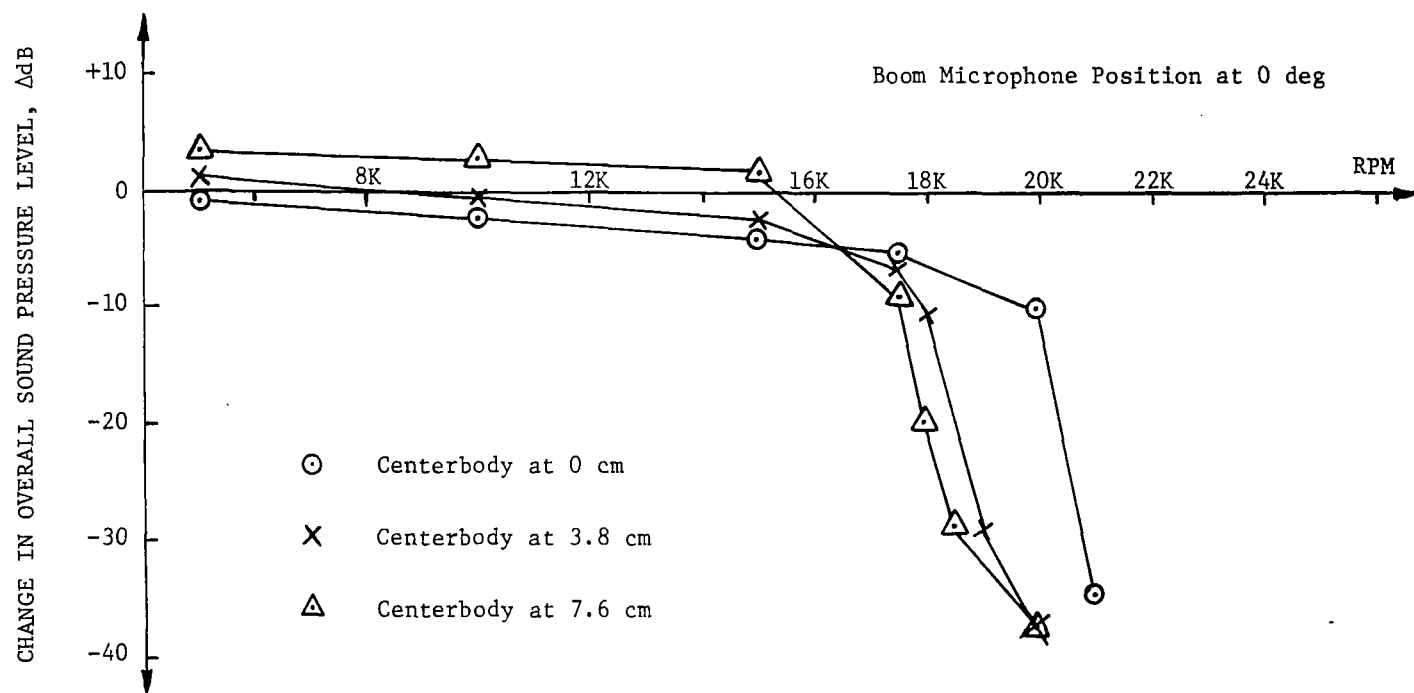


FIG.38 NOISE ATTENUATION FOR INLET CONFIGURATION 4

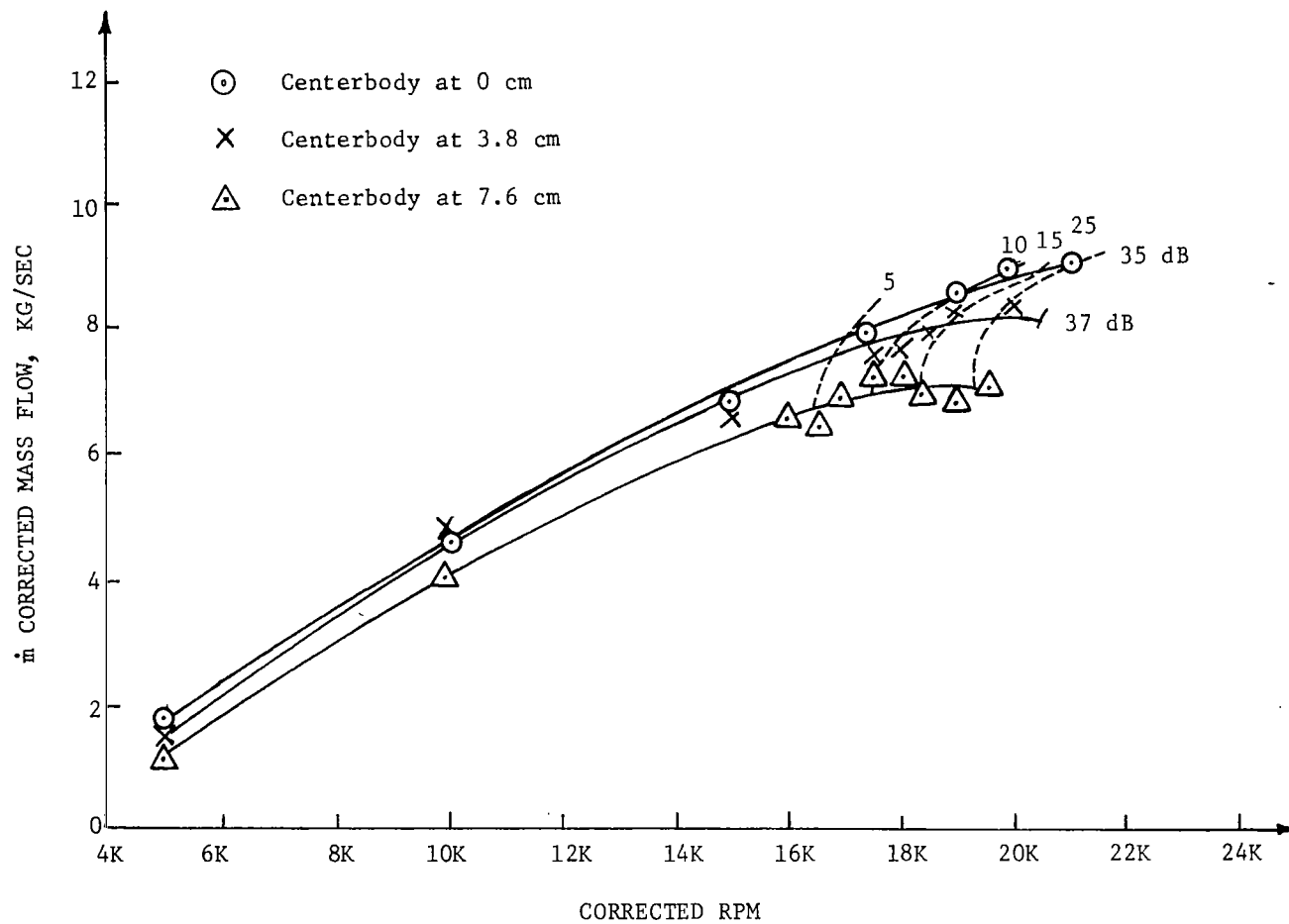


FIG.39 MASS FLOW FOR INLET CONFIGURATION 4

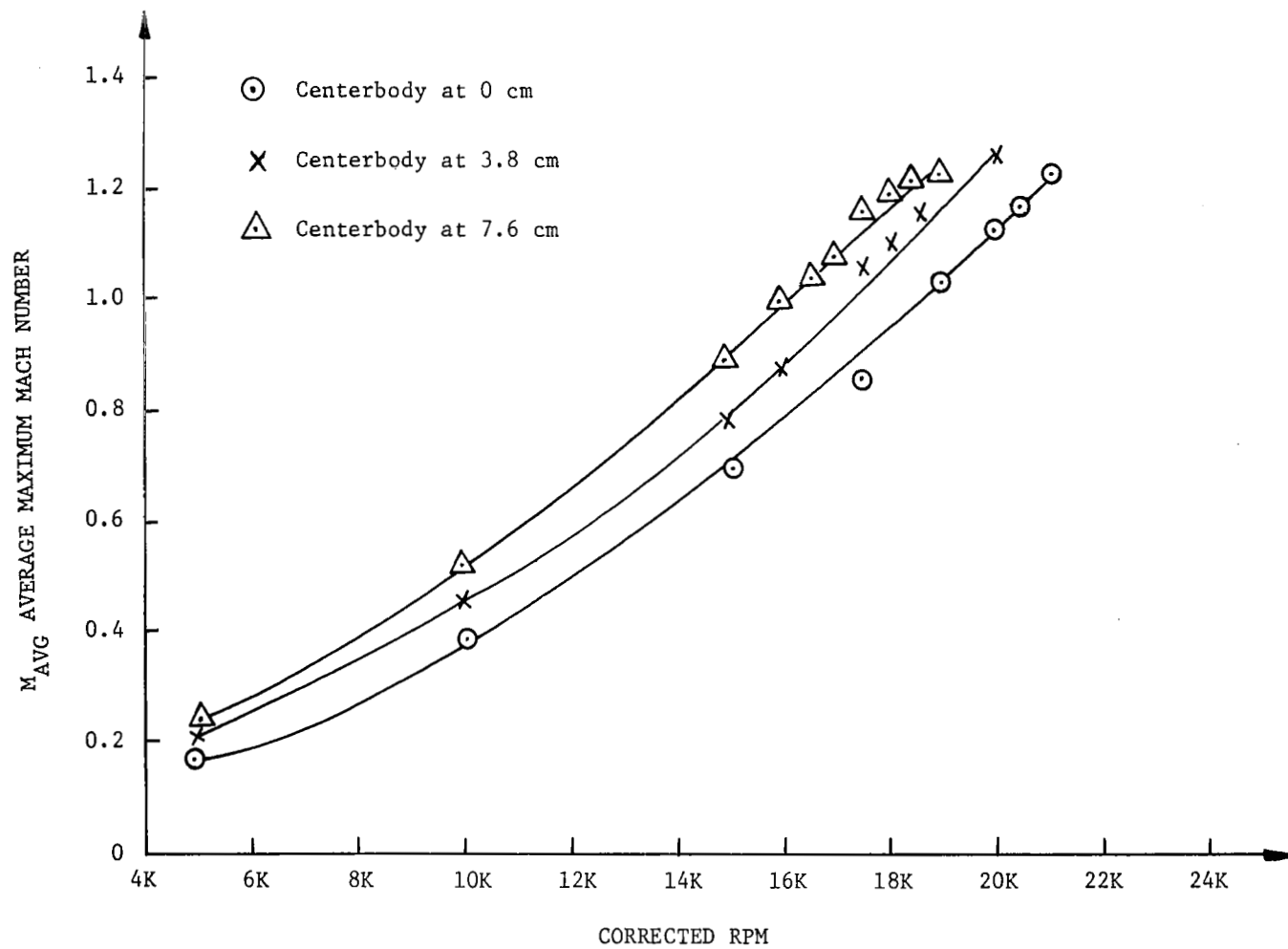


FIG.40 AVERAGE MAXIMUM MACH NUMBER FOR INLET CONFIGURATION 4

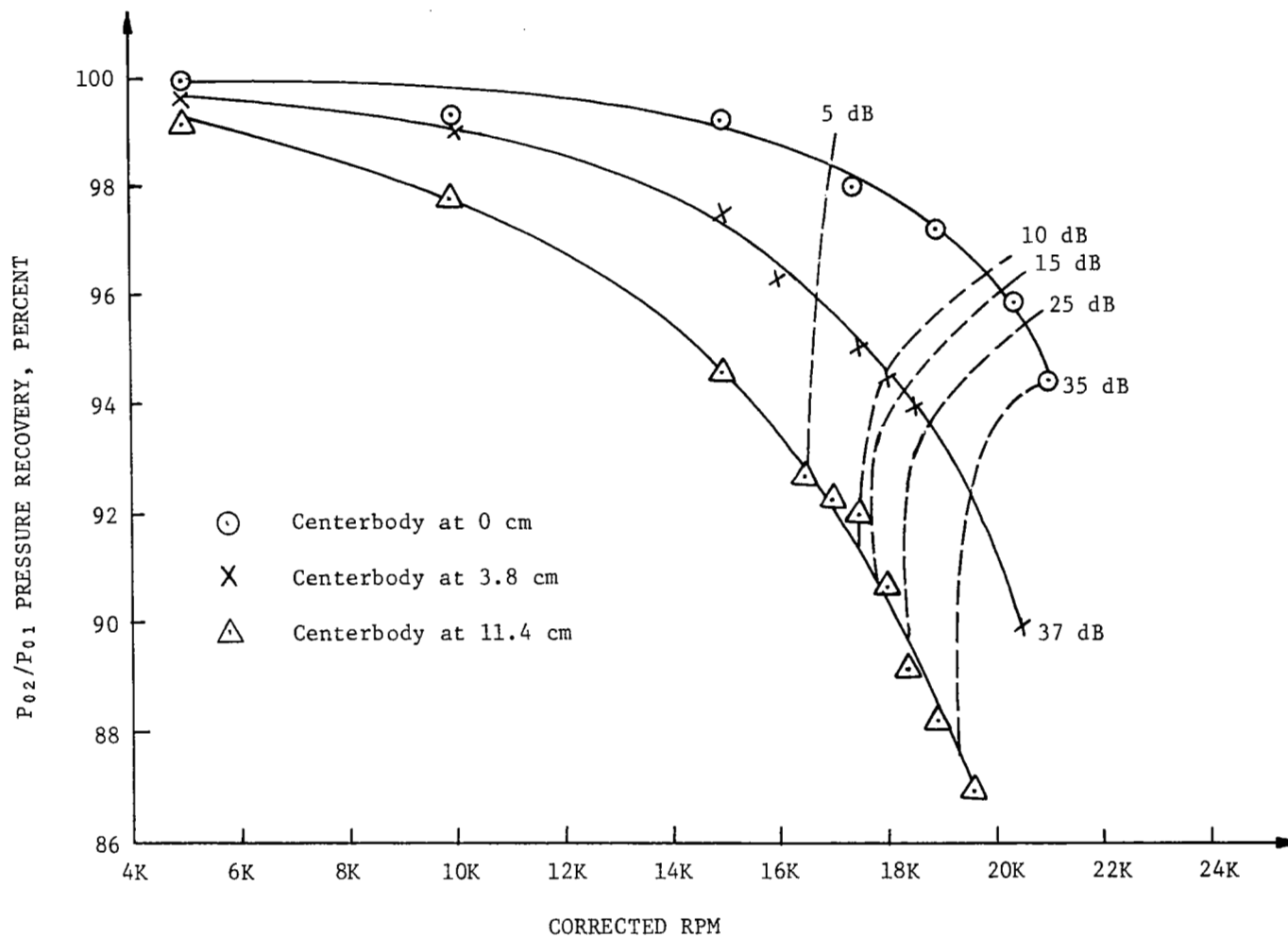


FIG.41 PRESSURE RECOVERY FOR INLET CONFIGURATION 4

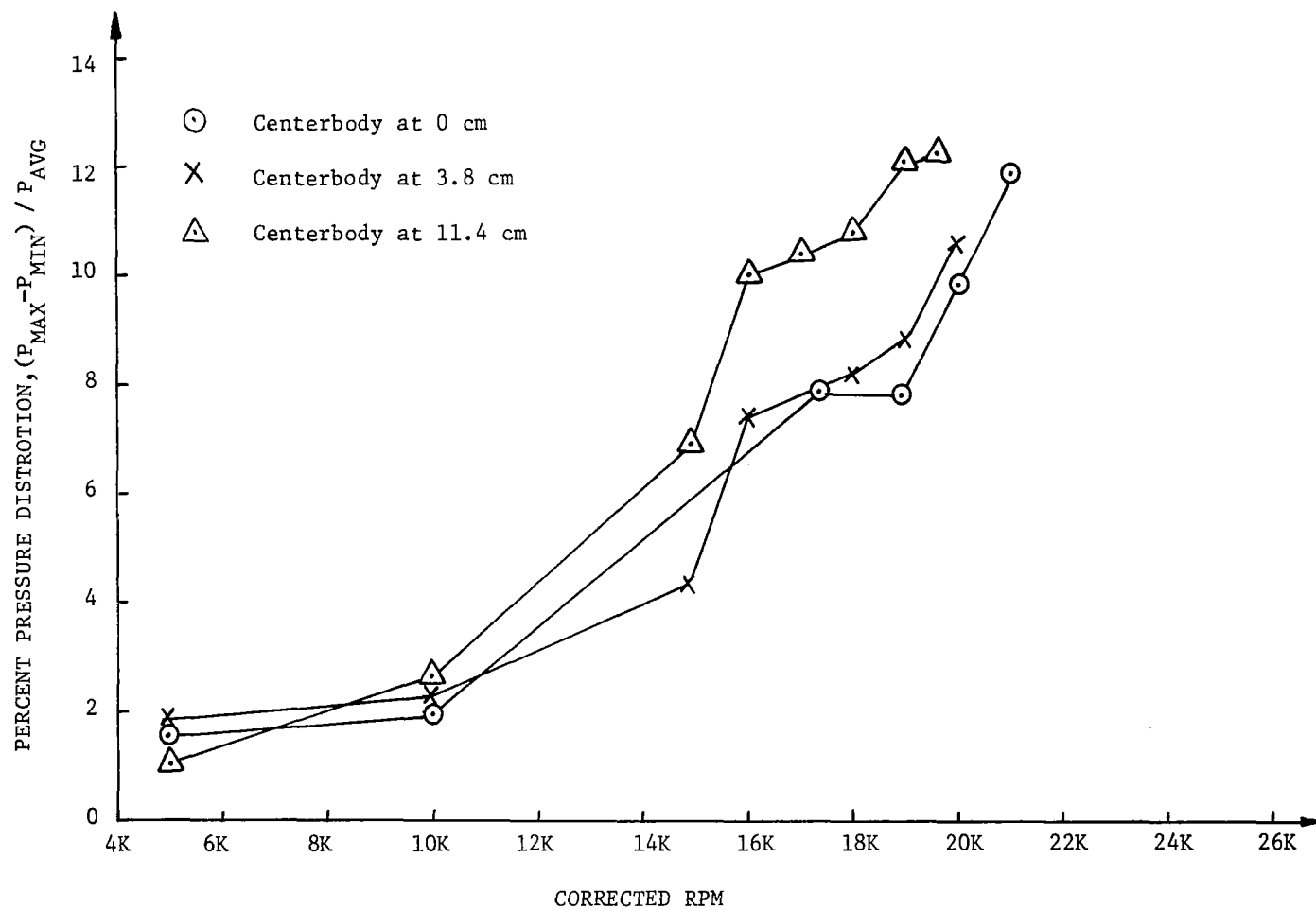


FIG.42 PRESSURE DISTORTION FOR INLET CONFIGURATION 4

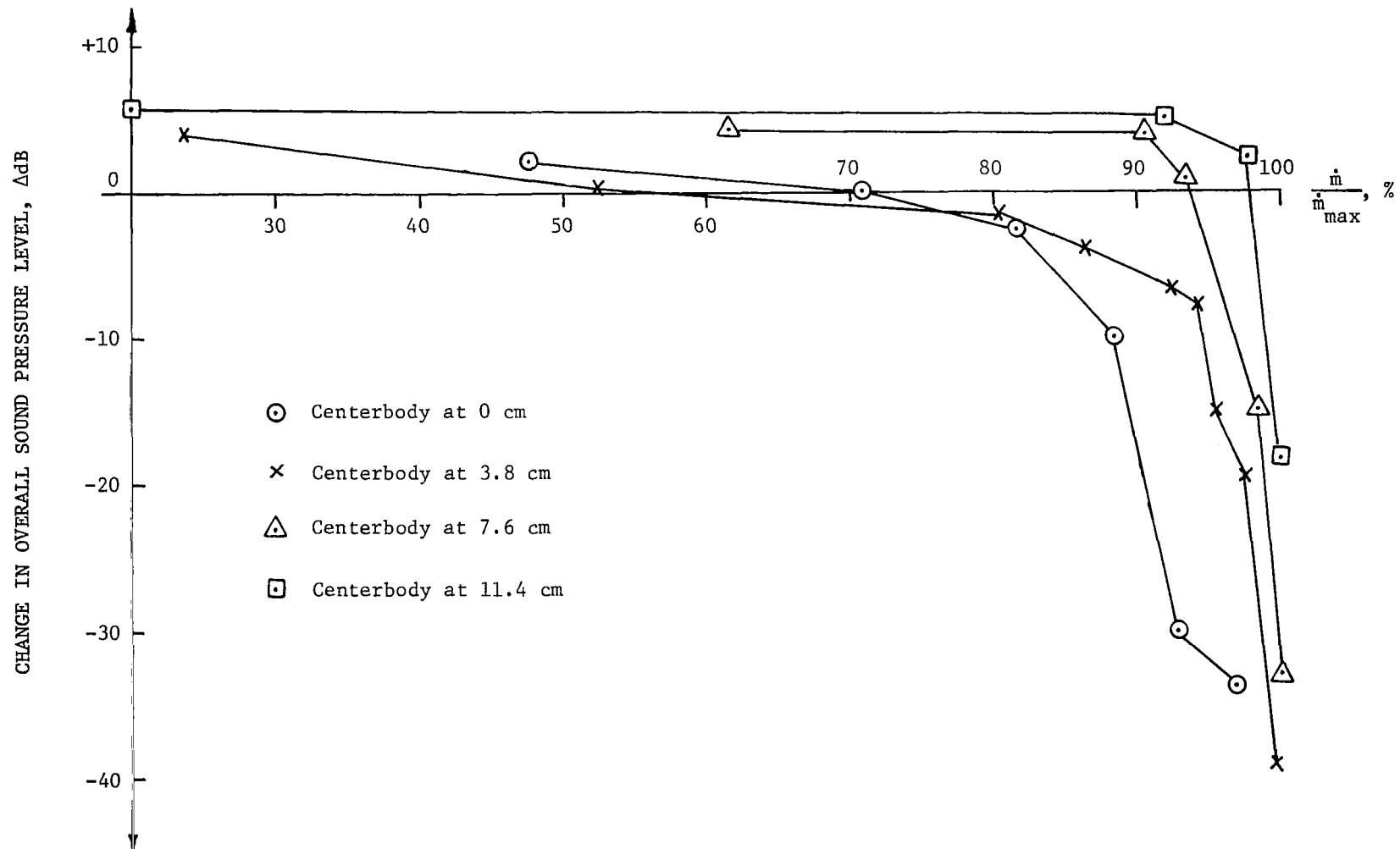


FIG.43 EFFECT OF PERCENTAGE OF MAXIMUM MASS FLOW ON NOISE ATTENUATION FOR INLET CONFIGURATION 2

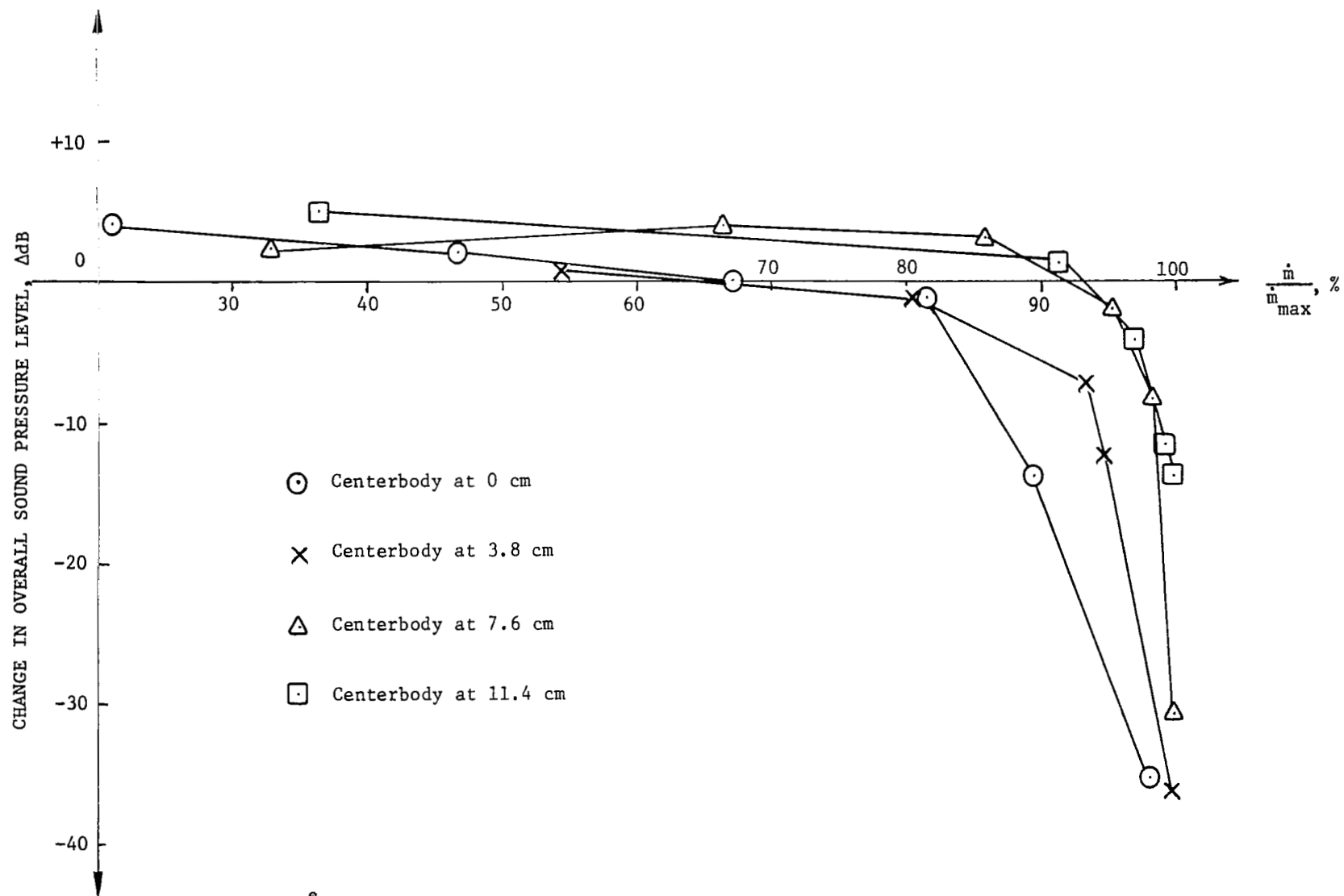


FIG.44 EFFECT OF PERCENTAGE OF MAXIMUM MASS FLOW ON NOISE ATTENUATION FOR INLET CONFIGURATION 3

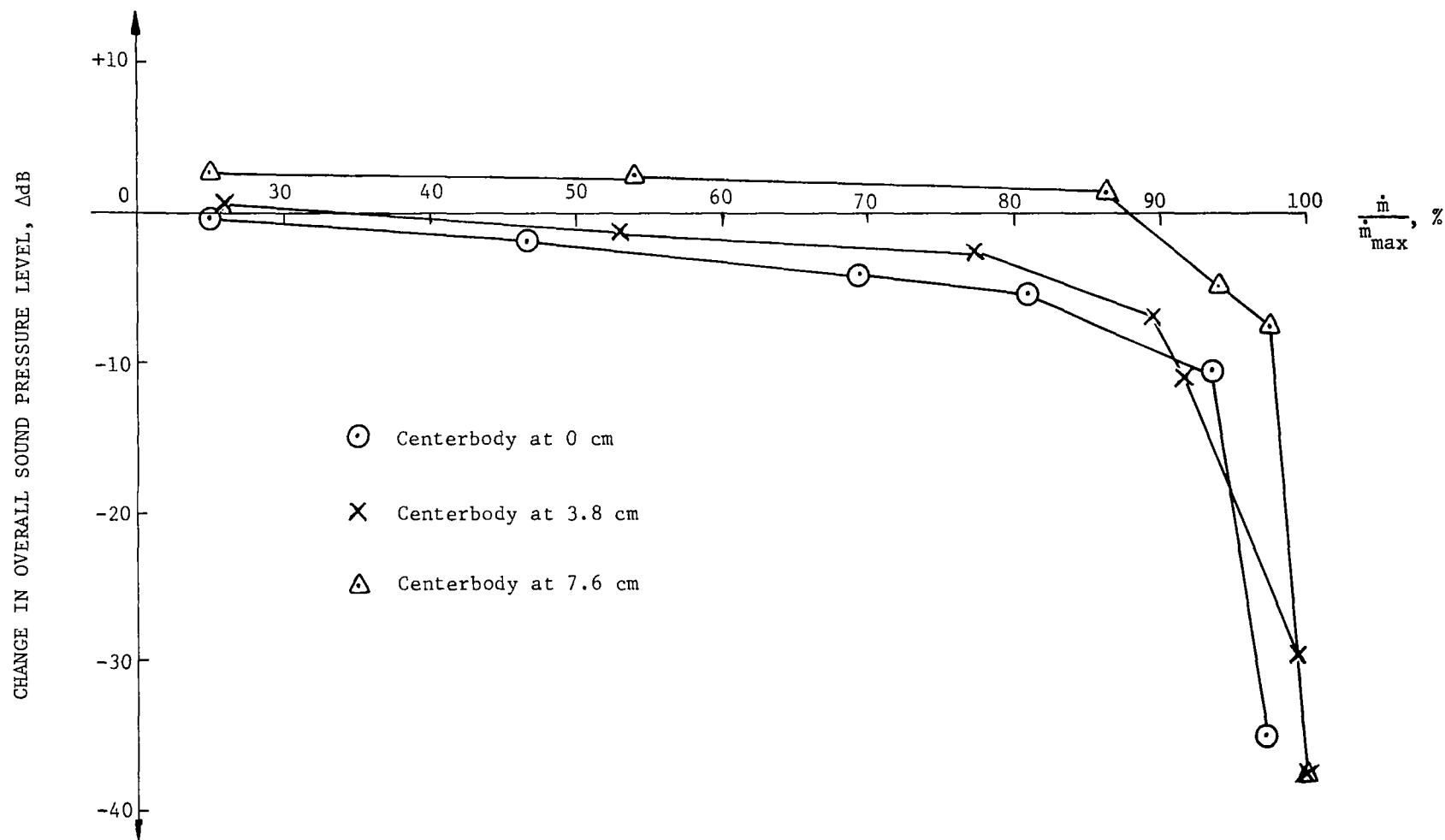


FIG.45 EFFECT OF PERCENTAGE OF MAXIMUM MASS FLOW ON NOISE ATTENUATION FOR INLET CONFIGURATION 4

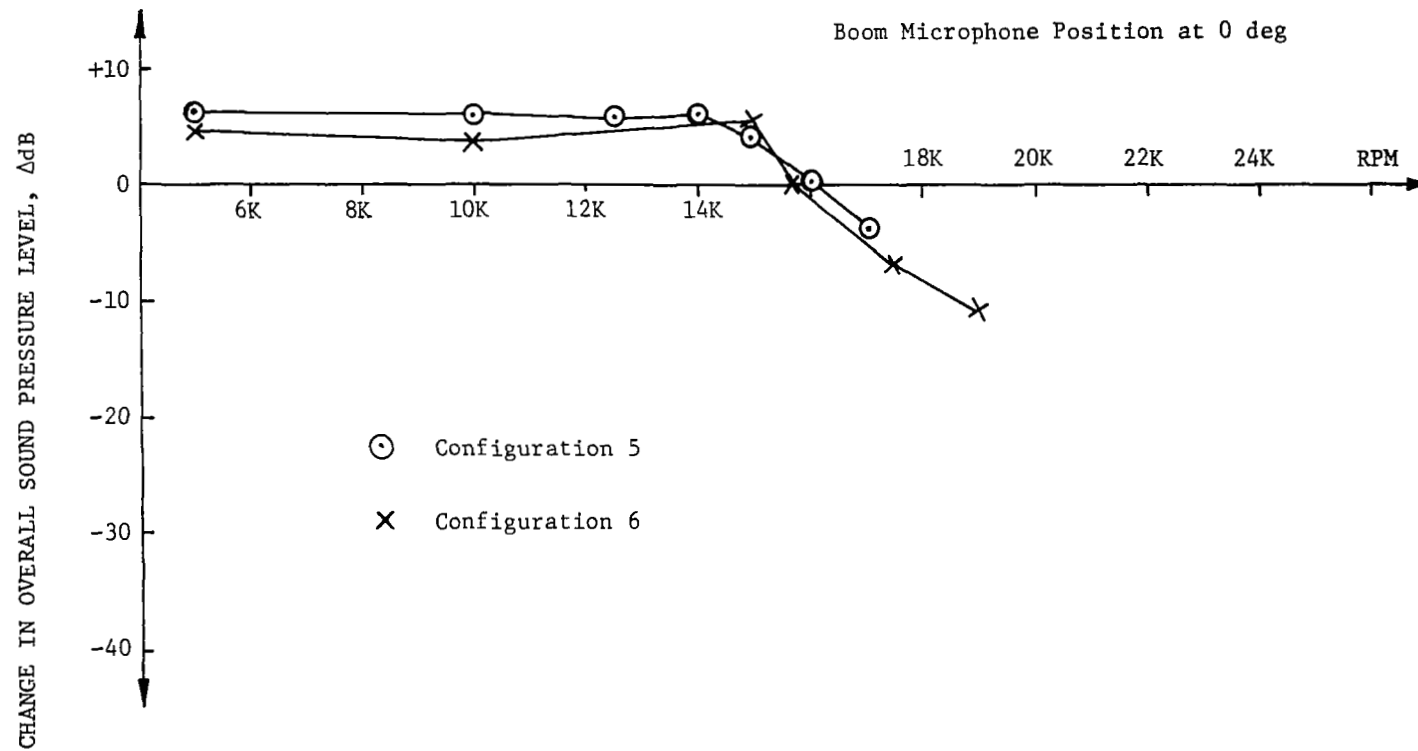


FIG.46 NOISE ATTENUATION FOR INLET CONFIGURATIONS 5 AND 6

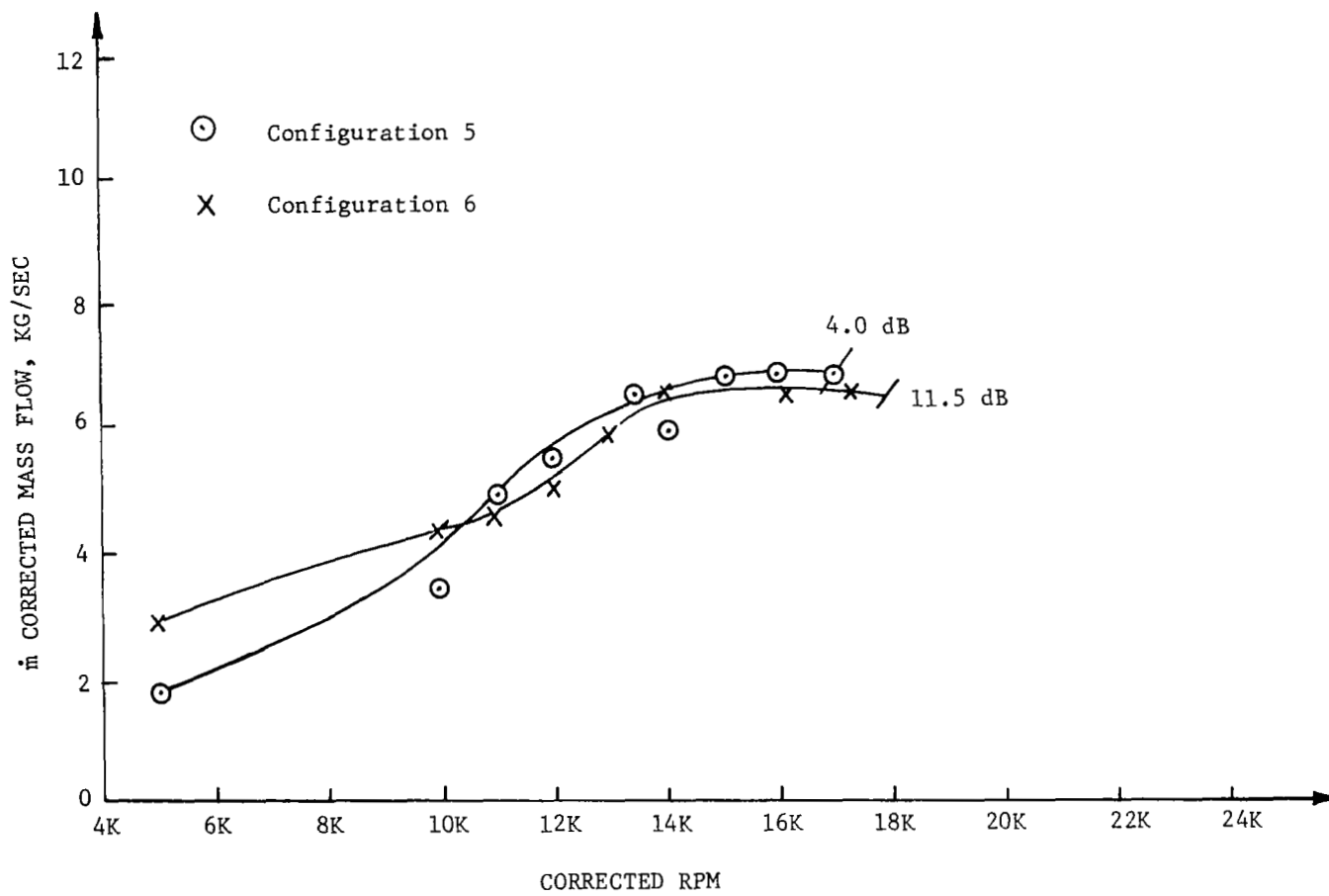


FIG.47 MASS FLOW FOR INLET CONFIGURATIONS 5 AND 6

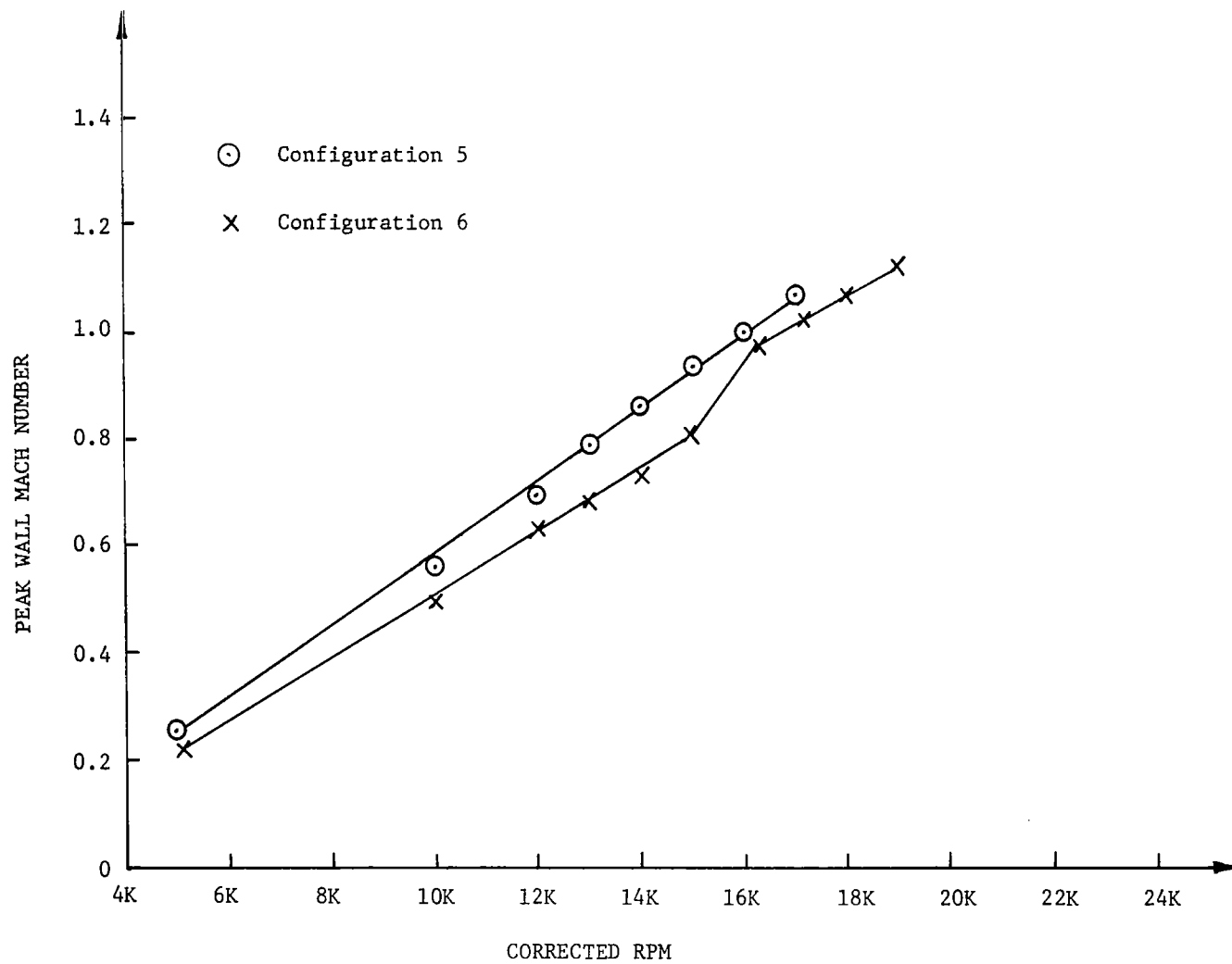


FIG.48 PEAK WALL MACH NUMBER OF INLET CONFIGURATIONS 5 AND 6

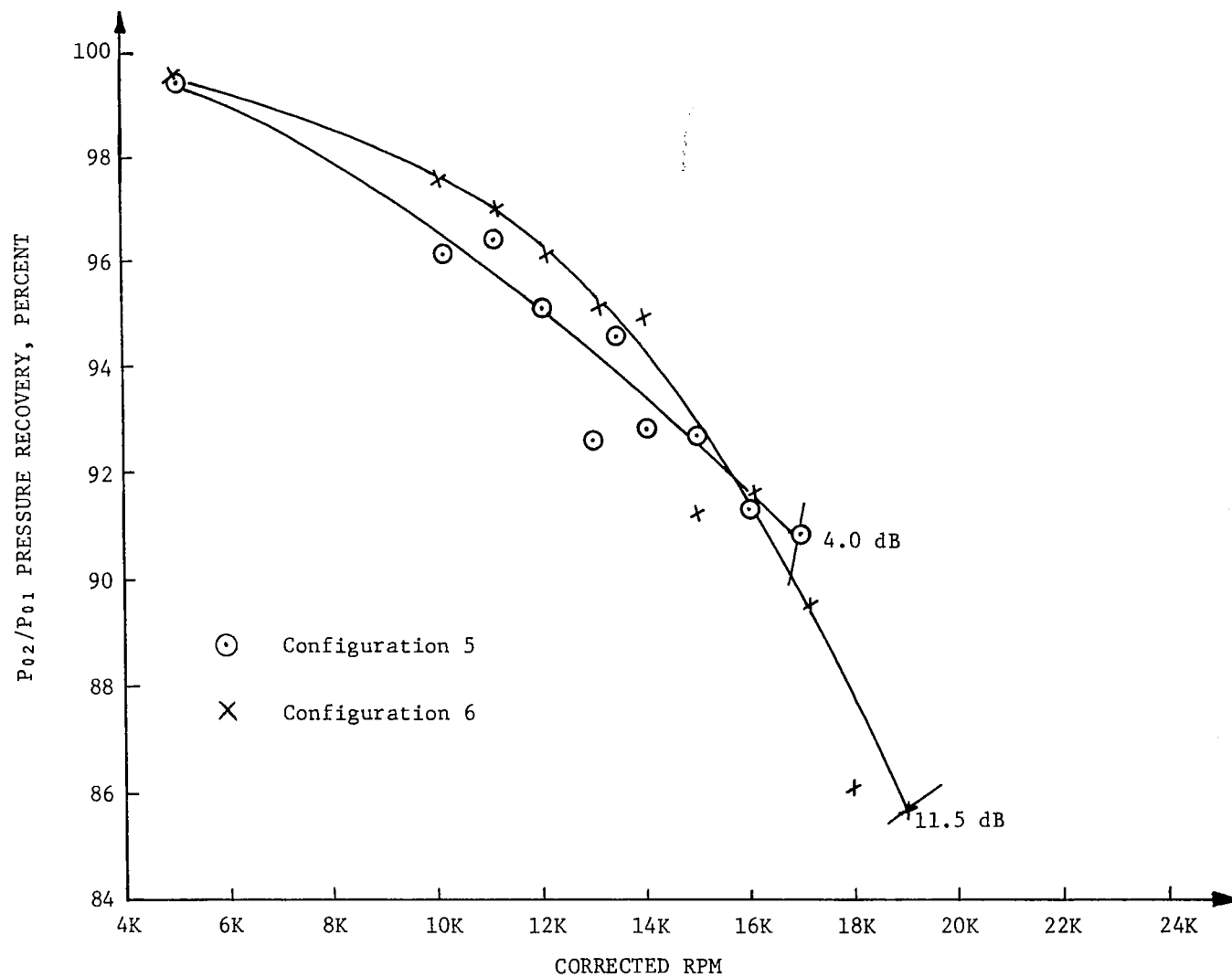


FIG.49 PRESSURE RECOVERY FOR INLET CONFIGURATIONS 5 AND 6

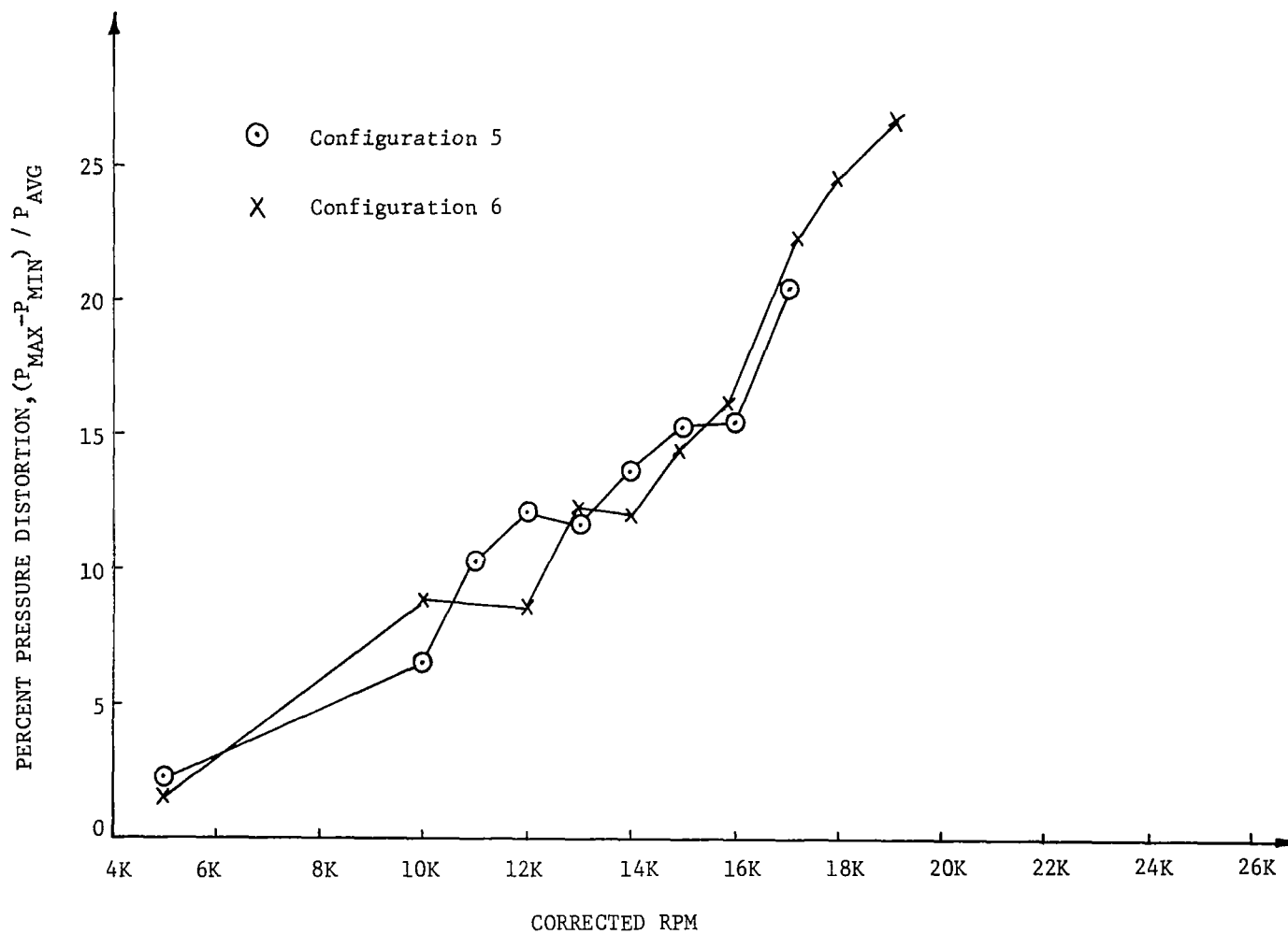


FIG.50 PRESSURE DISTORTION FOR INLET CONFIGURATIONS 5 AND 6

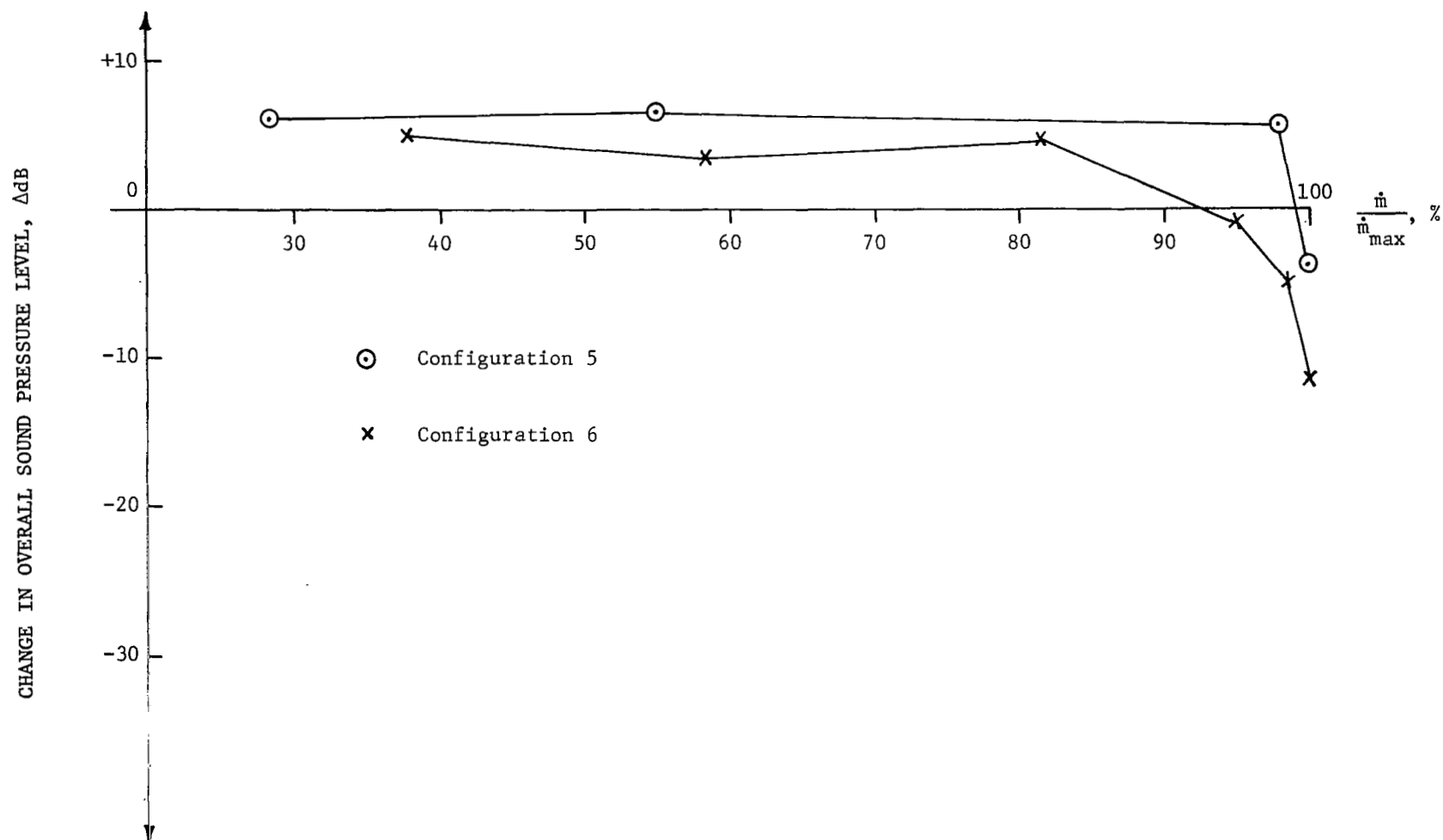


FIG.51 EFFECT OF PERCENTAGE OF MAXIMUM MASS FLOW ON NOISE ATTENUATION FOR INLET CONFIGURATIONS 5 AND 6

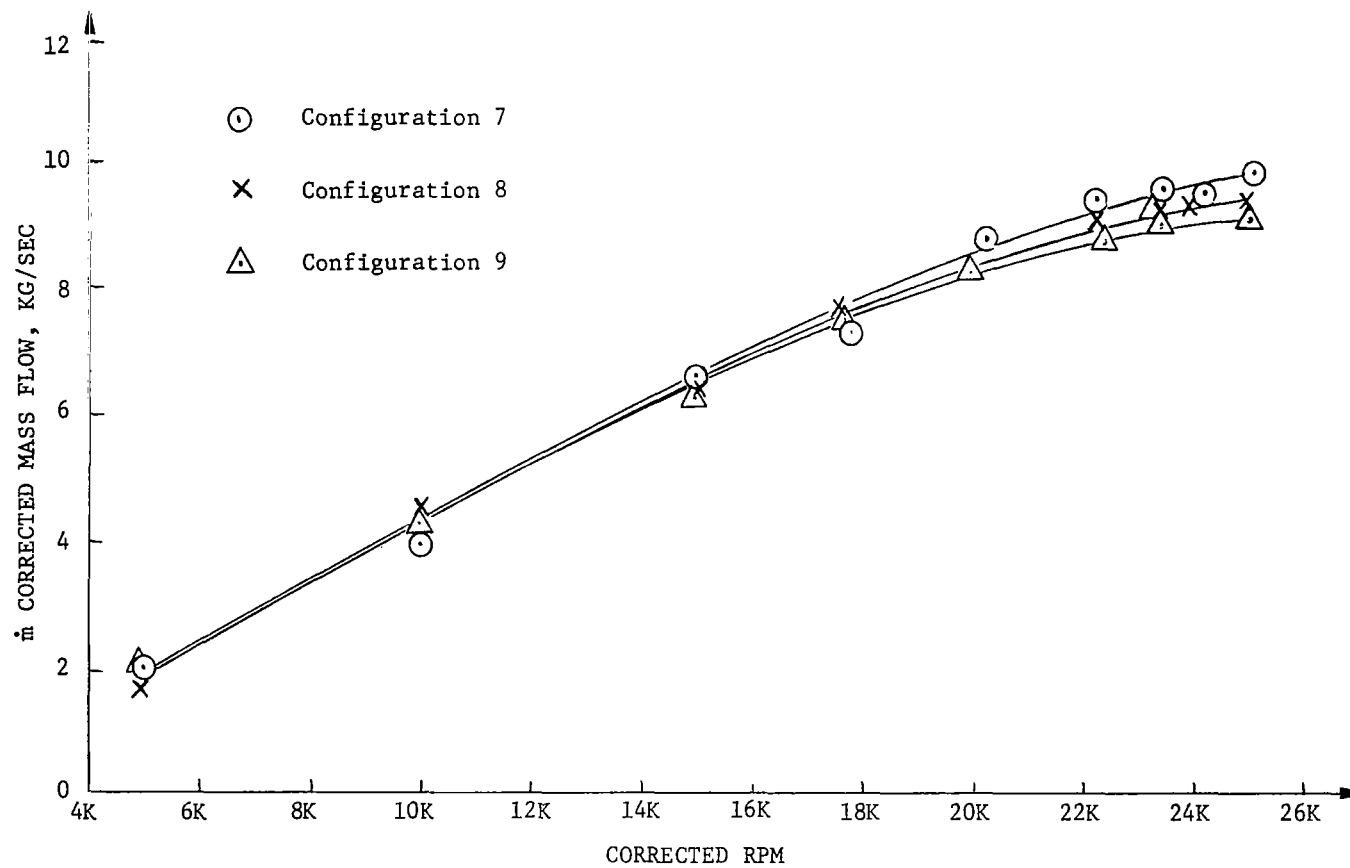


FIG.52 MASS FLOW FOR INLET CONFIGURATIONS 7, 8 AND 9

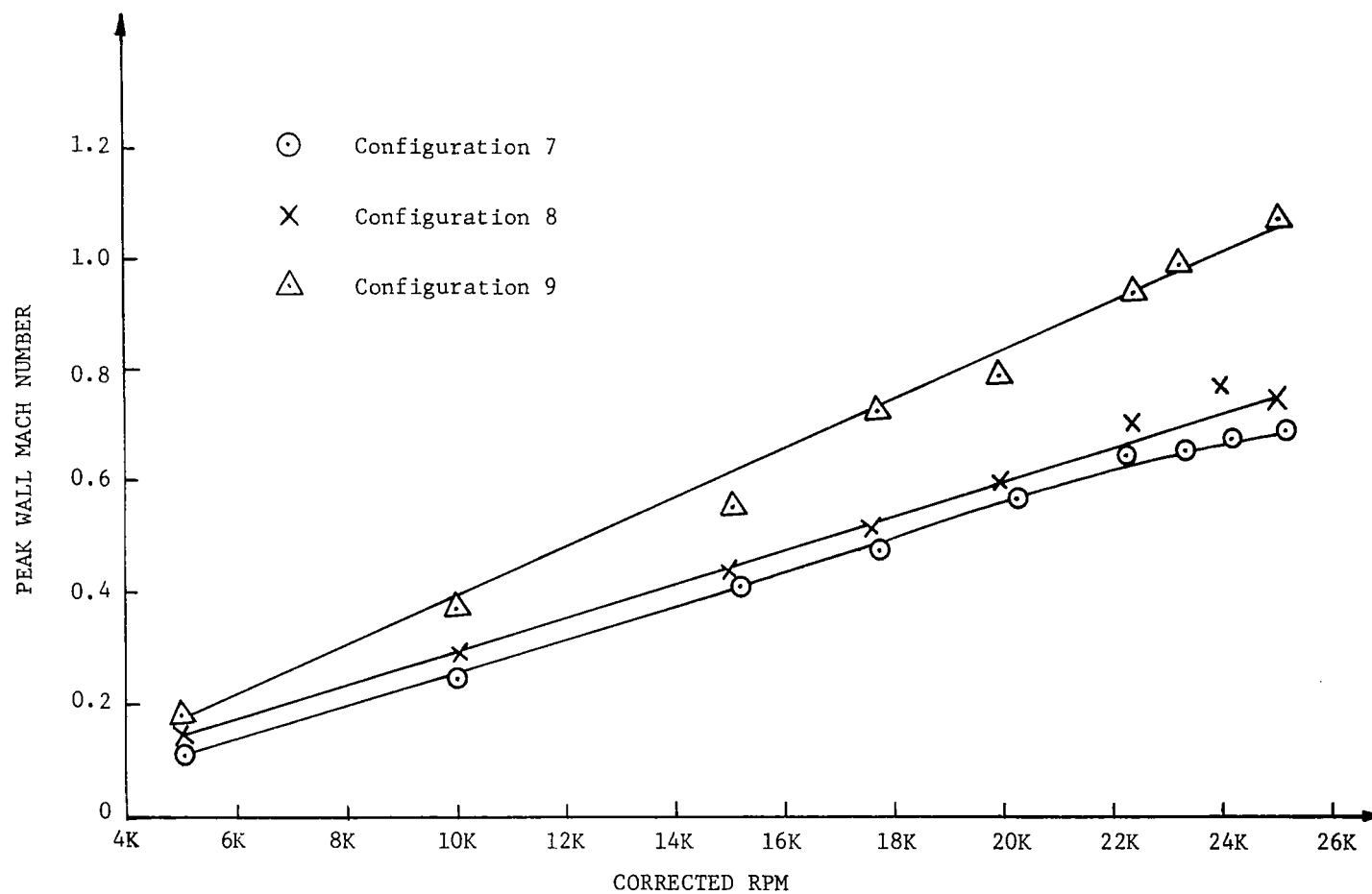


FIG.53 PEAK WALL MACH NUMBER OF INLET CONFIGURATIONS 7, 8 AND 9

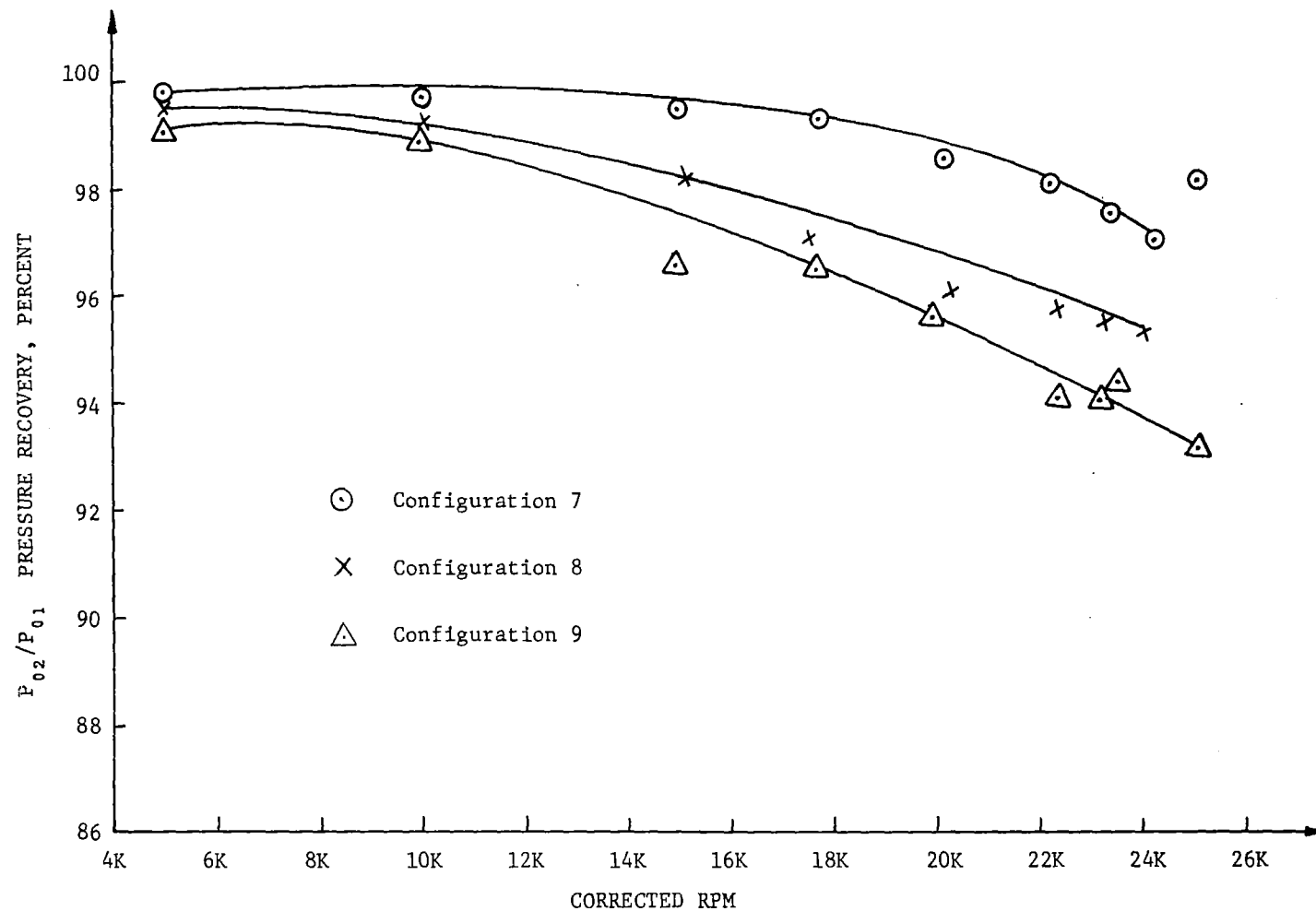


FIG.54 PRESSURE RECOVERY FOR INLET CONFIGURATIONS 7, 8 AND 9

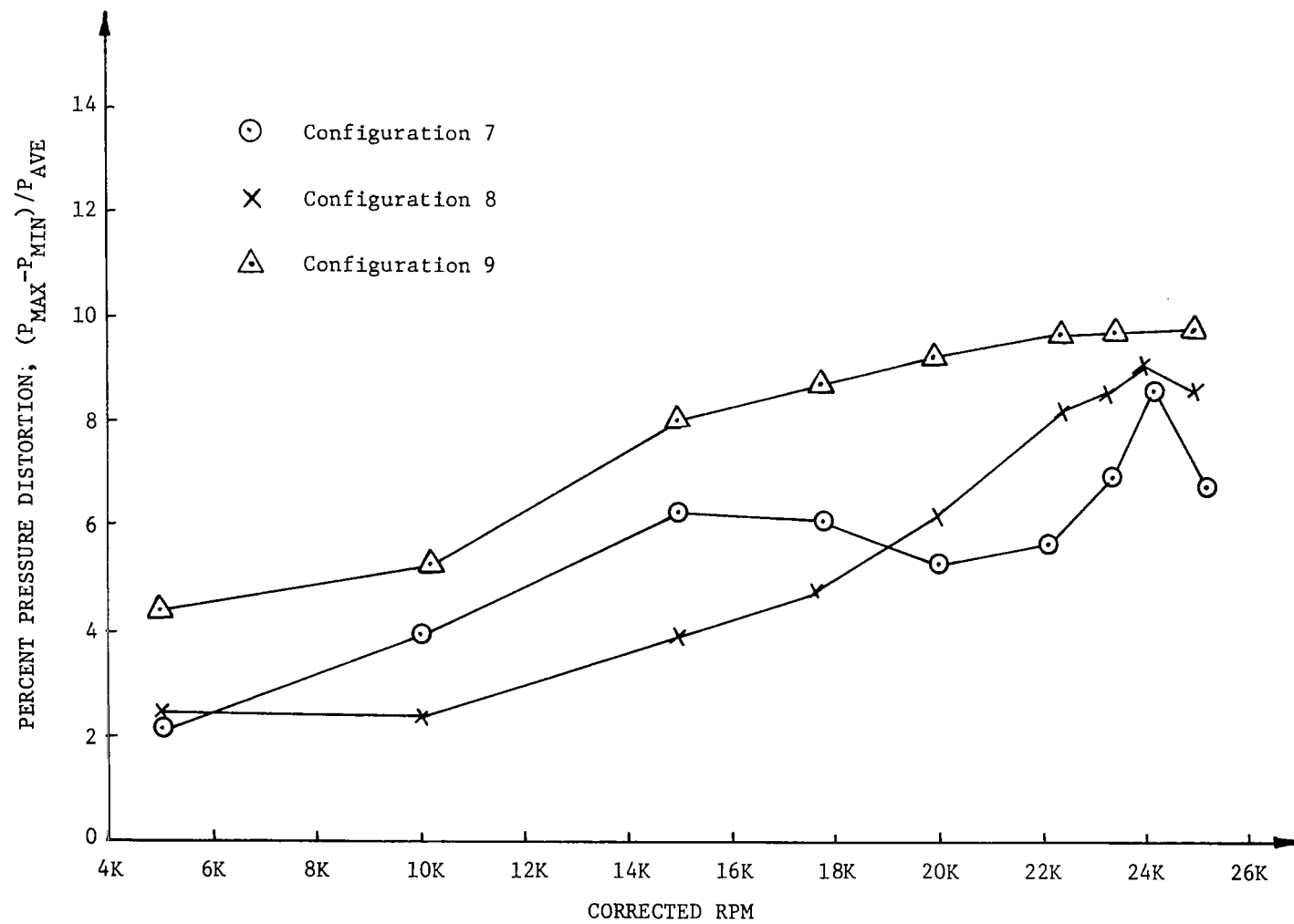


FIG.55 PRESSURE DISTORTION FOR CONFIGURATIONS 7,8,9

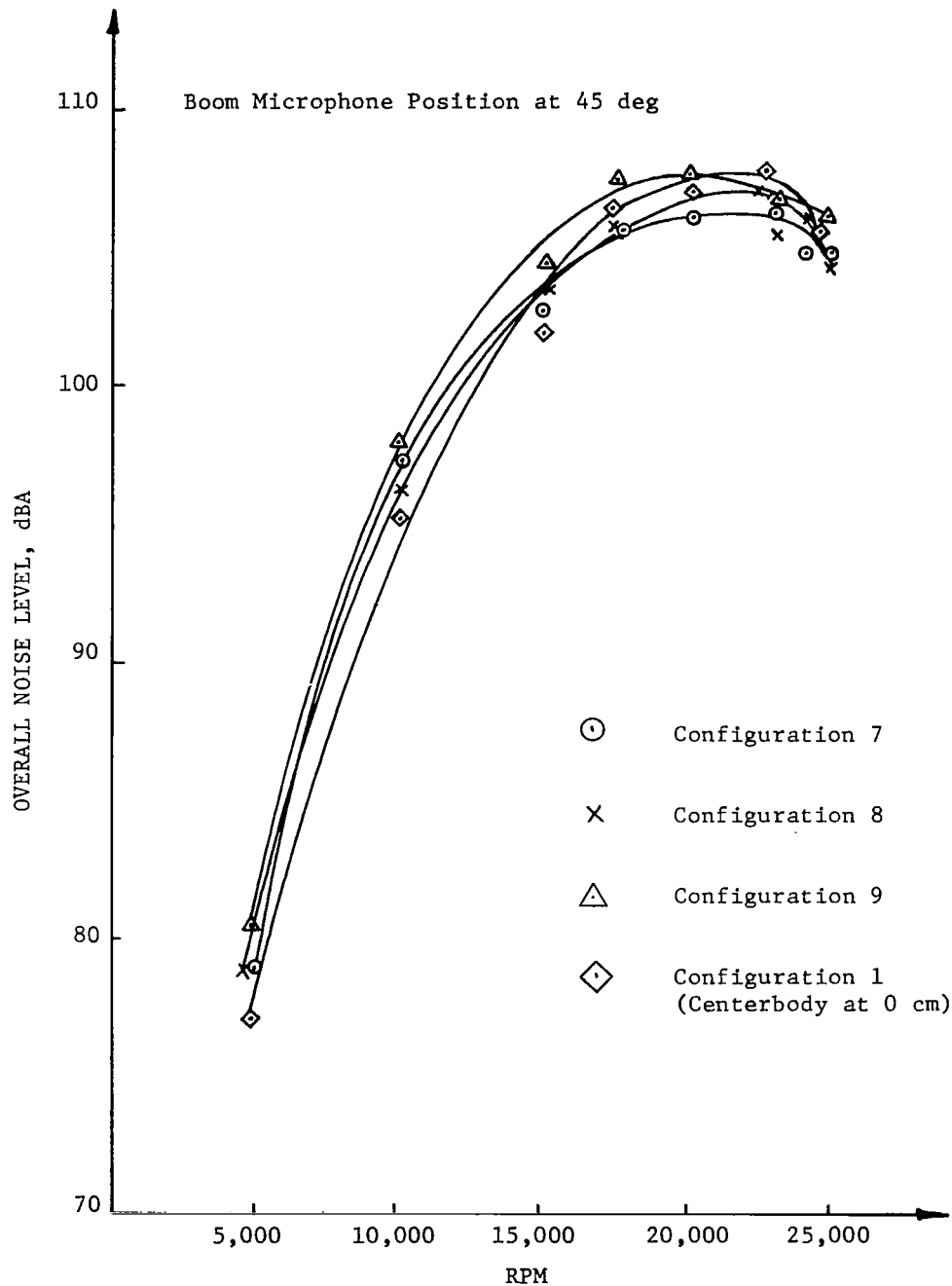


FIG.56 COMPARISON OF OVERALL NOISE ATTENUATION CHARACTERISTICS OF INLETS OPERATING AT SUBSONIC MACH NUMBERS

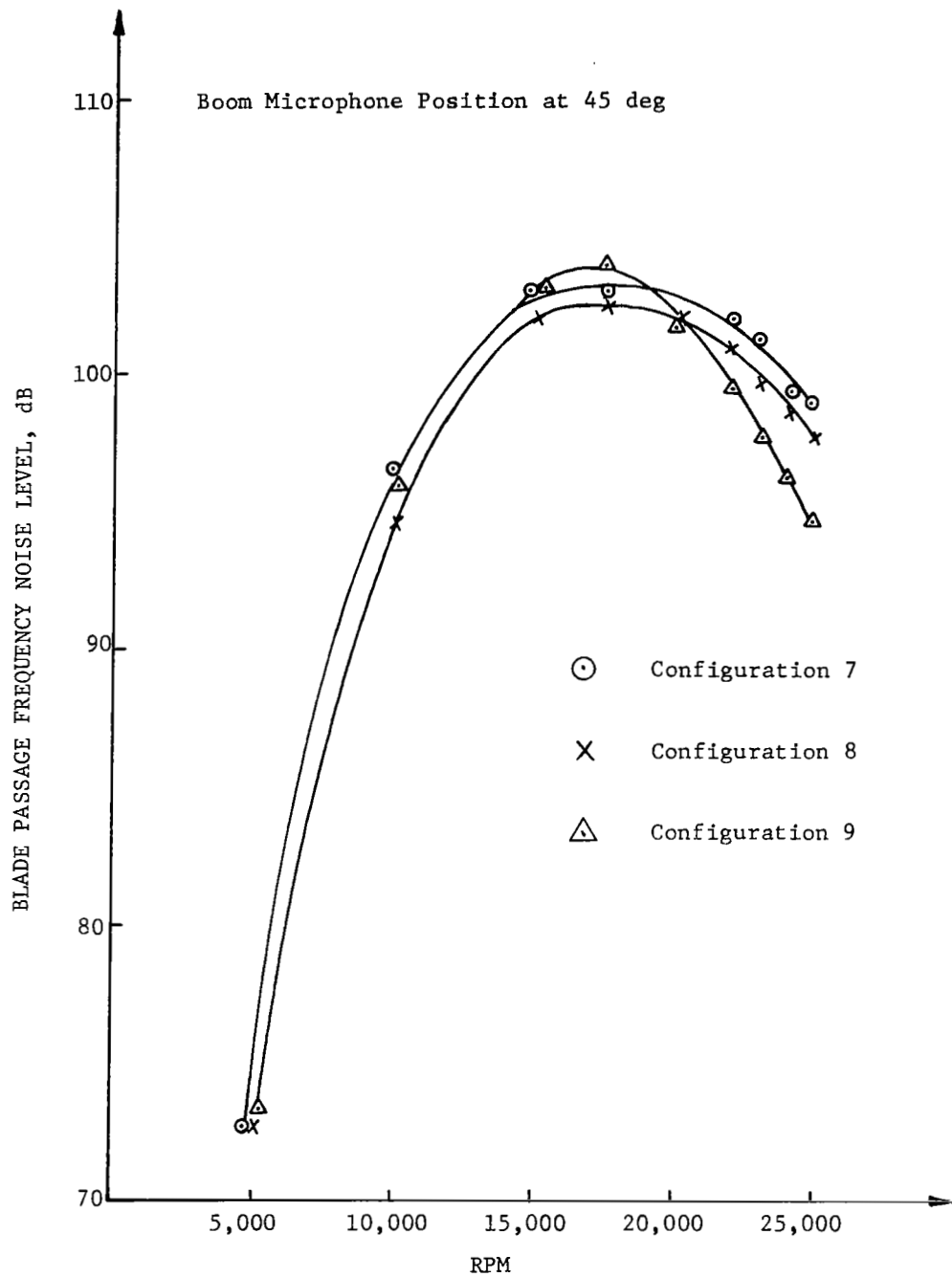


FIG.57 COMPARISON OF BLADE PASSAGE FREQUENCY ATTENUATION CHARACTERISTICS OF INLETS OPERATING AT SUBSONIC MACH NUMBERS

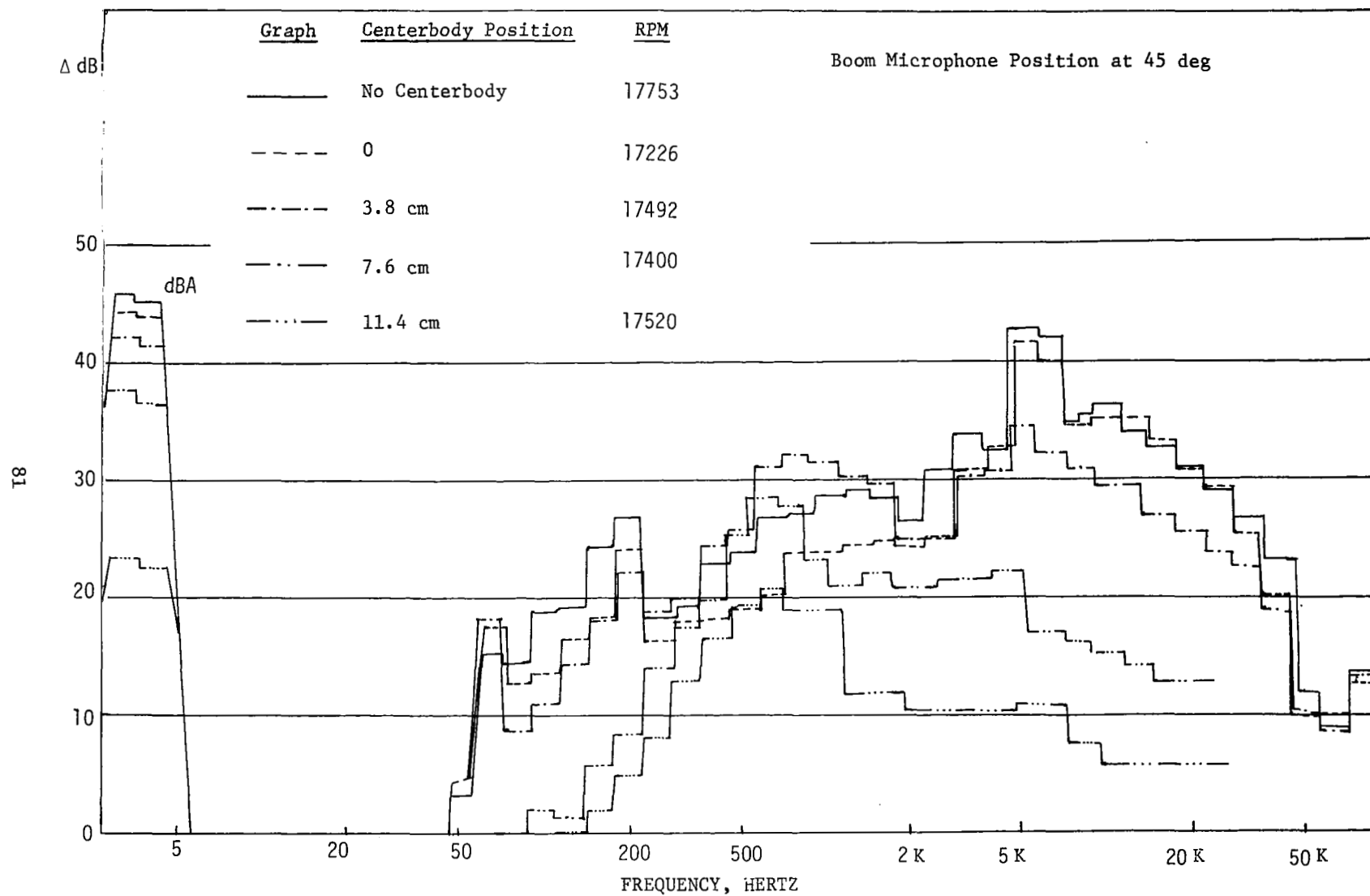


FIG.58 FREQUENCY SPECTRA FOR CONFIGURATION 2 AT 17,500 RPM

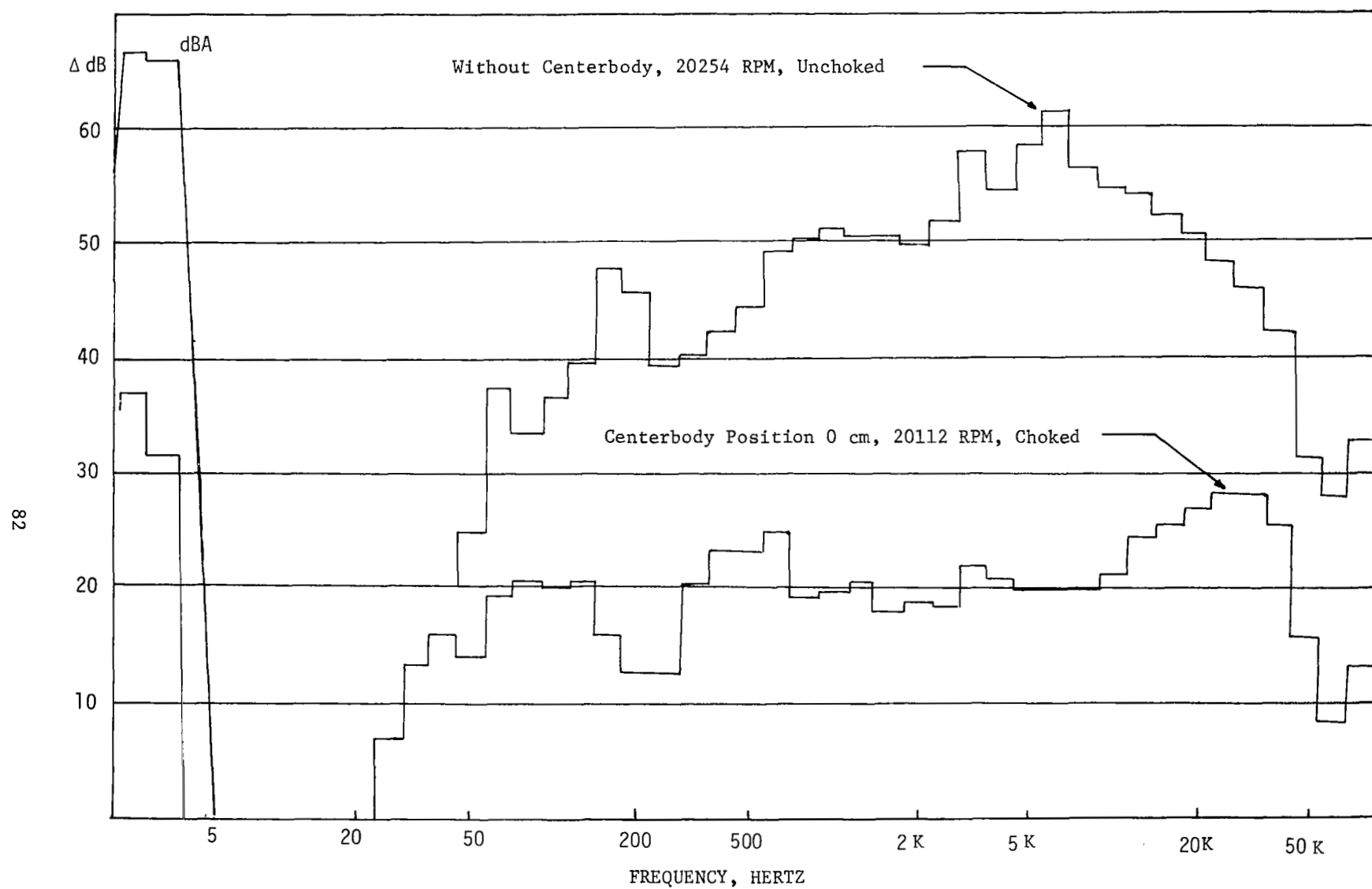


FIG.59 FREQUENCY SPECTRA FOR CONFIGURATION 2 AT 20,100 RPM

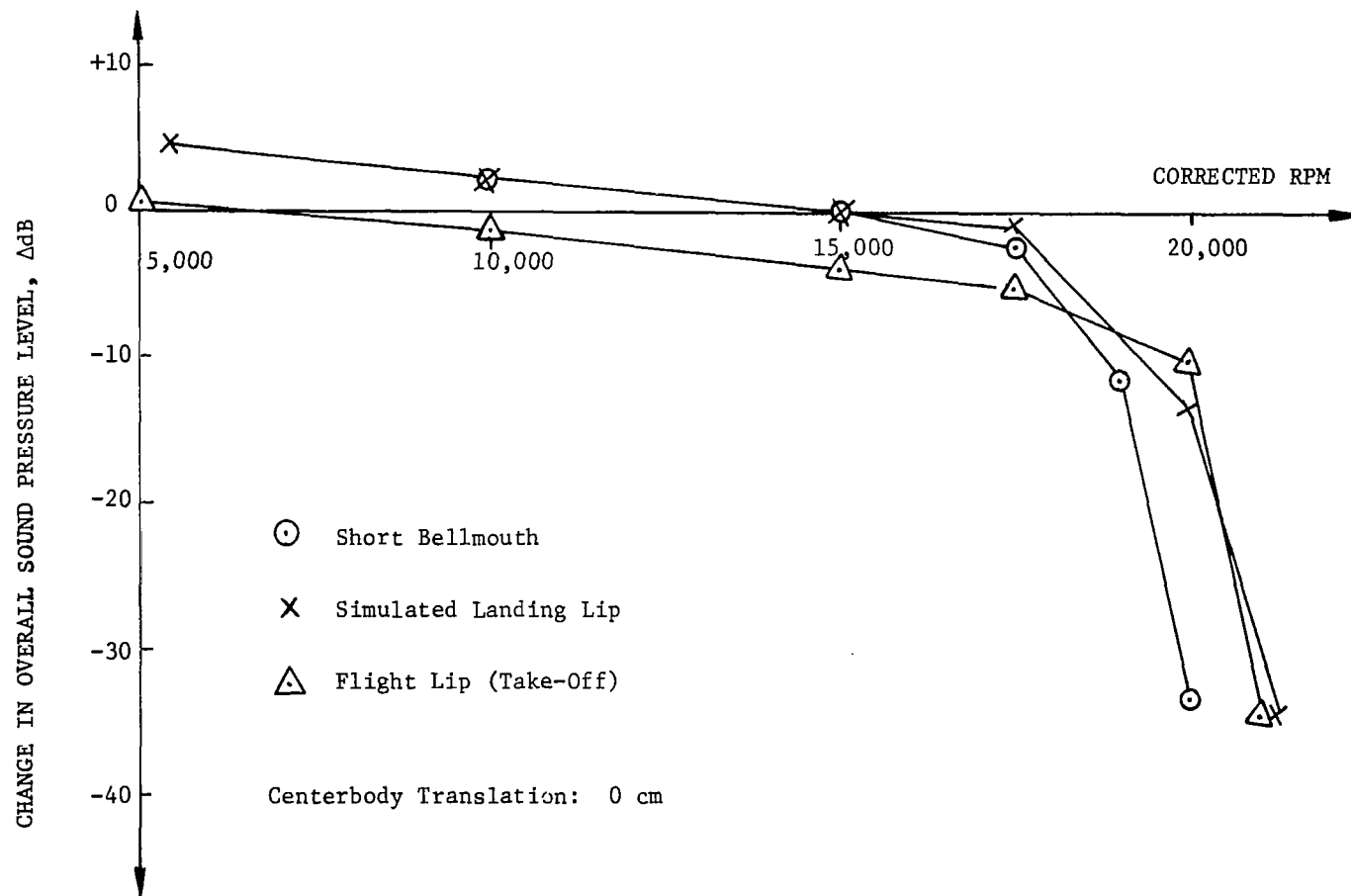


FIG.60 INFLUENCE OF LIP GEOMETRY ON NOISE ATTENUATION

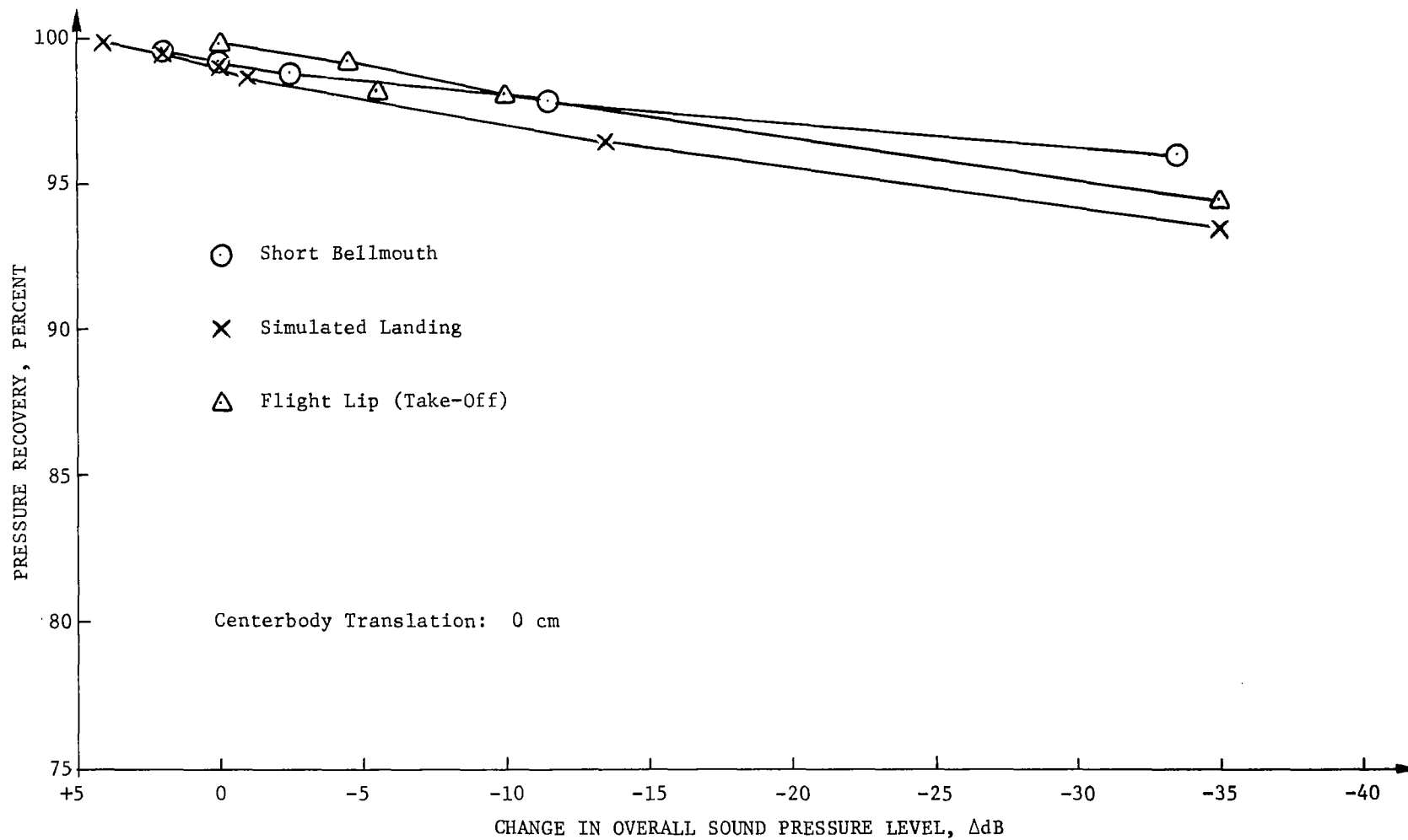


FIG.61 INFLUENCE OF LIP GEOMETRY ON NOISE ATTENUATION AND PRESSURE RECOVERY

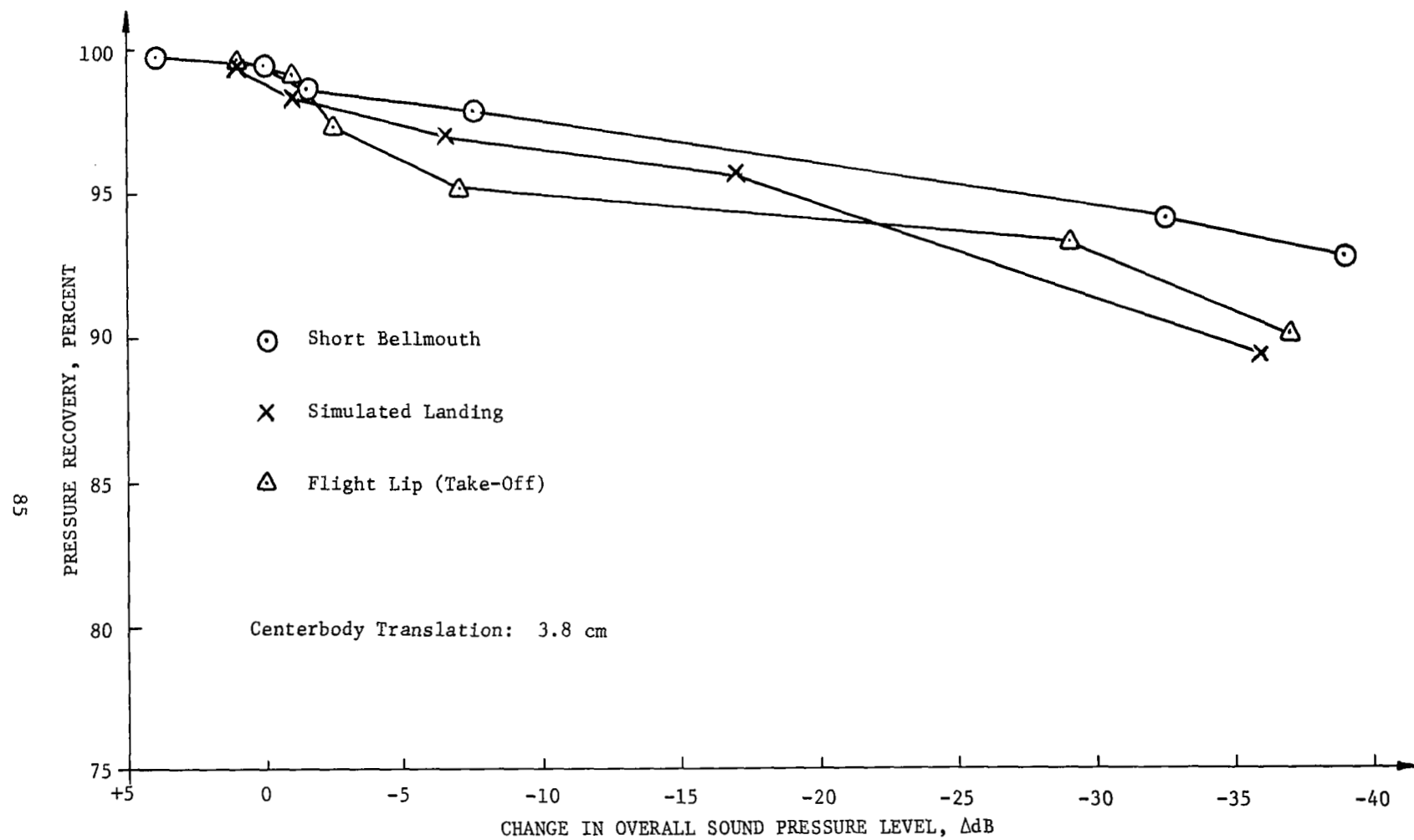


FIG.62 INFLUENCE OF LIP GEOMETRY ON NOISE ATTENUATION AND PRESSURE RECOVERY

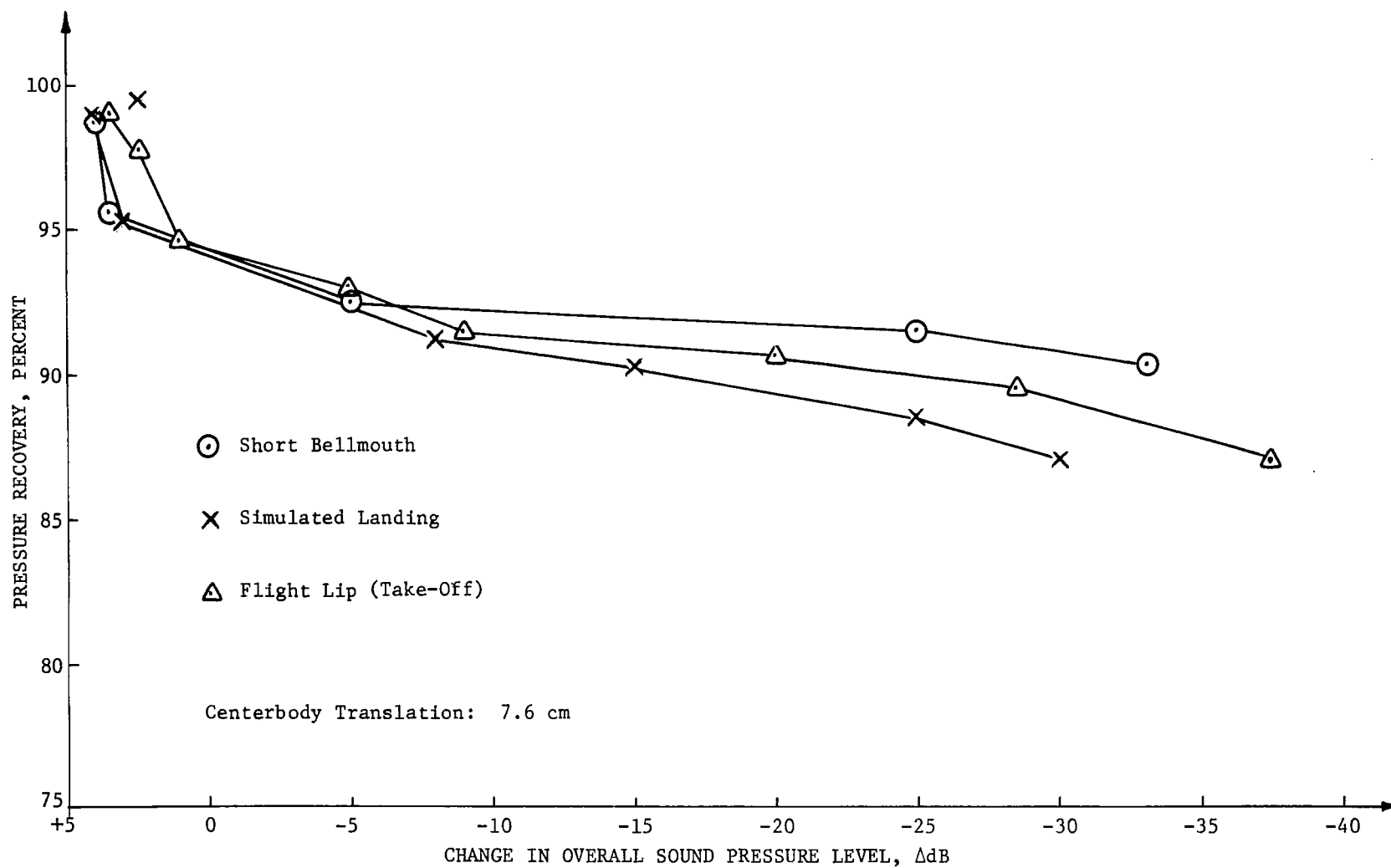


FIG.63 INFLUENCE OF LIP GEOMETRY ON NOISE ATTENUATION AND PRESSURE RECOVERY

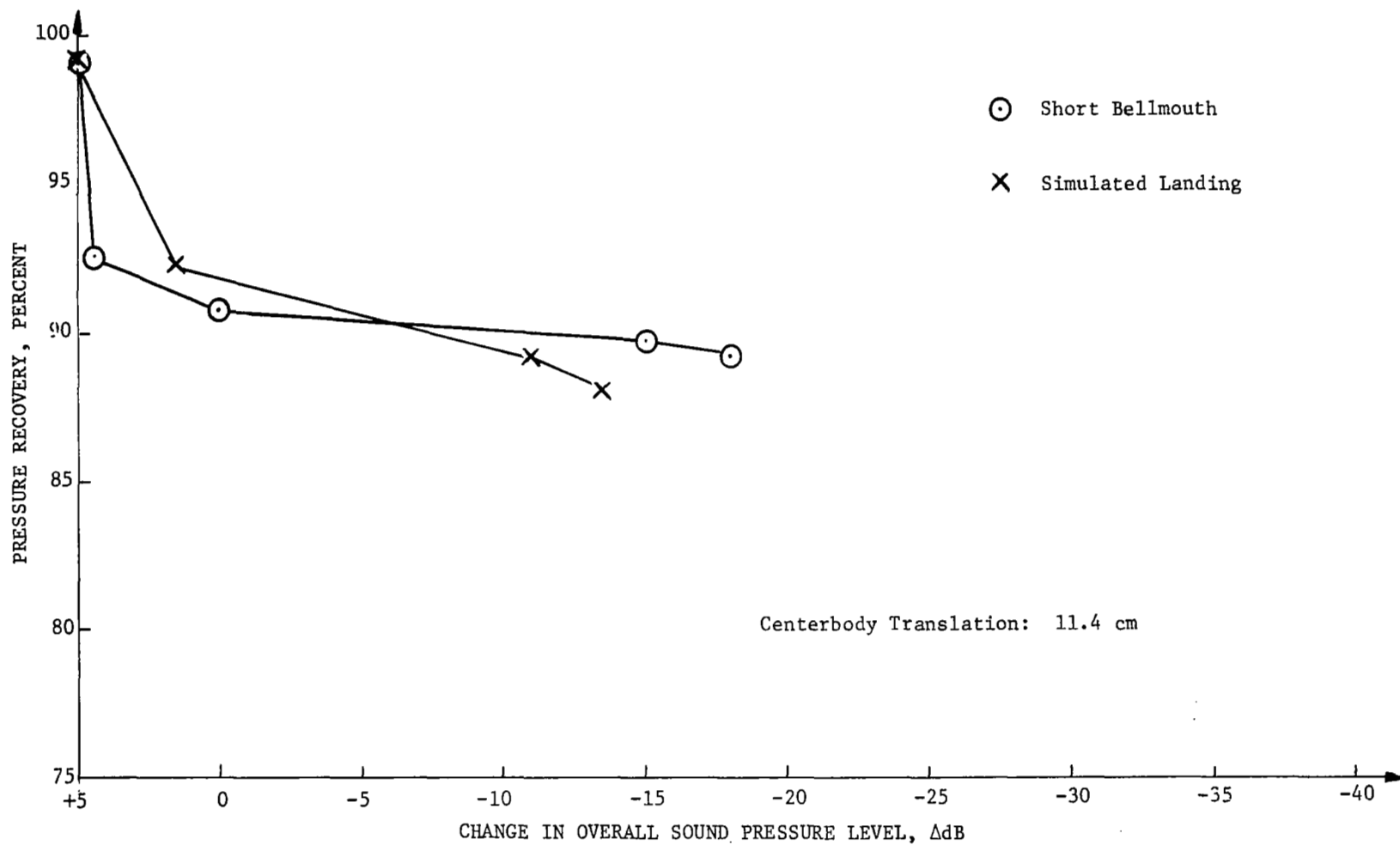


FIG.64 INFLUENCE OF LIP GEOMETRY ON NOISE ATTENUATION AND PRESSURE RECOVERY

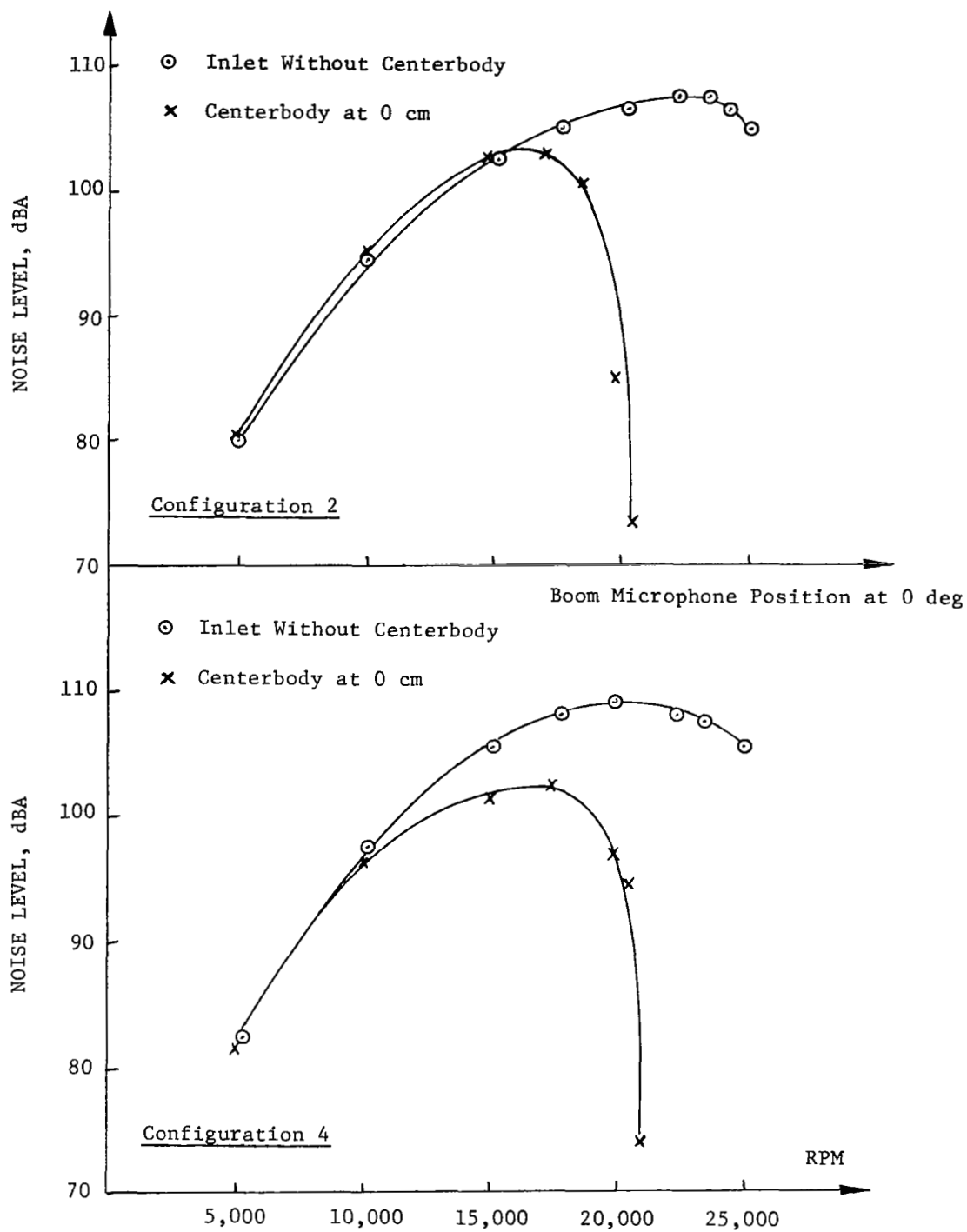


FIG.65 INFLUENCE OF CENTERBODY ON NOISE LEVEL

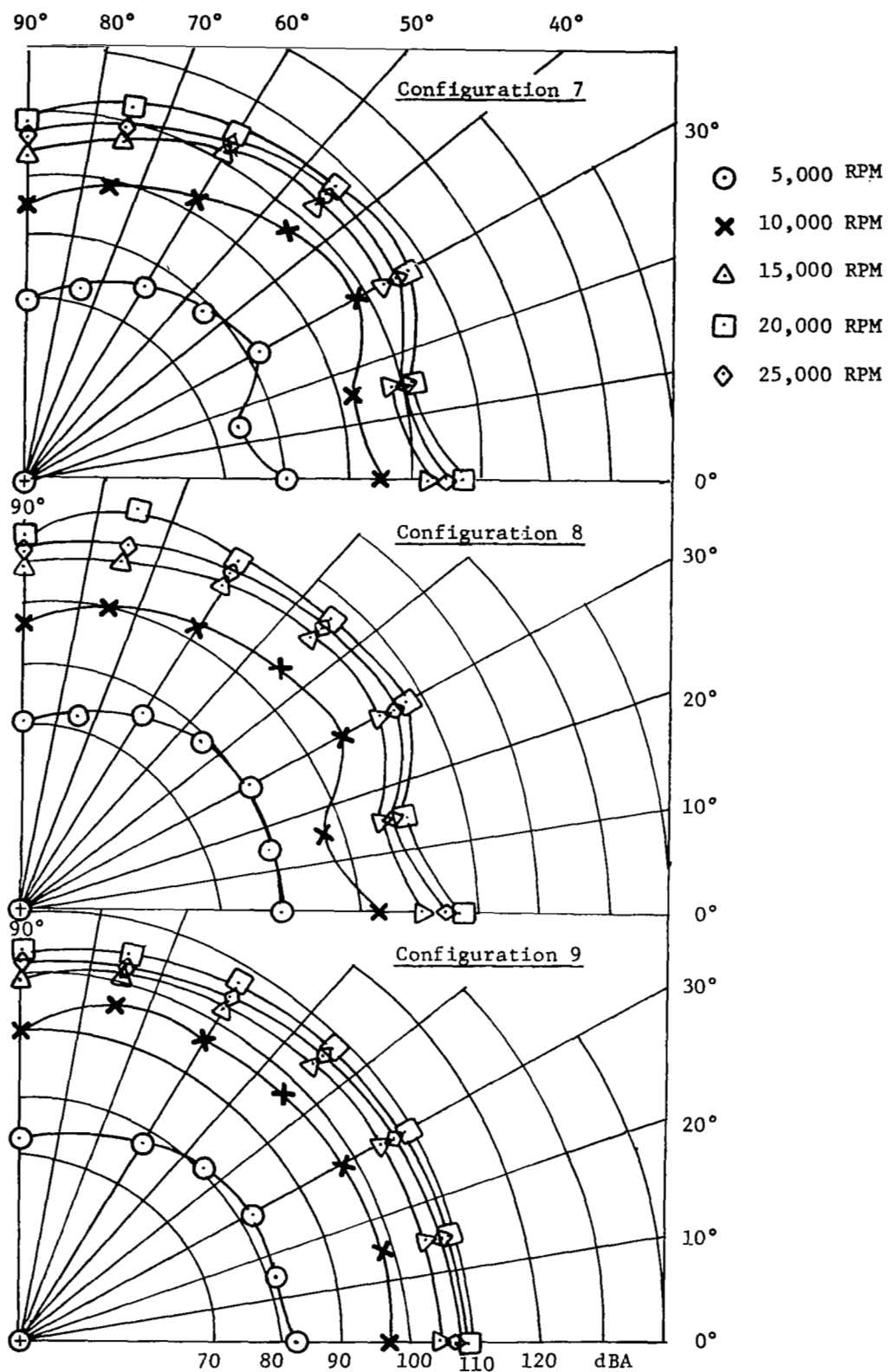


FIG.66 POLAR GRAPHS SHOWING THE INFLUENCE OF LIP GEOMETRY OF INLETS OPERATING AT SUBSONIC MACH NUMBER

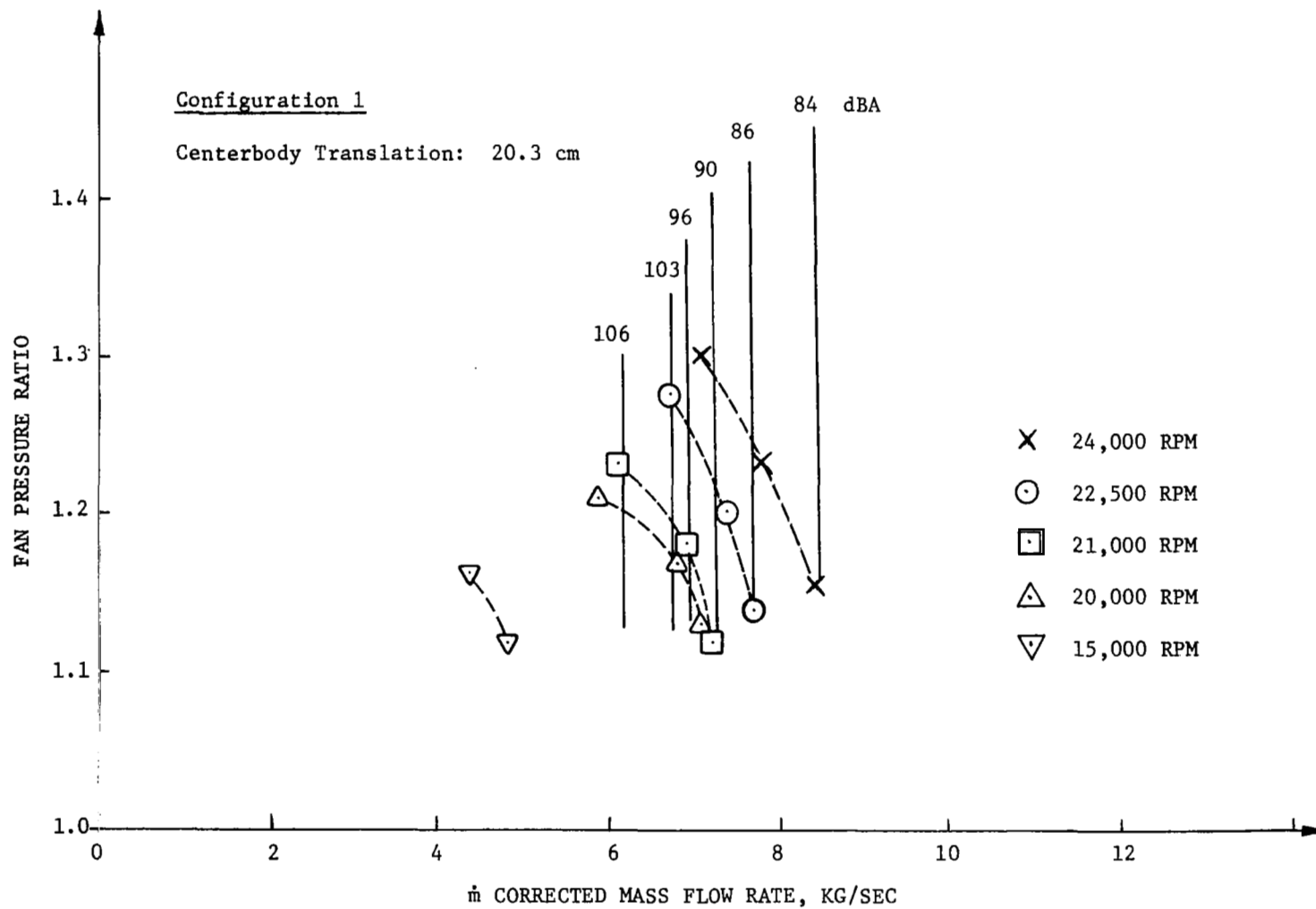


FIG.67 INFLUENCE OF COMPRESSOR PRESSURE RATIO ON NOISE

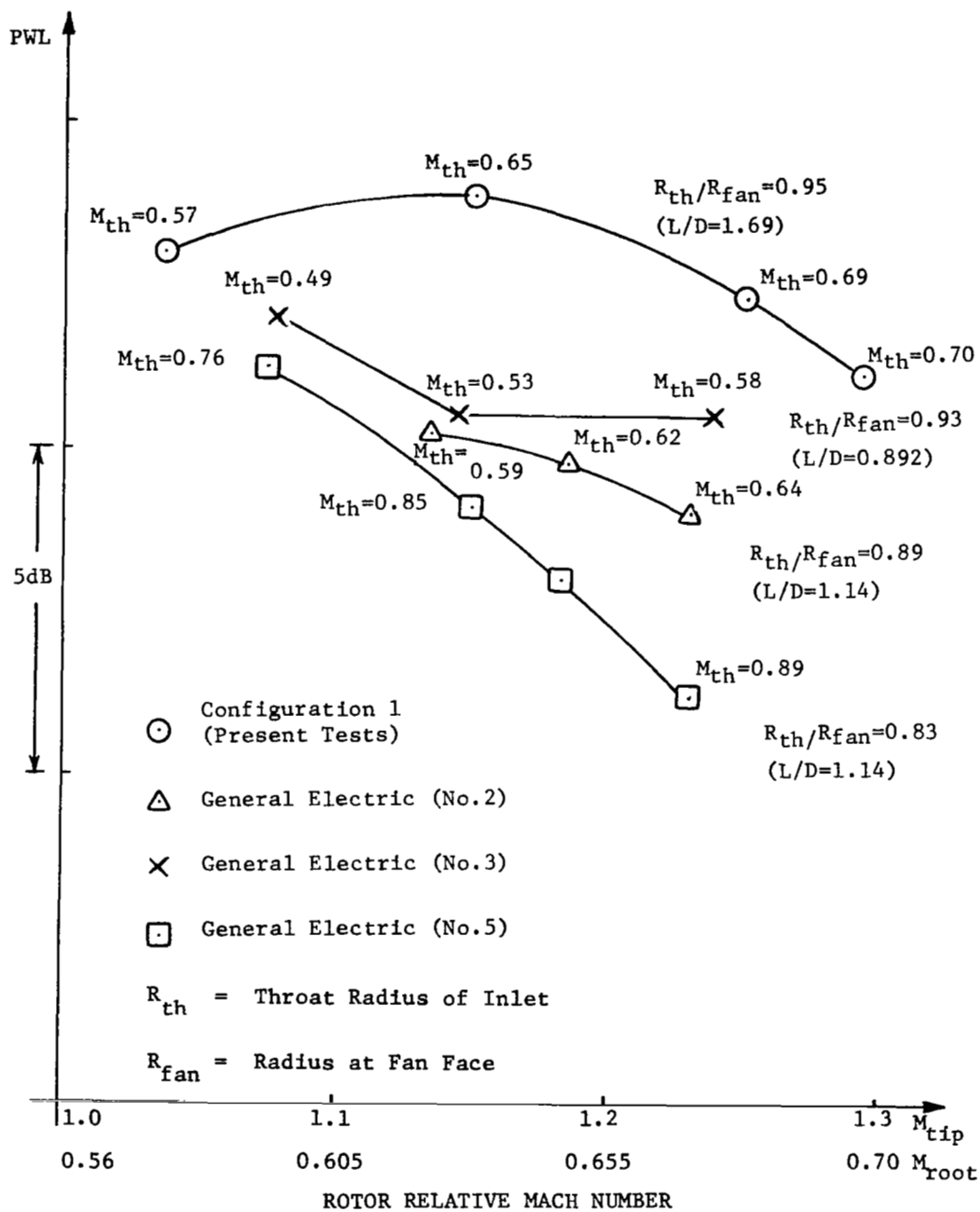


FIG. 68 COMPARISON OF NOISE ATTENUATION CHARACTERISTICS OF INLETS OPERATING AT HIGH SUBSONIC MACH NUMBER WITH COMPRESSOR OPERATING AT SUPERSONIC ROTOR TIP SPEED

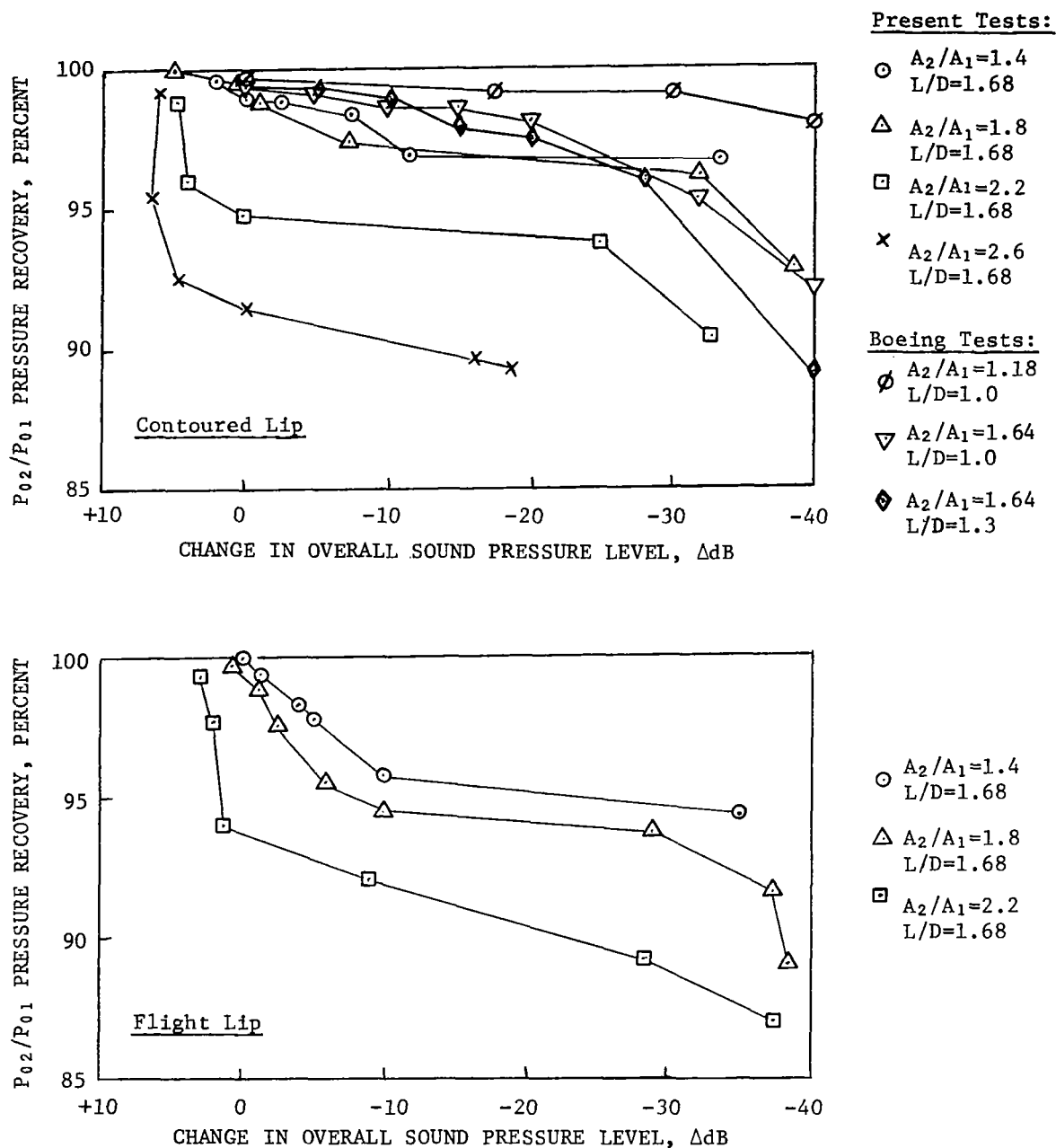


FIG.69 EFFECT OF AREA RATIO ON NOISE ATTENUATION AND PRESSURE RECOVERY

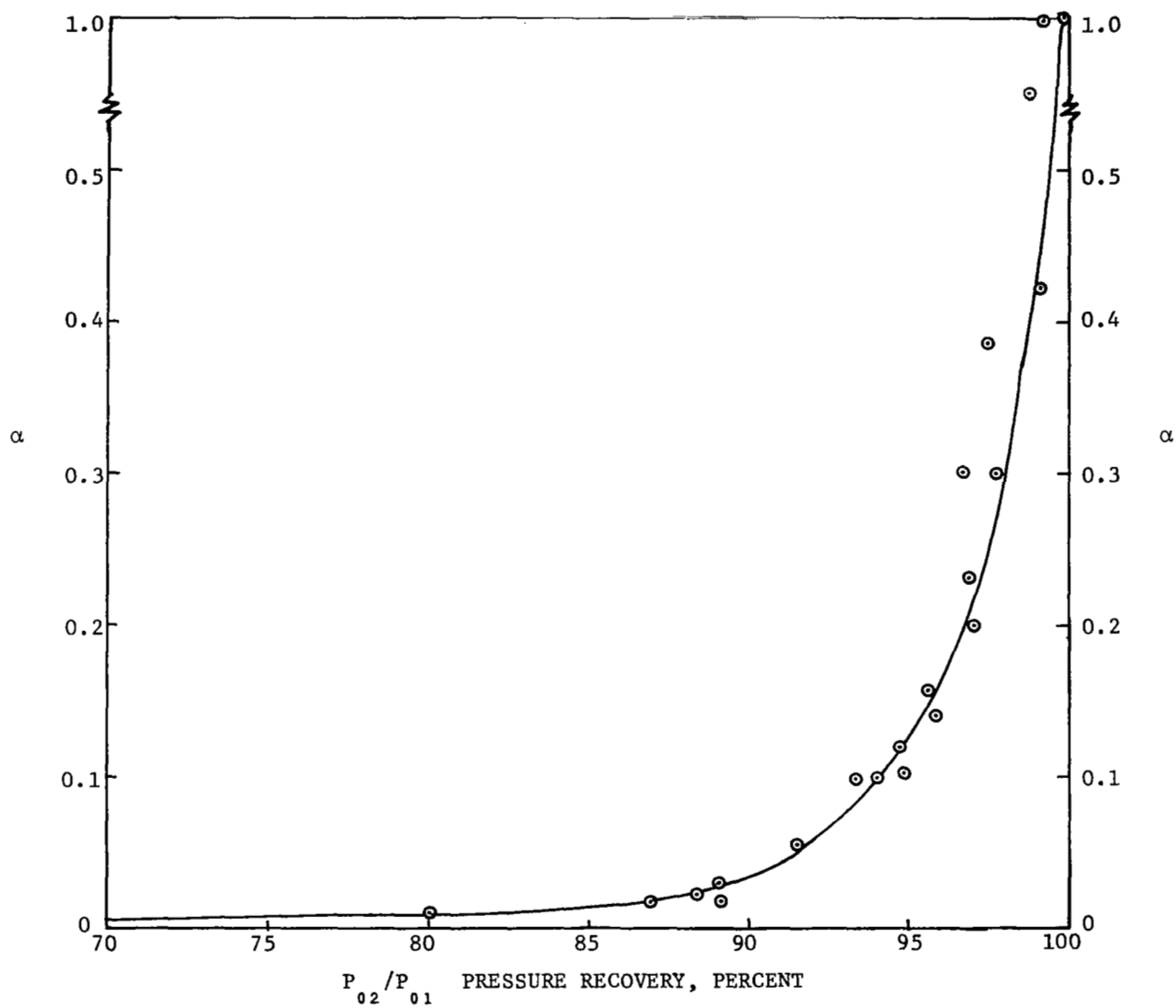


FIG.70 INFLUENCE OF PRESSURE RECOVERY ON THE EXPONENTIAL PARAMETER α

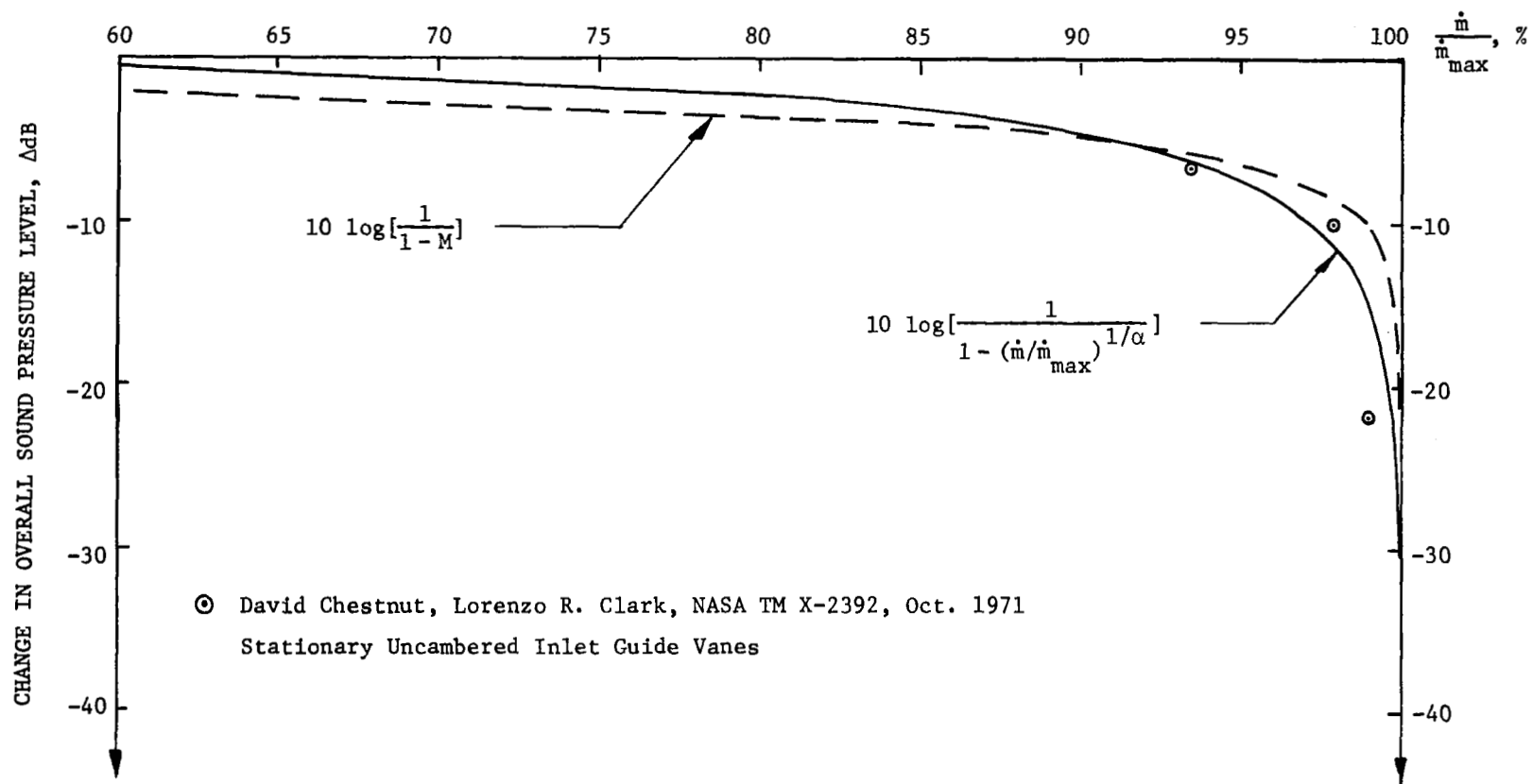


FIG.71 COMPARISON BETWEEN EMPIRICAL EQUATIONS AND EJECTOR TEST DATA

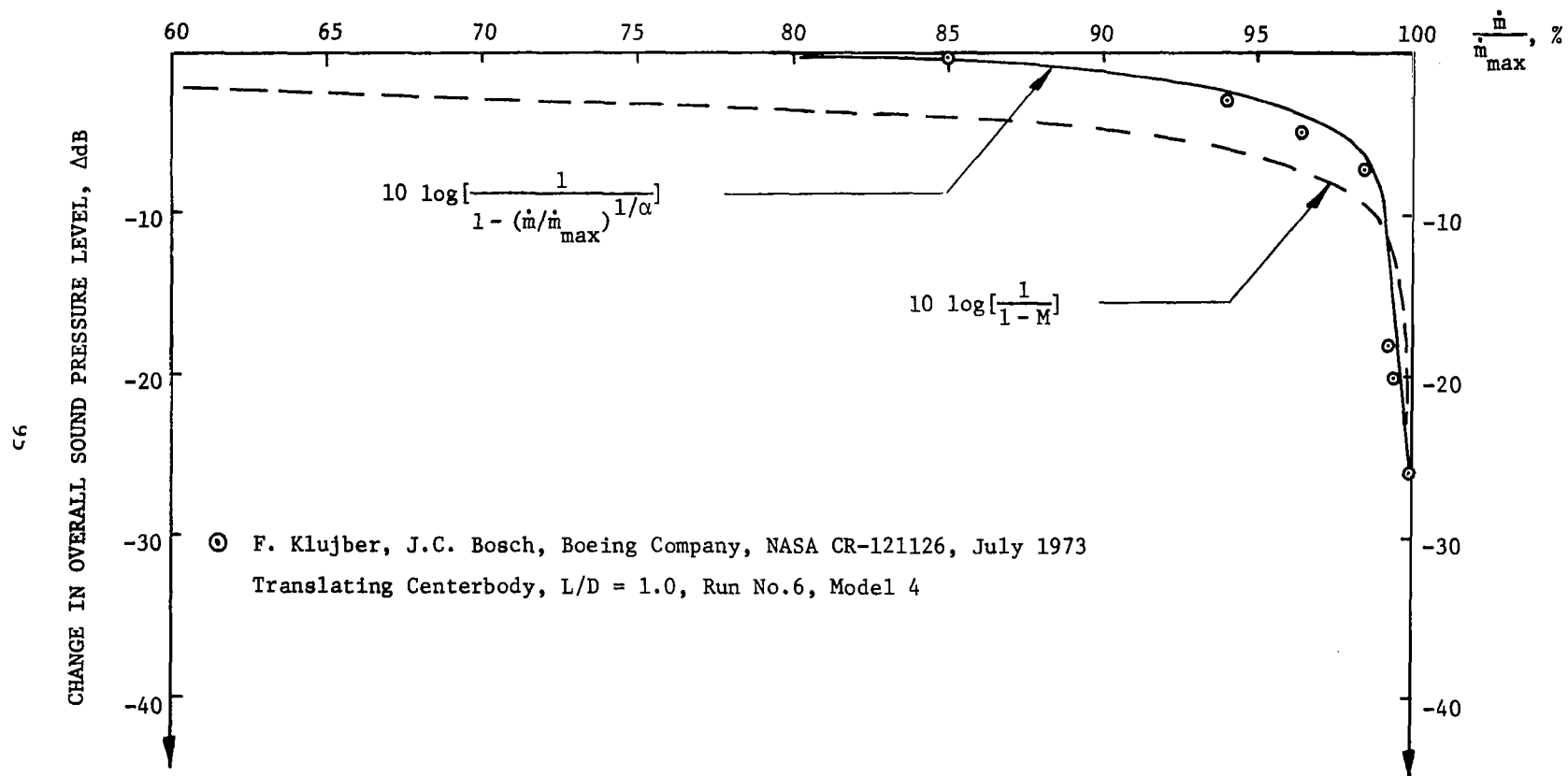


FIG.72 COMPARISON BETWEEN EMPIRICAL EQUATIONS AND COMPRESSOR TEST DATA

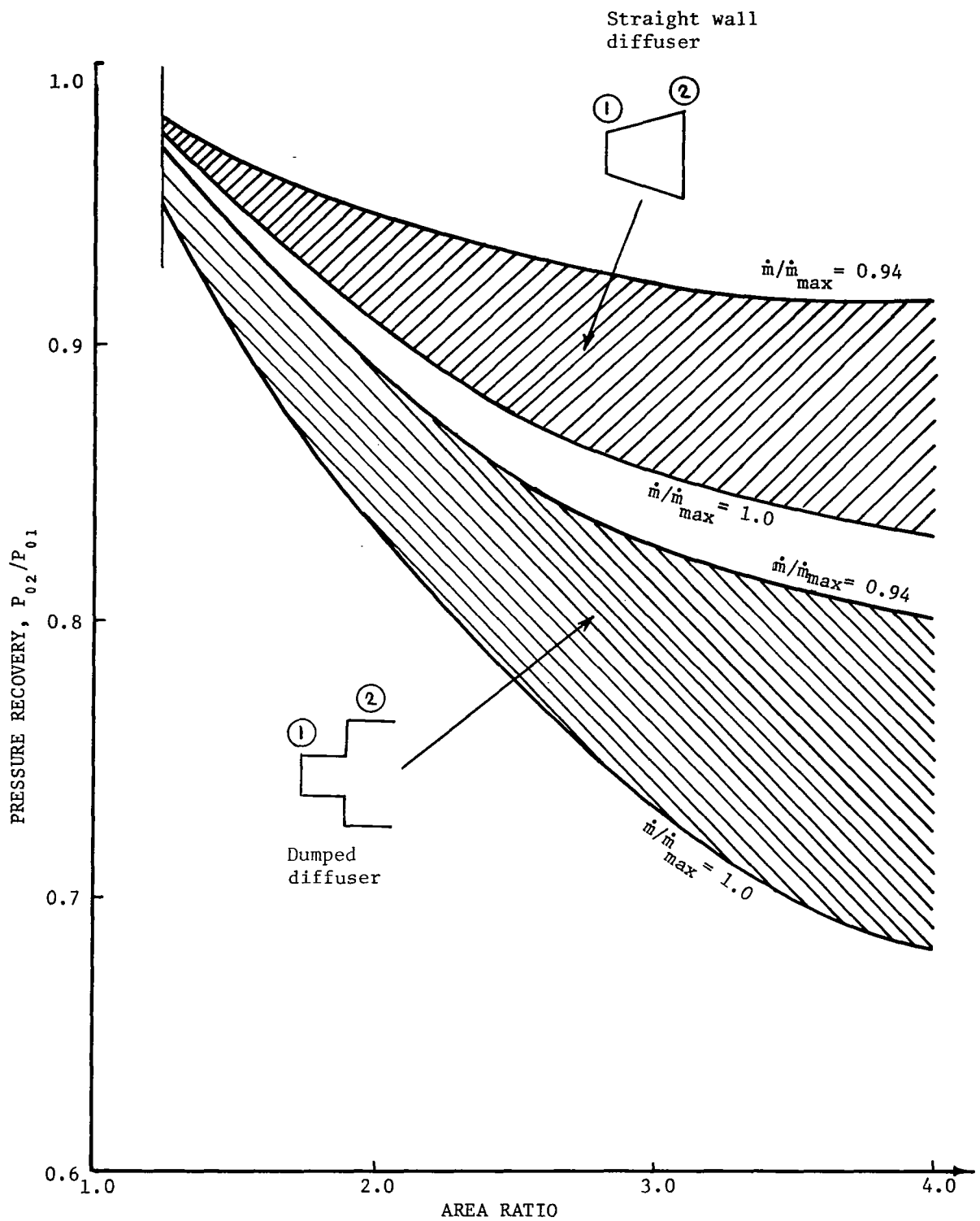


FIG.73 PRESSURE RECOVERY FOR DIFFUSERS WITH DIFFERENT AREA RATIOS

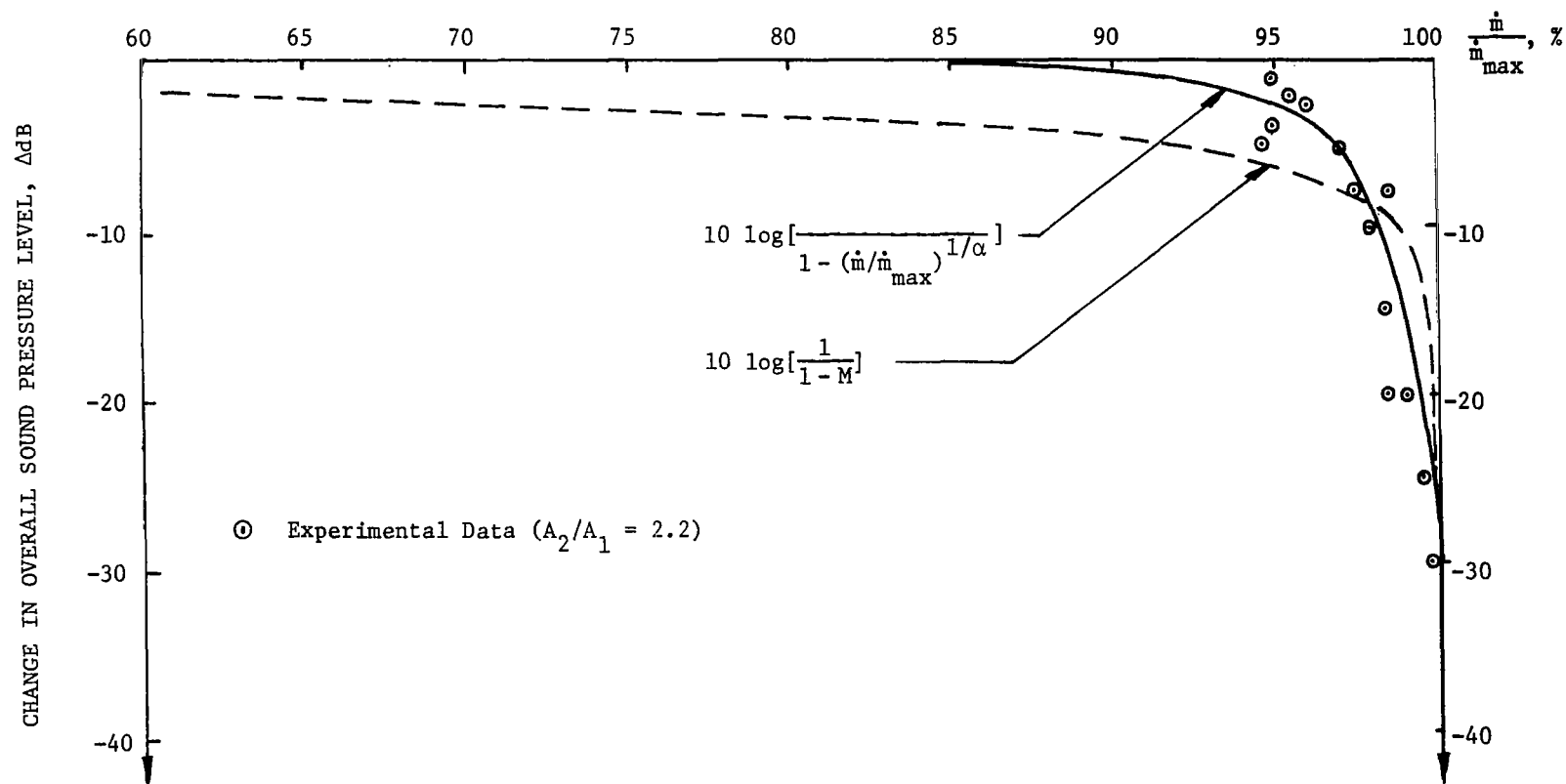


FIG.74 COMPARISON OF EMPIRICAL EQUATIONS WITH EXPERIMENTAL RESULTS

A P P E N D I X

TABLE A - REVIEW OF WORK ON SONIC AND NEAR-SONIC INLETS

Year	Author(s)	Paper	Type of Test
1961	Sobel and Welliver CURTISS-WRIGHT	<u>Noise-Control</u> , Vol.7, No.5	Sonic inlet tests with centerbody on compressor and Olympus-6 turbojet
1964	McKaig, BOEING	Document T6-3173	SST-type inlet on J-75 engine
1966	Sawhill, BOEING	Document D6A 10155-1	Ejector test with 12.7-cm SST-type inlet
1966	Anderson, BOEING	Document D6A 10378-1 TN	Ejector tests with 12.7-cm SST-type inlet
1967	Cawthorn et al., NASA	TN D-3929	SST-type inlet with Viper-8 jet engine
1968	E.B. Smith et al. GENERAL ELECTRIC	TR DS-68-7, Contract FA65WA-1236, FAA	Model cascade
1968	Chestnutt NASA	TN D-4682	Ejector tests with cambered and uncambered air-foils
1968	Higgins et al., BOEING	SP-189, pp. 197-215, NASA	JT3D engine with contracting cowl
1969	J.N. Smith and Higgins BOEING	Document D6-23469	JT3D engine
1970	Putnam and R.H. Smith NASA	TN D-5692	Static test with XB-70 airplane
1971	Chestnutt and Clark NASA	TM X-2392	Variable geometry cascade inlet tests with ejector
1972	Anderson et al., BOEING	Document D6-40208	Grid and radial type vane inlet with fan
1972	Lumsdaine SOUTH DAKOTA STATE U., UNIVERSITY OF TENNESSEE	<u>72 Inter-Noise Proceedings</u>	Model tests of several inlets with ejector
1973	Klujber, BOEING	Document D6-40855 (Vols. I, II, III)	Transonic 0.35-m dia. fan using inlets with low area ratio (max. $A_2/A_1 = 1.6$)

(cont.)

TABLE A cont.)

Year	Author(s)	Paper	Type of Test
1973	Miller and Abbott NASA	TM X-2773	Small fan with cross flow at various angles with translating centerbody (two positions only)
1973	Kutney GENERAL ELECTRIC	Work in progress (also G.E. Report No. R-73-AEG-412)	Tests with Langley transonic compressor with expanding centerbody ($A_2/A_1 = 2.6$)
1973	Compagnon GENERAL ELECTRIC	NASA CR-134495	Study of engine variable geometry systems with high Mach number inlets - collapsing cowl inlet recommended
1974	Lumsdaine UNIVERSITY OF TENNESSEE	Second Interagency Symposium on University Research in Transportation Noise	Tests with Langley transonic compressor with various area ratios and various types of inlets (max. $A_2/A_1 = 3.6$)
1974	Lumsdaine and Jibben SOUTH DAKOTA STATE U., UNIVERSITY OF TENNESSEE	To be presented at the 1975 ASME Automatic Control Conf., Houston, Texas	First test of an automatic control system designed for the choked inlet
1974	Groth NASA	AIAA paper 74-91	Translating centerbody with radial vanes tested with a J-85 engine
1974	Koch et al. ALLISON DIVISION, GM	AIAA paper 74-1098	Fixed geometry inlet tested with model fan (1/5 scale of advanced fan)
1974	Lumsdaine and Clark UNIVERSITY OF TENNESSEE and NASA	Second Interagency Symposium on University Research in Transportation Noise	Results of choked inlets tested with 30.5-cm fan
1975	Lumsdaine UNIVERSITY OF TENNESSEE	<u>75 Inter-Noise Proceedings</u>	Sonic and near-sonic inlet tests with NASA Langley transonic compressor
1975	B. Miller et al. NASA	NASA TM X-3222	Effect of lip design on acoustic and aerodynamic performance of high Mach number inlets, tests at different angles of attack in wind tunnel, siren source